Gauge theories of spin systems

A DISSERTATION
SUBMITTED TO THE FACULTY OF THE GRADUATE SCHOOL
OF THE UNIVERSITY OF MINNESOTA
BY

Jianlong Fu

IN PARTIAL FULFILLMENT OF THE REQUIREMENTS
FOR THE DEGREE OF
DOCTOR OF PHILOSOPHY

Natalia B. Perkins

May, 2019

Acknowledgements

It has been a nice experience for me to study for my PhD in University of Minnesota. There are a lot of things that I am grateful for and people that I am thankful to. First of all, I am grateful to my advisor, Professor Natalia Perkins, for her support throughout these years, including the chances to visit the Perimeter Institute and to attend various academic conferences. I am also very grateful to Professor Mikhail Voloshin, for the discussion with him and his encouragement. Moreover, I am thankful to J. Rau, M. Gingras, and J. Knolle for collaborations. In the end, I am thankful to the School of Physics of Astronomy in University of Minnesota, for providing a nice environment and resources for my graduate study.

Dedication

Dedicated to my parents

Abstract

In this dissertation, I discuss the gauge theory description of interacting spin systems, which results from the application of slave-particle approach. In particular, I discuss three types of gauge theory description. Starting from the Abrikosov fermion representation of spin, I review the effective SU(2) gauge theory of the Heisenberg model on the mean-field level. I then move on to study another types of spin representation, the Majorana fermion representation. After a discussion on the relationship between the three types of Majorana representation, namely the SO(3) Majorana representation, the SO(4) chiral representation and the Kitaev representation, I focus on the SO(3) Majorana representation and show that its non-local nature makes it equivalent to the Jordan-Wigner transformation of spin in both one-dimensional and two-dimensional space. To apply the SO(3) Majorana representation, I discuss three two-dimensional spin models, namely the Kitaev honeycomb model, the quantum XY model on honeycomb lattice and the 90° compass model on square lattice. Using the SO(3) Majorana representation, I demonstrate how to map the spin Hamiltonians into Z_2 lattice gauge theories with standard Gauss-law constraint. The mapping differs from the mean-field approach in that the resulting gauge theories are exact. In the third part of the dissertation, I discuss the application of non-local spin representations to some specific spin models. In particular, I review the effective U(1) lattice gauge theory for the spin ice model on pyrochlore lattice and discuss the potential application of staggered Abrikosov fermion representation in spin ice model and kagome antiferromagnetic model.

Contents

List of Tables

List of Figures

Chapter 1

Introduction

1.1 Condensed matter physics in a nutshell

To some extent, one of our most important knowledge of the universe we lived in is that the matter in the universe can be divided into small pieces [1]. To the best of our knowledge so far, the smallest pieces of the universe are the quarks and leptons and the gauge field particles [2, 3, 4, 5]. The theory describing the being and interaction of these particles is the Standard Model, which is a very successful theory whose predictions keeps being confirmed by experiments [3, 4, 5]. The Standard Model is a non-Abelian quantum field theory with the gauge group $\mathrm{SU}(3) \times \mathrm{SU}(2) \times \mathrm{U}(1)$, it incorporates three of the four fundamental interaction of the universe: the strong interaction, the weak interaction and the electromagnetic interaction [5]. Spontaneous breaking of the gauge symmetry through the Higgs mechanism brings masses to the particles of the Standard Model. The Standard Model is nontrivial in that it breaks some discrete symmetries, including parity symmetry; it also has complex mixing among its matter contents, the leptons [4, 5].

There is some evidence that the Standard Model is a low-energy effective field theory coming from a bigger theory that is only available at high enough energy scales. In particular, there is yet another type of interaction, the gravity, which cannot be treated within the same framework as the Standard Model. The theory behind the gravity force is the General Relativity, proposed by Einstein in 1915 [6]. General Relativity is a classical theory which relates the phenomenology of gravitation to the curving of the

spacetime manifold which is caused by the energy and momentum of the particles living in it. There have been several attempts to explore possibilities of a bigger framework of the theory. For example, string theory was proposed stating that the elementary particles we observe are all excited modes of elementary strings [7]. The strings interact in a way that no hard energy (or momentum) cutoff is needed to ensure the converging of the scattering amplitude. The string excitation spectrum is rich in a sense that it can incorporate all types of particles, including the boson and fermion and rank-2 tensor like the gravity. However, there is so far no evidence to show the existence of elementary strings. More generally, all the theories beyond Standard Model are not getting solid confirmation so far.

The details of the Standard Model can only be shown at relatively high energies. As the energy get lower, the matter tends to "condense". Quarks are glued together by gluons forming hardrons and mesons (due to the confinement of the SU(3) gauge theory, the quarks can never be detected individually). Protons and neutrons glued together to form nucleus which attaches electrons to form electrically neutral atoms. At even lower energy, the atoms form macroscopic matter that we encounter in our everyday life. The matter in our everyday life takes three phases, solid, liquid and gas. The number of atoms within macroscopic matter is large, typically of the order of 10^{23} or higher. Needless to say, the phenomenology of the macroscopic matter is quite different from the microscopic particles [8].

The macroscopic matter typically has three distinct properties. First, the number of the atoms and electrons within it is very large. Second, these large number of particles interact with each other in a complicated way. Third, the energy scale of the matter is relatively low. These three properties render the Standard Model almost irrelevant in describing the physics of the macroscopic matter. Instead, due to the large scale of the number of particles, we can normally apply statistical physics to study it [9, 10]. Also luckily enough, as the energy scale is low enough, the details of the complex structure of the Standard Model do not matter, instead we can use *effective field theories* to approximately describe the interaction between the particles. Therefore, a new type of theory has been developed in recent decades which is called *many-body theory* [10, 11, 12, 13]. The many-body theory is very important in that the rich structure and phenomena of the universe always involves macroscopic number of particles interacting

among themselves. Therefore, the development of the many-body theory takes place parallel with the quest for the ultimate theory of the universe. In some sense, both of these are essential to explain the rich phenomenology that is being observed. Recently, the research of macroscopic matter and many-body theory has developed into a new field called *condensed matter physics*. In condensed matter physics, the subfield of the solid state is usually called hard condensed matter, while the study of liquid and other form of matter (for example, life) is usually called soft condensed matter.

On one hand, the study of many-body physics should be familiar to physicists because of the similarity between quantum mechanics and statistical physics. Such similarity can be seen from the path integral formalism, and it results in the fact that the general structure of many-body theory is very similar with the quantum field theory of elementary particles [2, 10, 12, 13]. In light of this, as we shall see later in this thesis, the specific treatments of many many-body phenomena also borrow and share the concepts and methods of the quantum field theory (especially lattice gauge theory [14]). On the other hand, due to the large number of particles, the study of many-body theory is challenging. As we shall describe in greater detail later, a considerable amount of approximation is usually needed to work out some concrete predictions in many-body theory. Therefore, the possible number of interesting phenomena that can acquire a clear many-body theoretical description is limited. Here, before we jump into the details of the thesis, let's take a moment to give a brief description of some of the most interesting phenomena (or physics) in the many-body physics area.

To some extent, a great part of the most interesting physics in the hard condensed matter physics is related to "macroscopic quantum phenomena". According to common assumption, quantum mechanics only shows its peculiarities in the microscopic world, but experiments in condensed matter physics show that the macroscopic matter can also demonstrate "quantum mechanical behavior" which is unusual and cannot be explained by classical theory at all. In this regard, two interesting phenomena in condensed matter physics stands out, which is superfluidity and superconductivity [10, 12, 15, 16]. Superfluidity refers to the phenomenon that at low temperature, some liquids (say liquid helium) which consist of bosonic atoms can flow with *zero viscosity*. Superconductivity is the phenomenon that below a certain temperature, the electrical resistance of some materials drops down to zero. While superfluidity can be explained by the Bose-Einstein

condensation of a bosonic system [10], the explaination of superconductivity is more complex. It took people a long time to realize that the Fermi surface of some fermionic system can be unstable when interaction is adiabatically turned on, this observation is called "Cooper instability" [15]. At low temperature the fermionic system is unstable and particles near the Fermi surface tend to pair up and form bosonic "Cooper pair". At low temperatures, such Cooper pair will Bose condense and thus cause superfluidity. The superfluidity of Cooper pairs then explains the superconductivity phenomena [12, 15]. On the other hand, there is another type of macroscopic quantum phenomena which is restricted to the two-dimensional electronic systems, that is the Qantum Hall Effect (QHE). Theoretically, it was shown by Thouless *et al* that the Hall conductivity, calculated quantum mechanically is necessarily quantized for two dimensional electronic systems, the quantization is related to geometric quantity called the (first) Chern number [13, 17, 18]. Needless to say, there are other types of fascinating physical phenomena that have been or are being understood in condensed matter physics. These research works make the condensed matter physics one of the most fast developing field in physics.

In this thesis, I will focus on another sub-field of (hard) condensed matter physics, the spin systems [19]. As we shall explain later in this chapter, the interacting spin systems can sometimes be seen as the large coupling limit of half-filled electronic systems in which electrons are nearly static. However, the theoretical methods developed to study the spin systems share a lot of similarities with the "free electron" limit in which electrons are "moving freely". On the other hand, as we shall see, these theoretical methods also have some similarities with the (lattice) gauge theories in elementary particle physics (although some of the concepts are not understood in exactly the same way). In light of these, I will begin the discussion with a background description of the spin systems starting with general electronic many-body theory.

1.2 Spin interaction from correlated electron Hamiltonian

To study a system of electrons on a lattice, we have to make some approximations. When the temperature is low, the electrons tend to localize in adjacent to each individual atom neucleus, thus it is reasonable to describe the electron states using a basis labeled

by their location in the lattice. Under second quantization, the electron states are thus denoted by creation and annihilation operators $c^\dagger_{i\sigma}$ and $c_{i\sigma}$, in which i labels the lattice sites the electron reside in and σ denotes the spin states of the electron. Such approximation is usually taken as the starting point of the many-body theory and it is called "tight-binding approximation". Using the tight-binding approximation, it is then possible to write down the electronic Hamiltonian [12].

$$\mathcal{H} = \sum_{ij} t_{ij} c^\dagger_{i\sigma} c_{j\sigma} + \sum_{ii'jj'} U_{ii'jj'} c^\dagger_{i\sigma} c^\dagger_{i'\sigma'} c_{j'\sigma'} c_{j\sigma} \tag{1.1}$$

As can be seen from Eq. 1.1, the many-body electronic Hamiltonian contains two parts. The first part is a hopping term which denotes the second quantized kinetic energy of the electronic system. Here we usually assume that in the hopping term, the two sites i and j are nearest neighbours of the lattice under the tight-binding approximation (higher-order hopping term generally have much smaller t parameter as their wavefunction hardly overlap). The second term is an interaction term, in which the parameter $U_{ii'jj'}$ comes from the electron-electron interaction. As discussed in the previous section, due to the low energy scale, it is usually sufficient to approximate the interaction strength U to be a constant depending on the locations of the electrons (such an approximation has also been used in the Fermi theory of the Weak interaction in particle physics [4]).

For the next step, let's take a closer look at the interaction term [12]. First of all, the U parameters for $i = j$ and $i' = j'$ are generally large due to the fact that the overlapping of wavefunction is the largest in this situation. The term

$$\sum_{i \neq i'} U_{ii'ii'} c^\dagger_{i\sigma} c^\dagger_{i'\sigma'} c_{i'\sigma'} c_{i\sigma} = \sum_{i \neq i'} V_{ii'} n_i n_{i'}, \tag{1.2}$$

in which $n_i = \sum_\sigma c^\dagger_{i\sigma} c_{i\sigma}$ denotes the electron number on each site, is called the "direct term". This term denotes the density-density interaction in the electronic system. Second, the U parameters of the situation $i' = j$ and $j' = i$ in Eq. 1.1 are usually comparable to the direct term. We have

$$\sum_{i \neq j} U_{ijji} c^\dagger_{i\sigma} c^\dagger_{j\sigma'} c_{i\sigma'} c_{j\sigma} = -2 \sum_{i \neq j} J^F_{ij} (\boldsymbol{S}_i \cdot \boldsymbol{S}_j + \frac{1}{4} n_i n_j), \tag{1.3}$$

in which we have defined $J_{ij}^F = U_{ijji}$. The (second-quantized) spin operator is defined as

$$\boldsymbol{S}_i = \frac{1}{2} c_{i\alpha}^\dagger \boldsymbol{\sigma}_{\alpha\beta} c_{i\beta}, \tag{1.4}$$

with $\sigma_{\alpha\beta}$ being the Pauli matrix. To derive Eq. 1.3, we used the identity

$$\boldsymbol{\sigma}_{\alpha\beta} \cdot \boldsymbol{\sigma}_{\gamma\delta} = 2\delta_{\alpha\delta}\delta_{\beta\gamma} - \delta_{\alpha\beta}\delta_{\gamma\delta}. \tag{1.5}$$

From Eq. 1.3 we can see that the exchange term in the electron interaction contains a *ferromagnetic interaction* whose strength is J_{ij}^F and is positive. Finally, the situation with the largest U parameters in Eq. 1.1 comes from the on-site Coulomb interaction in which $i = i' = j = j'$. Let us define $U_{iiii} = \frac{U}{2}$ then we have the term

$$\sum_{i\sigma\sigma'} U_{iiii} c_{i\sigma}^\dagger c_{i\sigma'}^\dagger c_{i\sigma'} c_{i\sigma} = \sum_i U n_{i\uparrow} n_{i\downarrow}. \tag{1.6}$$

in which $\uparrow$ and $\downarrow$ label the specific spin state up and down. This term (Eq. 1.6) is also called *Hubbard interaction*.

In many cases the coupling parameters U of the Hubbard term of interaction are so large that it is reasonable to ignore other terms in the summation of the interaction term in 1.1 and just keep the Hubbard term. Under such approximation, the Hamiltonian takes a simple form

$$\mathcal{H} = t \sum_{\langle ij \rangle} c_{i\sigma}^\dagger c_{j\sigma} + U \sum_i n_{i\uparrow} n_{i\downarrow}. \tag{1.7}$$

This Hamiltonian, in which the kinetic energy term is the nearest-neighbour hopping, is called the *Hubbard model* [12, 13]. It is the simpliest and probably the most important and commonly used model for certain correlated electronic systems. The Hubbard model captures two important features of the electronic system, first the hopping term is the kinetic energy of the electrons and the second term is the on-site repulsive interaction term for electrons.

There are two interesting limits of the Hubbard model Eq. 1.7. The first limit is $U \ll t$. In this limit the kinetic energy of the electrons dominates and the interaction among the electrons provides a perturbation. Without the perturbation, the system is a free electron system and the ground state of it can be easily obtained by going to

the Fourier space. The perturbation coming from interactions can be treated using the standard quantum field theory method [10, 20]. The other limit, which is what we are interested in and focus on in this thesis, is the *strong coupling limit* $t \ll U$. In this limit, the interaction term dominates and the ground state of the system is a *half-filled* system with a single electron per site. This ground state leaves the interaction term of the Hubbard model being zero. Any other state with additional number of electron (or hole) which violates the half-filling will have potential energy higher than the ground state at least on the scale of U. Thus the system is *gapped* [13, 21]. The kinetic term in this limit will serve as a perturbation. Using standard perturbation method we can obtain a second-order perturbation from the kinetic term

$$\mathcal{H}_2' = J \sum_{\langle ij \rangle} \boldsymbol{S}_i \cdot \boldsymbol{S}_j, \tag{1.8}$$

in which the coupling strength $J = \frac{4t^2}{U}$ and the spin operator is defined in Eq. 1.4. Eq. 1.8 is the Hamiltonian of an *antiferromagnet*, it is also known as the *Heisenberg spin Hamiltonian*. When the system is in the large coupling limit, the unperturbed ground state is half-filled with zero energy as stated above, in the case the only relevant term in the electronic Hamiltonian is the antiferromagnetic interaction Eq. 1.8.

In this way, we have found the usual spin interaction term in the most simple (and yet general) correlated electronic Hamiltonian Eq. 1.1. It can be either ferromagnetic, from the exchange term Eq. 1.3, or antiferromagnetic, from the on-site Hubbard term Eq. 1.8. In real materials, the electron Hamiltonian is usually much more complex and the corresponding spin interaction Hamiltonian can also take various forms. In this regard, in later chapters of the thesis, we will study various types of spin Hamiltonian, some of which has real material realizations. In the thesis, we shall focus on the antiferromagnetic spin Hamiltonians in which the spin coupling $J > 0$. Before we move on, it is useful to take a moment to emphasize the importance of the study of the spin Hamiltonian (Eq. 1.8) as the large coupling limit of the electronic systems. On one hand, the study of spin systems is important in real materials. In insulators where the system is gapped and in large coupling limit, spin interaction can be the dominant term in the Hamiltonian (while in metals where the systems are in the free-electron limit, the spin interactions can be less important) [8]. On the other hand, the study of spin

systems can be useful in other fields such as quantum computing [22, 23]

1.3 The study of spin systems

1.3.1 General methods for spin systems

To study the spin Hamiltonian Eq. 1.8, people have developed various approaches. In this section we first briefly summarize some of the methods used. The first method is the *spin path integral* [13, 24, 25, 26]. To define a spin path integral one should first define the spin coherent states. In a general spin-S system, the coherent state is labeled by a vector with unit length in the three-dimensional space, it satisfies $\boldsymbol{S}|\boldsymbol{n}\rangle = \boldsymbol{n}|\boldsymbol{n}\rangle$. With proper definition of the coherent states [13, 26], we can write the partition function as

$$Z = \mathrm{tr} e^{-\beta\mathcal{H}} = \int D\boldsymbol{n} \exp(iS\sum_i S_{WZ}[\boldsymbol{n}] - i\int_0^T dt \sum_{ij} JS^2 \boldsymbol{n}(i,t)\cdot\boldsymbol{n}(j,t)), \qquad (1.9)$$

in which the term S_{WZ} is the Wess-Zumino action, it has a clear geometric intepretation which is the area the vector $\boldsymbol{n}(i,t)$ swept on the unit sphere in each path in the path integral [13]. Using this partition function, one can work out the simpliest case, the one-dimensional quantum spin chain, in detail, the resulting Lagrangian is the following [13]

$$\mathcal{L}(\boldsymbol{n}) = \frac{1}{2g}(\frac{1}{v_s}(\partial_0\boldsymbol{n})^2 - v_s(\partial_1\boldsymbol{n})^2) + \frac{\theta}{8\pi}\epsilon_{\mu\nu}\boldsymbol{n}\cdot(\partial_\mu\boldsymbol{n}\times\partial_\nu\boldsymbol{n}). \qquad (1.10)$$

in which $\boldsymbol{n}$ is a unit vector and $g = \frac{2}{S}$, $v_s = 2a_0JS$ and $\theta = 2\pi S$. In the Lagrangian, the first term is usually refered to as *non-linear sigma model* and the second term is a *topological term*. Interesting analysis on the Lagrangian 1.10 and then on the one-dimensional spin model can be made based on the topological term and renormalization group [13], details of this study is beyond the scope of this thesis.

For the one-dimensional spin-$\frac{1}{2}$ Heisenberg chain, the exact solution can be obtained by the *Bethe ansatz* [13, 27]. On the other hand, there is another method that was developed to the study of one-dimensional spin chain and is more commonly used, that is the *Jordan-Wigner transformation* [13, 89, 90]. As will be discussed in detail in Chapter 3, the Jordan-Wigner transformation defines a non-local mapping between spin-$\frac{1}{2}$ operators and a complex fermion operator connecting to a half-infinite fermionic operator

creating a quantum kink. The definition of the Jordan-Wigner (JW) transformation is given by Eq. 3.32.

The spin path integral method, Bethe ansatz and JW transformation are generally useful for any quantum spin systems regardless of the actual spin ground states, there are other types of treatments designed for certain types of spin ground states. For an interacting spin system, the ground state is sometimes *ordered*. If so, according to the Landau's theory of phase transtition, there is expected to be a phase transition between the ordered state and the disordered states when temperature gets higher [9]. For an ordered spin ground state, it is sometimes useful to write the spin operators in terms of a bosonic operator using the Holstein-Primakoff transformation [12, 28]

$$\hat{S}_i^- = a_i^\dagger \sqrt{2S - a_i^\dagger a_i}, \qquad \hat{S}_i^+ = \sqrt{2S - a_i^\dagger a_i}\, a_i, \qquad \hat{S}_i^z = S - a_i^\dagger a_i. \tag{1.11}$$

This transformation holds for any spin S, the spin operators are denoted by $\hat{S}$ and a_i is the bosonic annihilation operator. This bosonic operator is actually representing the *spin-wave excitation* of an ordered spin ground state, it is also called *magnon*.

On the other hand, it is also possible that the spin ground state is not ordered, in other words, this type of spin ground state *does not break any symmetry* (especially the spin rotation symmetry). This kind of spin ground state is proposed and studied only recently and it is called the *quantum spin liquid* (QSL) states [29, 30, 31, 32, 33, 34, 35, 36, 22]. To study the quantum spin liquid states, there are many other methods developed [33]. In the next section, we are going to briefly review these methods and set a stage for the discussion for later sections.

1.3.2 Quantum spin liquid states and gauge theories for spin systems

As discussed above, the quantum spin liquid is a type of spin ground state in which no symmetry is broken. The possibility of such states in real model is usually ensured by *frustration*, either from the specific lattice structure or from competing spin interactions. For the first case, we can think about a model on a triangular lattice, spins located on the sites of the lattice interact with their nearest neighbours with antiferromagnetic Ising coupling (the Hamiltonian only involves $S_i^z S_j^z$ terms). For each triangle in the lattice, the interaction terms on the three bonds cannot be satisfied at the same time. In this

case, the ground state is not ordered on the z-direction, instead, it is a superposition state. For the second case, the lattice itself might not be frustrating but the spin Hamiltonian takes a special form such that the ground state cannot be ordered. Later in this thesis, we will discuss the Kitaev honeycomb model which falls into this category [23].

The quantum spin liquid states are interesting in general because it cannot be described by Landau's characterization of phases by explicit symmetry of states [9]. States of such kind are generally considered to possess *topological order* [13, 30, 37, 38, 39]. Moreover, quantum spin liquid states usually possess non-trivial *quantum entanglement* [30, 33]. Besides, there has been evidence showing that there is connection between the quantum spin liquid states and high-T_c superconductivity [40]. Although the quantum spin liquid states are interesting, the study of the properties of such states is challenging because of lack of order. In recent years some new methods have been developed to describe quantum spin liquid states, including the resonant-valence-bond (RVB) method [13, 29, 41, 42] and slave-particle approach [30, 38, 39, 40, 43, 44, 45, 46, 47, 48, 49, 50, 51, 52]. In this thesis, we will put considerable focus on the slave-particle approach, we shall see that the application of slave-particle approach usually maps the spin interaction into some (lattice) gauge theories. In order to lay the foundation for future chapters, here we will give a brief description of the slave-particle approach and the resulting gauge theories.

The first step of the slave-particle approach is to write the spin operators in terms of bosonic or fermionic particle operators (such artificial particles are usually called *spinon*). The most commonly used ones are the Abrikosov fermion representation (which will be discussed in detail in Chapter 2) and the Schwinger boson representation. When constructing such mapping between the spin operator and the particle operators, some *redundancy* is necessarily brought in. To see this let's take a brief look at the Abrikosov fermion represetation,

$$\boldsymbol{S}_i = \frac{1}{2} f^\dagger_{i\alpha} \boldsymbol{\sigma}_{\alpha\beta} f_{i\beta}, \tag{1.12}$$

in which the $f_{i\sigma}$ is the annihilation operator of the fermionic spinon. Although the representation 1.12 happens to take the same form as the second-quantization of spin operators in Eq. 1.4, the physical meanings of the spinon (denoted by f_i) and electron

operator (denoted by c_i) are different. We will emphasize this point again in Chapter 2. In order to make sure that the spin algebra is faithfully represented, we have to require that there is a single spinon on each spin site, this means $\sum_\alpha f_{i\alpha}^\dagger f_{i\alpha} = 1$. Notice that on the right-hand side of Eq. 1.12, if we rotate the phase of the fermionic spinon $f_i \to f_i e^{i\phi}$, the left-hand side, which is the spin operator, remains unchanged. This symmetry is local, meaning that the phases of the spinon operators on each site can be independently chosen such that the physical spin operators are unaffected. This $U(1)$ local symmetry is similar to the gauge symmetry of the standard quantum field theory [2, 3], therefore, we would call such symmetry a *gauge symmetry* that comes in the slave-particle approach of spin systems. In Chapter 2 we will discuss such gauge symmetry in detail and we will show that the full gauge group for this case is SU(2) instead of U(1). Importantly we should also note the limitation of such terminology, especially when comparing with the gauge symmetry in the Standard Model; they are not the same because while the former is brought in by hand with the particular spin representation, the gauge symmetry in standard model is chosen by *nature*. Nevertheless, as we will see in later chapters, the construction of the theory allows us to borrow the methods of the quantum gauge theory (especiall lattice gauge theory) to study the system of spinons.

One of the most significant difficulty of the slave-particle approach is that the resulting Hamiltonian after replacing spin operators using spin representations is usually quartic in spinons. Thus in most cases the analysis of the ground state and the excitation spectrum can be performed only at the mean-field level. Although this approach can be justified in some limits, its applicability to physical spin models is questionable in many cases. In some rare cases, exact solution of the QSL Hamiltonian is achievable. Such solutions not only give us a chance to study the QSL states thoroughly in the model itself, but also provide us with opportunities to compare the applicability of other approximate theoretical methods. Of particular interest in this regard is the Kitaev honeycomb model which describes a system of spin-1/2 on sites of a honeycomb lattice interacting via Ising-like nearest-neighbor exchange interactions [23]. This model is not only exactly solvable with a QSL ground state, but also realizable in materials [23, 53, 54]. In particular, recent years have seen much progress in identifying candidate materials for realizing the Kitaev QSL, such as the honeycomb iridates A_2IrO_3 [55, 56, 57, 58, 59], honeycomb ruthenium chloride $\alpha-RuCl_3$ [60, 61, 62], and another

5d Ir honeycomb compound $H_3LiIr_2O_6$ [63, 64, 65, 66, 67]. The exact solution of the Kitaev honeycomb model has been achieved by a slave-particle representation of spins using four Majorana fermions in an extended Hilbert space [23]. Using this representation, Kitaev demonstrated that the low-energy physics of the original spin model can be understood by studying a system of Majorana fermions coupled to a static Z_2 gauge field in the extended Hilbert space. From this, it is explicitly showed that the ground state of the model is a gapless Z_2 QSL, while the fractionalized excitations are gapless (or gapped) Majorana fermions and gapped Z_2 gauge fluxes [23].

The slave particle representation of spin used in the exact solution of the Kitaev model belongs to a special type of spin representations, the *Majorana representations*. Majorana fermions are real fermions that have the properties that they anticommute with each other and they are antiparticle of themselves (see Chapter 3 for details). The Majorana representation of spin has a long history. Besides Kitaev representation with four Majorana fermions [23], two other types of Majorana representation of spin are known. The first one was introduced in the 1970s [68, 69, 70, 71, 72, 73, 74, 75, 76]. This representation contains three Majorana fermions transforming under SO(3), thus we will call it *SO(3) Majorana representation*. As we will discuss in detail in Chapter 3, the SO(3) Majorana representation has a significant advantage over the Kitaev representation that no unphysical states is involved [72, 73]. Using this representation, various spin models have been studied on the mean-field level including one-dimensional spin chain [75] and two-dimensional triangular lattice [76, 77]. The second type of Majorana fermion representation was introduced by Chen *et al* in their study of QSL realized on a two-dimensional square lattice using projective symmetry group (PSG) method [78]. We will call it *SO(4) chiral Majorana representation* for the reasons that will become clear later. Previous works of the Majorana representations of spin ususally studied the spin models on the mean field level [76, 77]. Similar to other types of slave-particle representations, the Majorana representations have gauge redundancy, since they are real, the gauge group is Z_2.

1.4 Motivation and outline of the dissertation

As we discussed before, the study of quantum spin models (especiall quantum spin liquid states) using slave-particle approach usually results in some lattice gauge theories. This motivates me to explore more of the mapping between strong correlated electronic systems in condensed matter physics and lattice gauge theories that are usually discussed in particle physics. In this regard, I will start with a review of the application of the Abrikosov fermion representation to the spin liquid states, in particular I will show how the SU(2) gauge structure emerges in the mean-field treatment. Then I will move on to the Majorana representation. I will first discuss the three known types of Majorana representation in detail. In particular I will show that one way to connect these three Majorana representation in a coherent framework is by referring to the spinor representation of the SO(4) group [74]. I will then focus on the SO(3) Majorana represenation and show its advantage over the other two. Knowing its non-local nature, I will argue that the SO(3) Majorana representation is equivalent to the Jordan-Wigner transformation in both 1D and 2D [79]. Motivated by the Kitaev's exact solution of the Kitaev model using the Kitaev representation, I will discuss the application of the *SO(3) Majorana representation* in spin models. In this regard, I will discuss first the Kitaev model itself, then I will move on to two other spin models which do not possess exact solvability, namely the quantum XY model on honeycomb lattice and the 90° compass model on square lattice.

My application of the SO(3) Majorana representation in the three spin models all result in Z_2 lattice gauge theories. In particular, the Z_2 gauge theory for the Kitaev model takes the standard form which highlights its exact solvability. On the other hand, the Z_2 for the other two models are nontrivial and no exact physical argument can be made without making approximations to the Z_2 lattice gauge theory. In some sense, such application of SO(3) Majorana representation is unique from previous studies in that the resulting Z_2 lattice gauge theories are exact and no approximation is brought in to obtain them. The resulting Z_2 gauge theories can serve as a platform for further approximations.

For the next part, I will discuss some exotic spin representations that have been applied in spin models with special lattice geometry. One distinct example of this

kind is the *quantum spin ice* model [32]. The existing theory of the quantum spin ice model using non-local spin representation results in a U(1) lattice gauge theory [80, 81]. Beforing ending the thesis, I will briefly discuss this theory and propose another non-local spin representation that can potentially be applied to quantum spin ice model in 3D and Heisenberg model on kagome lattice in 2D.

To summarize, the rest of the dissertation is organized as follows. In Chapter 2 I will review the Abrikosov fermion slave-particle approach to spin models and explore the resulting SU(2) gauge structure on the mean-field level. In Chapter 3, I will move on to discuss the three types of Majorana representations and the relationship between them. In particular, I will focus on the SO(3) Majorana representation and discuss its equivalence with the Jordan-Wigner transformation. In Chapter 4 I will apply the SO(3) Majorana representation in three spin models, namely the Kitaev model, the quantum XY model on honeycomb lattice and the 90° compass model on square lattice. Using the SO(3) Majorana representation I will develop a method to map the original spin Hamiltonians to Z_2 lattice gauge theories. In Chapter 5, I will review the existing theory of quantum spin ice model which features a U(1) lattice gauge theory. I will then propose another type of non-local spin representaion and discuss its potential application in various spin models. The dissertation ends in Chapter 6 with a discussion on the results and an outlook for future studies.

Chapter 2

Slave particle approach: SU(2) gauge theory on the mean field level

2.1 Basics of the Abrikosov fermion spin representation

In this chapter, we are going to review and discuss the SU(2) slave particle approach to spin models [30, 40, 43, 44, 47, 49, 50, 51]. The model Hamiltonian we will study is the standard Heisenberg Hamiltonian.

$$\mathcal{H} = J \sum_{ij} \boldsymbol{S}_i \cdot \boldsymbol{S}_j, \tag{2.1}$$

in which $\boldsymbol{S}_i$ is the spin-$\frac{1}{2}$ operators and the spin-spin interaction is usually taken to be between nearest neighbours i and j. It is generally nontrivial to study this Heisenberg Hamiltonian in full detail. If we know that the system has ordered ground state, then the excitations are described by magnons, as described in Chapter 1. However, if it is possible that the ground state is not ordered, for example, a spin liquid state, then the magnon description will not work. As mentioned in Chapter 1, in this case one can use the slave particle approach. In this chapter we will be using fermionic slave particles

(i.e. fermionic spinons). To this end, one can write the spin operators as

$$\boldsymbol{S}_i = \frac{1}{2} f^\dagger_{i\alpha} \boldsymbol{\sigma}_{\alpha\beta} f_{i\beta}, \tag{2.2}$$

here we have introduced the fermionic spinon operator $f_{i\alpha}$ with spin $\alpha = \uparrow, \downarrow$, satisfying the standard fermionic anticommutation relation $\{f_{i\alpha}, f^\dagger_{j\beta}\} = \delta_{ij}\delta_{\alpha\beta}$ (other anticommutators vanish identically). This representation of spin Eq. 2.2 is also called *Abrikosov fermion representation* [81]. Note that the spinon is different from real electron in that the former is purely artificial particle operators, in this regard, the spinons do not have electric charge although the theory has a U(1) gauge symmetry (or in other words, we will never be interested in the electric charge of the spinon). To highlight the difference between the spinon and real electron, the spinon is denoted by f while the real electron is denoted by c (see Chapter 1).

For the representation 2.2 to produce the correct spin algebra, it can be shown that one additional condition is needed

$$f^\dagger_{i\uparrow} f_{i\uparrow} + f^\dagger_{i\downarrow} f_{i\downarrow} = 1. \tag{2.3}$$

If we use $n_{i\alpha} = f^\dagger_{i\alpha} f_{i\alpha}$ to denote the number of fermion of spin α, then the condition 2.3 means that only one spinon is occupying each site.

In order to apply the representation in the Heisenberg model, one simply have, using Eq. 2.2 and the spin identity 1.5 [30],

$$\boldsymbol{S}_i \cdot \boldsymbol{S}_j = \sum_{\alpha\beta} \left(-\frac{1}{4} f^\dagger_{i\alpha} f_{i\alpha} f^\dagger_{j\beta} f_{j\beta} - \frac{1}{2} f^\dagger_{i\alpha} f_{j\alpha} f^\dagger_{j\beta} f_{i\beta} \right). \tag{2.4}$$

That means that the Heisenberg model Hamiltonian can be written in terms of spinon fields as

$$\mathcal{H} = -J \sum_{ij} \boldsymbol{S}_i \cdot \boldsymbol{S}_j = J \sum_{ij} \sum_{\alpha\beta} \left(\frac{1}{4} f^\dagger_{i\alpha} f_{i\alpha} f^\dagger_{j\beta} f_{j\beta} + \frac{1}{2} f^\dagger_{i\alpha} f_{j\alpha} f^\dagger_{j\beta} f_{i\beta} \right). \tag{2.5}$$

One can easily notice that the Eq. 2.5 is a four-fermion interacting Hamiltonian, it is by no means simplier than the original interacting electron Hamiltonian Eq. 1.1. The only difference is that in this case the matter field is spinon instead of real electron. In some

sense, Eq. 2.5 is harder to solve because there is no small parameter to perform a perturbative study. The only possible way to proceed is to use a *mean-field approximation*, the theoretical foundation of which is the *Hubbard-Stratonovich transformation* of *path integral formalism of many-body physics* [12]. Here we should pause and give a brief summary of the path integral formalism of many-body physics to lay the foundation for future discussion.

To introduce the field theoretical description of many-body physics, we start with the standard correlated electron Hamiltonian Eq. 1.1 and the thermal partition function of the system is

$$\mathcal{Z} = \mathrm{tr} e^{-\beta(\mathcal{H}-\mu N)}, \tag{2.6}$$

in which μ is the chemical potential. From now on, we will take $\mu = 0$ for simplicity. In order to define the path integral, we introduce *coherent states*, these states are eigenstates of the particle creation and annihilation operators. For our case, we need the *fermionic coherent states* and the eigenvalues are *Grassmann numbers* (Grassmann numbers are numbers that are anticommuting with each other). With these we have for fermionic coherent states $|\xi\rangle$, $c_i|\xi\rangle = \xi_i|\xi\rangle$ and ξ is a Grassmann number. Specifically such states can be written as $|\xi\rangle = \exp(-\sum_i \xi_i c_i^\dagger))|0\rangle$. These coherent states are usefull to transform operators into fields. With the aid of coherent states, one can rewrite the trace in the partition function 2.6 in terms of a path integral [12]

$$\mathcal{Z} = \int D(\bar{\xi}, \xi) e^{-S[\bar{\xi},\xi]}, \tag{2.7}$$

in which the action

$$S[\bar{\xi}, \xi] = \int_0^\beta d\tau [\bar{\xi}\partial_\tau \xi + \mathcal{H}(\bar{\xi}, \xi)]. \tag{2.8}$$

In the action the field ξ and $\bar{\xi}$ take values in the Grassmann number space. To get the $\mathcal{H}(\bar{\xi}, \xi)$ one simply replaces the electron creation operator with field $\bar{\xi}$ and the annihilation operators with field ξ.

As the original second-quantized Hamiltonian 1.1, the action itself will contain interaction terms that are quartic in fermionic fields ξ, $\bar{\xi}$. To treat these quartic terms, one can apply a mathematic trick based on Gaussian integral, the *Hubbard-Stratonovich transformation* (HS transformation), in which we will introduce a new set of fields to

rewrite the path integral. Specifically, the quartic terms in ξ can always be decoupled in the following way $\bar{\xi}\bar{\xi}\xi\xi \to \hat{\rho}_m V_{mn}\hat{\rho}_n$, in which the $\hat{\rho}$ are bilinear in $\bar{\xi}$ and ξ and m and n are some labels of the bilinear. The following identity provides the foundation of the HS transformation:

$$\exp[-\hat{\rho}_m V_{mn}\hat{\rho}_n] = \int D\phi \exp[-\frac{1}{4}\phi_m V^{-1}_{mn}\phi_n - i\phi_m\hat{\rho}_m]. \tag{2.9}$$

This identity can be easily proved by Gaussian integral in various forms. Using the identity 2.9, one transforms a term quartic in the matter fields into a path integral of a new field ϕ, the effective action of the new auxiliary field contains quadratic terms in ϕ and interaction terms $\phi\xi\xi$ etc. In this way we can effectively get rid of the quartic terms in the original action 2.8. In reality, the newly introduced field ϕ can be chosen in various ways depending on how we define the bilinear field $\hat{\rho}$, different choice is sometimes called different *channels*.

The final form of the path integral after the HS transformation reads

$$\int D\phi D(\bar{\xi},\xi)\exp[-S_{\text{eff}}[\phi,\bar{\xi},\xi]]. \tag{2.10}$$

From this one can obtain the effective Hamiltonian from the effective action $S_{\text{eff}}[\phi,\bar{\xi},\xi]$, which reads $\mathcal{H}_{\text{eff}}[\phi,\bar{\xi},\xi]$. Under certain circumstancies, one can then make the assumption that the quantum fluctuations of the auxiliary field ϕ are small, in this case one can replace the field ϕ by its average value $\langle\phi\rangle$, then the new effective Hamiltonian $\mathcal{H}_{\text{eff}}[\langle\phi\rangle,\bar{\xi},\xi]$ is called the *mean-field Hamiltonian* because the average value of the field ϕ has the physical meaning of the "mean-field" of the bilinear field $\hat{\rho}$ [12]. The mean-field Hamiltonian typically does not contain fermionic quartic terms and can be solved easily. To make sure that the mean-field Hamiltonian captures that essential physics of the original model, in which the auxiliary field ϕ is always fluctuating, we have to make sure that the fluctuation is "relatively small". One key criteria for this is that the actual average of the auxiliary field cannot be zero.

We have briefly discussed the mean-field approach and the HS transformation, we are now ready to move back to the spinon quartic Hamiltonian 2.5 and discuss the gauge structure emerging from its mean-field treatment.

2.2 Mean-field theory and SU(2) gauge structure

Now we turn to study the spin Hamiltonian Eq. 2.5 on the mean-field level following Refs. [30, 40]. First we remind ourself that the Abrikosov fermion representation 2.2 only works under the condition that there is one fermion per site. To be precise, the constraint is that

$$f_{i\alpha}^{\dagger} f_{i\alpha} = 1, \qquad f_{i\alpha} f_{i\beta} \epsilon_{\alpha\beta} = 0, \tag{2.11}$$

in which the $\epsilon_{\alpha\beta}$ is nonvanishing only when $\alpha \neq \beta$. The second constraint is actually equivalent to the first constraint in 2.11.

To apply mean-field theory, as discussed in the previous section, the key step is to choose the auxiliary fields that are expected to have non-vanishing expectation values for the ground states. In general there are various choices of such auxiliary fields in terms of fermion bilinears in the Hamiltonian 2.5 [51]. Different choices of the auxiliary field correspond to the assumption that the ground state has different types of *orders*. Here, following Ref [30] we choose the following auxiliary fields

$$\begin{aligned} \eta_{ij}\epsilon_{\alpha\beta} &= -2\langle f_{i\alpha} f_{j\beta}\rangle, \qquad \eta_{ij} = \eta_{ji}, \\ \chi_{ij}\delta_{\alpha\beta} &= 2\langle f_{i\alpha}^{\dagger} f_{j\beta}\rangle, \qquad \chi_{ij} = \chi_{ji}^{\dagger}. \end{aligned} \tag{2.12}$$

Applying only these two types of auxiliary fields in the Hamiltonian assumes at the same time that $\langle f_{i\alpha} f_{j\alpha}\rangle = 0$ and $\langle f_{i\alpha}^{\dagger} f_{j\beta}\rangle = 0$ for $\alpha \neq \beta$ and so on. On the other hand, to impose the constraints 2.11, one has to introduce some *Lagrange multiplier* in the path integral formalism. To this end, we will denote the Lagrange multiplier fields by a_i^{μ}, in which $\mu = 1, 2, 3$. Integrating out the multiplier fields will automatically impose the certain constraints in the path integral. Using the definition of auxiliary fields 2.12 to decouple the quartic fermionic terms in 2.5, including the multiplier, we can read off the effective Hamiltonian from the path integral

$$\begin{aligned} \mathcal{H}_{\text{eff}} = &\sum_{ij} -\frac{3}{8} J[(\chi_{ij} f_{i\alpha}^{\dagger} f_{j\alpha} + \eta_{ij} f_{i\alpha}^{\dagger} f_{j\beta}^{\dagger}\epsilon_{\alpha\beta} + \text{H.c.} - |\chi_{ij}|^2 - |\eta_{ij}|^2)] \\ &+ \sum_i \{a_i^3 (f_{i\alpha}^{\dagger} f_{i\alpha} - 1) + [(a_i^1 + i a_i^2) f_{i\alpha} f_{i\beta}\epsilon_{\alpha\beta} + \text{H.c.}]\}, \end{aligned} \tag{2.13}$$

in which the summation over repeated spin indices is assumed. In the effective Hamiltonian 2.13, the fields χ_{ij}, η_{ij} and a_i^μ are all fluctuating, meaning that they are to be integrated in the path integral formalism. Under such assumption, the effective theory is still *exact*.

The approximation is brought in when we neglect the fluctuation of the auxiliary fields and assume that χ_{ij}, η_{ij} and a_i^μ are nonvanishing constants. Such treatment corresponds to taking the mean-field. For the mean-field treatment to make sense, one need to proceed according to the following procedures. First, pick up a choice of the mean-fields values for χ_{ij}, η_{ij} and a_i^μ, then solve the effective Hamiltonian 2.13 and find its ground states. Second, check if the ground state satisfies the *self-consistent* equations (or the definition of the auxiliary fields) Eq. 2.12, and check if the ground states satisfies the constraint on the mean-field level, namely

$$\langle f_{i\alpha}^\dagger f_{i\alpha}\rangle = 1, \qquad \langle f_{i\alpha} f_{i\beta}\epsilon_{\alpha\beta}\rangle = 0. \tag{2.14}$$

Third, if the checking of the second step is satisfied, then the mean-field solution is *good*, otherwise, one should change the mean-field values and repeat the first and second steps.

The effective Hamiltonian 2.13 and the constraints 2.11 has SU(2) local symmetry [82, 83]. To see this, we can rewrite the Hamiltonian with the definition of a fermionic doublet

$$\psi = \begin{pmatrix} \psi_1 \\ \psi_2 \end{pmatrix} = \begin{pmatrix} f_\uparrow \\ f_\downarrow^\dagger \end{pmatrix}, \tag{2.15}$$

and the auxiliary fields grouped into a matrix

$$U_{ij} = \begin{pmatrix} \chi_{ij}^\dagger & \eta_{ij} \\ \eta_{ij}^\dagger & -\chi_{ij} \end{pmatrix} = U_{ji}^\dagger. \tag{2.16}$$

Then the effective Hamiltonian can be written as

$$\mathcal{H}_{\text{eff}} = \sum_{ij} \frac{3}{8} J \left[\frac{1}{2} \text{tr}(U_{ij}^\dagger U_{ij}) - (\psi_i^\dagger U_{ij} \psi_j + \text{H.c.}) \right] + \sum_i a_i^\mu \psi_i^\dagger \sigma^\mu \psi_i, \tag{2.17}$$

in which $\mu = 1, 2, 3$ and the σ^μ are the three Pauli matrices. On the mean-field level, the U_{ij} matrices are assumed to be constants and the constraint 2.11 on the mean-field

level is written as

$$\langle \psi_i^\dagger \sigma^\mu \psi_i \rangle = 0. \tag{2.18}$$

The Hamiltonian 2.17 and the constraints 2.18 have a local SU(2) symmetry, both of these are invariant under local transformation

$$\psi_i \to W_i \psi_i, \qquad U_{ij} \to W_i U_{ij} W_j^\dagger, \tag{2.19}$$

in which W_i is a SU(2) matrix depending on the sites i. The existance of such SU(2) local symmetry alters the definition of the mean-field treatment described above. To understand this better, let us examine the physical meaning of the mean-field states.

As discussed before, each *good* mean-field state corresponds to a certain choice of the matrix U_{ij} and parameters a_i^μ. The mean-field states satisfy the constraints 2.18 on the mean-field level. However, such mean-field states, although self-consistent with the Hamiltonian and constraints, are not *physical states* of the *original Hamiltonian*. For a physical states, the constraints of a single fermion occupation 2.11 must be satisfied rigorously. To get from the mean-field states $|\psi_{\text{mean}}\rangle$ to physical states $|\psi_{\text{phys}}\rangle$, a *projection* is needed [30],

$$|\psi_{\text{phys}}\rangle = \hat{\mathcal{P}} |\psi_{\text{mean}}\rangle. \tag{2.20}$$

With the definition of the projection, one can understand the physical meaning of the SU(2) local symmetry, that is the transformed parameters U_{ij} correspond to the same physical state after the projection as the untransformed ones. More precisely, we have

$$|\psi_{\text{phys}}\rangle = \hat{\mathcal{P}} |\psi_{\text{mean}}^{(U_{ij})}\rangle = \hat{\mathcal{P}} |\psi_{\text{mean}}^{(W_i U_{ij} W_j^\dagger)}\rangle. \tag{2.21}$$

This implies that the local SU(2) symmetry is *unphysical* and is only a local *redundancy* of the theory. In light of this, we will refer to this symmetry as the *SU(2) gauge symmetry* of the Hamiltonian 2.17 and constraints 2.18.

To gain a full description of the spin systems, the mean-field ground states alone are clearly not enough. We should also include the fluctuation of the parameters U_{ij} and a_i^μ, it is sometimes reasonable to assume that such fluctuation is small. Therefore, the full spectrum of the spin model 2.5 under the mean-field treatment is the fermion spinon ψ and the (small) fluctuations of the parameters U_{ij} and a_i^μ. Because of the SU(2) gauge

symmetry however, certain fluctuations of U_{ij} are not physical, for example, multiplied by a SU(2) matrix which is close to the identity. Because the U_{ij} can in general be any matrix, it is quite challenging to study the general case in detail. On the contrary, sometimes one needs to make assumptions to fix the structure of U_{ij} to facilitate the discussion. Such assumptions of the U_{ij} are generally called *mean-field ansatz*.

Under some circumstances, the U_{ij} matrix can be written as [40]

$$U_{ij} = \bar{U}_{ij} e^{i a_{ij}^{\mu} \sigma^{\mu}}, \tag{2.22}$$

in which $\bar{U}_{ij}$ is a constant matrix. If $\bar{U}_{ij}$ commutes with all the SU(2) matrices, then we can separate phase fluctuations in the SU(2) manifold $e^{i a_{ij}^{\mu} \sigma^{\mu}}$ from the matrix U_{ij}. Replacing the U_{ij} with the constant $\bar{U}_{ij}$, the SU(2) gauge symmetry is then captured by the field a_{ij}^{μ}. In this case, the mean-field spectrum contains fermionic spinon ψ, SU(2) gauge fluctuation a_{ij}^{μ} and multiplier a_i^{μ}. With such construction, we have mapped the Heisenberg spin Hamiltonian Eq. 2.1 into a SU(2) gauge theory of spinon coupled to gauge fluctuations.

Before moving on, we will mention a few mean-field ansaetze for $\bar{U}_{ij}$ following Ref [40] for Heisenberg spin models on the *two-dimensional square lattice*.
(i) the "π-flux state"

$$\bar{U}_{\boldsymbol{i},\boldsymbol{i}+\boldsymbol{x}} = -i(-1)^{i_y}\chi, \qquad \bar{U}_{\boldsymbol{i},\boldsymbol{i}+\boldsymbol{y}} = -i\chi. \tag{2.23}$$

(ii) the "staggered flux state"

$$\bar{U}_{\boldsymbol{i},\boldsymbol{i}+\boldsymbol{x}} = -\sigma^3\chi - i(-1)^{i_x+i_y}\Delta, \qquad \bar{U}_{\boldsymbol{i},\boldsymbol{i}+\boldsymbol{y}} = -\sigma^3\chi + i(-1)^{i_x+i_y}\Delta. \tag{2.24}$$

(iii) the "Z_2 gapped state"

$$\begin{aligned} &\bar{U}_{\boldsymbol{i},\boldsymbol{i}+\boldsymbol{x}} = \bar{U}_{\boldsymbol{i},\boldsymbol{i}+\boldsymbol{y}} = -\chi\sigma^3, \qquad \bar{U}_{\boldsymbol{i},\boldsymbol{i}+\boldsymbol{x}+\boldsymbol{y}} = \eta\sigma^1 + \lambda\sigma^2, \\ &\bar{U}_{\boldsymbol{i},\boldsymbol{i}-\boldsymbol{x}+\boldsymbol{y}} = \eta\sigma^1 - \lambda\sigma^2, \qquad a_i^{2,3} = 0, \qquad a_i^1 \neq 0. \end{aligned} \tag{2.25}$$

In all these definitions, the i_x, i_y are the position coordinates of the site if we put the lattice on a grid and $\chi, \Delta, \eta, \lambda$ are all constant parameters.

So far we have briefly reviewed the mean-field treatment of the Heisenberg spin

model using the slave-particle approach (or Abrikosov fermion representation) and discussed the origin of the SU(2) gauge structure of the mean-field theory. Before ending this chapter, we will discuss briefly the generalization of the Abrikosov fermion representation in various forms.

2.3 Generalization and discussion

There are a few possible generalizations of the Abrikosov fermion representation discussed in the previous chapter. In this section, we briefly mention two generalizations without going into details. And then we will give a discussion on the SU(2) slave particle approach and the mean-field treatment.

Firstly it has been shown that the spinon doublet and the SU(2) gauge structure can be developed in a more compact form. To this end, we follow Ref [78] and define a 2×2 matrix in terms of spinon fields

$$F_i = \begin{pmatrix} f_{i\uparrow} & f_{i\downarrow}^\dagger \\ f_{i\downarrow} & -f_{i\uparrow}^\dagger \end{pmatrix}. \tag{2.26}$$

The matrix F_i has the following properties. The left multiplication of a SU(2) matrix on F_i is spin rotations (in terms of the spinon field f_i) and the right multiplication of a SU(2) matrix on F_i corresponds to the SU(2) gauge transformation described above. In terms of this new object, the spin operator can be written as

$$\boldsymbol{S}_i = -\frac{1}{4}\mathrm{tr}(\boldsymbol{\sigma} F_i F_i^\dagger). \tag{2.27}$$

As described above, the spin operator is invariant under gauge transformation $F_i \to F_i U_i$ in which U_i is a SU(2) matrix. One can define another object

$$\boldsymbol{G}_i = \frac{1}{4}\mathrm{tr}(F_i \boldsymbol{\sigma} F_i^\dagger). \tag{2.28}$$

In terms of $\boldsymbol{G}_i$ the single fermion occupation constraint 2.11 can be expressed as

$$\boldsymbol{G}_i = 0. \tag{2.29}$$

One can then construct the mean-field Hamiltonian using the new objects $\boldsymbol{S}_i$ and $\boldsymbol{G}_i$, keeping in mind that these two objects exaust all kinds of fermionic bilinears on a single site [78].

Another generalization of the Abrikosov fermion representation is to generalize to the case in which vacant site and double-occupation are allowed. This case is relevant in the doped materials (for example, high-T_c superconductors) [40]. In this kind of materials, the interaction of electrons is not just the spin-spin interaction but more complex. For a single site, there are four possible states, which are vacant state, a single electron state with spin up or down and a double occupation state with two electrons. To represent these states properly, we use the most general *slave-boson representation* to write a single electron operator in the following way [40, 84]

$$c_{i\sigma}^{\dagger} = f_{i\sigma}^{\dagger} b_i + \epsilon_{\sigma\sigma'} f_{i\sigma'} d_i^{\dagger}, \tag{2.30}$$

in which $\epsilon_{\uparrow\downarrow} = -\epsilon_{\downarrow\uparrow} = 1$. In the slave-boson representation 2.30 the $c_{i\sigma}$ is the electron operator, the $f_{i\sigma}$ is the spinon operator described in previous sections, bosonic b_i operator annihilates the vacant state in which there is no spinon, and bosonic d_i operator annihilates the double-occupation state. The representation 2.30 can reproduce all the commutation of the electron operator with the following constraint

$$f_{i\uparrow}^{\dagger} f_{i\uparrow} + f_{i\downarrow}^{\dagger} f_{i\downarrow} + b_i^{\dagger} b_i + d_i^{\dagger} d_i = 1. \tag{2.31}$$

The physical meaning of the constraint follows from the definition of these slave-particle operators. From the general representation 2.30 we can see the difference between electron operator and the spinon operator clearly. If the onsite interaction is strong such that double occupation states are prohibited, then the representation 2.30 can be simplified as $c_{i\sigma}^{\dagger} = f_{i\sigma}^{\dagger} b_i$ [40]. If further more vacant states are also prohibited, then we have $c_{i\sigma}^{\dagger} \to f_{i\sigma}^{\dagger}$. This is the case in which the Hamiltonian is purely spin-spin interaction and the Abrikosov fermion representation 2.2 coincides with the second-quantized spin operator in terms of electron operators Eq. 1.4.

Before closing this chapter, let us summarize what we have discussed for the mean-field approach of the slave-particle approach. To study the general Heisenberg model on lattices, one starts with the slave-particle representation (in this chapter, we have

focused on the Abrikosov fermion representation) to write spin operators in terms of bilinears of fermionic operators called spinons, in this process, some constraints (such as single occupation) must be imposed to reproduce the spin algebra. The Heisenberg Hamiltonian is then transformed into terms quartic in fermion operators. To handle such quartic terms, one apply the HS transformation and introduce auxiliary fields, whose physical meaning is the average of fermionic bilinears. After the HS transformation, one finds that the effective Hamiltonian with the spinon and auxiliary fields have some gauge symmetry, in our case with the Abrikosov fermion, the gauge group is SU(2). The next step is to have some assumptions about the fluctuation of the auxiliary fields, the mean-field approach. Under such mean-field assumptions, the effective Hamiltonian now becomes a gauge theory with spinons coupling to SU(2) gauge fields.

The origin of the gauge symmetry is rooted in the redundancy of the representation itself. The SU(2) mean-field gauge theory itself has a few limitations that are needed to be taken care of. First, it is generally a difficult task to determine the proper choice of auxiliary fields in various cases; second, the assumptions of the mean-field theory about the smallness of the fluctuations are usually questionable; third, it is not an easy task to handle a non-abelian SU(2) gauge theory in general. These considerations motive people to find different routes to study spin systems. In the following chapters, I will discuss an alternate way to treat spin systems by using the Majorana representations. Although still a slave particle approach, the gauge redundancy of Majorana representation is only Z_2. I will also discuss methods to map various spin models in 2D to Z_2 lattice gauge theories without using the mean-field methods.

Chapter 3

Majorana representations of spin

Having discussed the application of the Abrikosov fermion representation to spin models, we now move on to another type of spin representation, the Majorana representation. In this chapter, we will first give a detailed description of the three types of Majorana representations of spin and discuss the relationship between them using the spinor representation of the SO(4) group. Then we will focus on the properties of the SO(3) Majorana representation. Due to its non-local nature, we will show that it is equivalent to the Jordan-Wigner transformation in both one dimensional and two dimensional space. This discussion will help to clarify the properties of the Majorana representations of spin, in particular, the SO(3) Majorana representation. Understanding such properties will lay foundation for the application of the SO(3) Majorana representation in spin models, which will be discussed in the next chapter.

3.1 Three types of Majorana representations

The three types of Majorana representations of spin-1/2 degrees of freedom fall into two categories: the SO(3) Majorana representation uses three Majorana fermions to represent a single spin operator while the Kitaev representation and the SO(4) chiral Majorana representation use four Majorana fermions to represent a single spin operator. As a basic criteria the representation needs to satisfy the spin-1/2 algebra, namely,

$$\sigma^{\alpha}\sigma^{\beta} = \delta^{\alpha\beta} + i\epsilon^{\alpha\beta\gamma}\sigma^{\gamma}, \qquad \alpha, \beta, \gamma = x, y, z. \tag{3.1}$$

Below we discuss the details of the three types of representations starting with the SO(3) Majorana representation.

3.1.1 SO(3) Majorana representation

In order to introduce the SO(3) Majorana representation, we first define three Majorana fermions η_i^α, $\alpha = x, y, z$ for each spin σ_i^α (throughout this section, we use i and j to label the position of the spin and Majorana fermion). They satisfy the following anti-commutation relations,

$$\{\eta_i^\alpha, \eta_j^\beta\} = 2\delta_{ij}\delta^{\alpha\beta}. \tag{3.2}$$

The SO(3) Majorana representation of spin is given by [68, 69, 70, 71, 72, 73, 74, 75, 76]

$$\sigma_i^x = -i\eta_i^y\eta_i^z, \qquad \sigma_i^y = -i\eta_i^z\eta_i^x, \qquad \sigma_i^z = -i\eta_i^x\eta_i^y. \tag{3.3}$$

The three Majorana fermions η_i^x, η_i^y and η_i^z form the fundamental representation of group SO(3), corresponding to the SU(2) rotation of spin. We can define a SO(3) singlet operator γ_i using the Majorana fermion operators [72, 73, 74, 76],

$$\gamma_i = -i\eta_i^x\eta_i^y\eta_i^z. \tag{3.4}$$

The SO(3) singlet operator commutes with Majorana fermions on the same site $[\gamma_i, \eta_i^\alpha] = 0$, and it anticommutes with Majorana fermions on different sites $\{\gamma_i, \eta_j^\alpha\} = 0$, with $i \neq j$. Therefore it commutes with all spin operators, $[\gamma_i, \sigma_j^\alpha] \equiv 0$, no matter if $i = j$ or $i \neq j$. Furthermore, it follows that the γ_i operator is a constant of motion because it commutes with all kinds of spin Hamiltonian [72, 73, 74, 76].

In terms of the SO(3) singlet we have another form of SO(3) Majorana representation (3.3)

$$\sigma_i^x = \gamma_i\eta_i^x, \qquad \sigma_i^y = \gamma_i\eta_i^y, \qquad \sigma_i^z = \gamma_i\eta_i^z. \tag{3.5}$$

From this expression, we can easily see the SO(3) structure; also this form has certain advantages since γ operators are constants of motion.

For the next step, we pair up Majorana fermions η^x and η^y and define complex

fermion

$$c_i^\dagger = \frac{1}{2}(\eta_i^x + i\eta_i^y), \qquad c_i = \frac{1}{2}(\eta_i^x - i\eta_i^y). \tag{3.6}$$

In terms of these complex fermions we have the spin raising and lowering operators

$$\sigma_i^+ = \frac{1}{2}(\sigma_i^x + i\sigma_i^y) = \eta_i^z c_i^\dagger, \quad \sigma_i^- = \frac{1}{2}(\sigma_i^x - i\sigma_i^y) = c_i \eta_i^z. \tag{3.7}$$

And there is another form with the SO(3) singlet,

$$\sigma_i^+ = \frac{1}{2}\gamma_i(\eta_i^x + i\eta_i^y) = \gamma_i c_i^\dagger, \quad \sigma_i^- = \frac{1}{2}\gamma_i(\eta_i^x - i\eta_i^y) = \gamma_i c_i. \tag{3.8}$$

On the other hand, in terms of complex fermion (3.6), the z component of the spin operators is written as

$$\sigma_i^z = 2c_i^\dagger c_i - 1 = 2n_i - 1. \tag{3.9}$$

Here and hereafter in this thesis, we use $n_i = c_i^\dagger c_i$ to label the number of complex fermions. With the complex fermion, we can find a useful relation between γ operator and the η^z operators,

$$\gamma_i = \sigma_i^z \eta_i^z = (2n_i - 1)\eta_i^z = -(-1)^{n_i}\eta_i^z, \tag{3.10}$$

in which we have used the fact that $(-1)^{n_i} = (1 - 2n_i)$ for the fermion number n_i can only take two values 0 and 1.

At this stage it is important to analyze the Hilbert space of the Majorana fermions introduced to represent the spin space. Suppose we have N spins in our spin model, then the original spin Hilbert space has dimension 2^N. We introduce 3 Majorana fermions to represent each spin, each Majorana fermion has Hilbert space dimension $\sqrt{2}$ [76], thus the dimension of the Hilbert space of the Majorana fermions is $2^{\frac{3N}{2}}$. The dimension of the Majorana fermion Hilbert space is $2^{\frac{N}{2}}$ larger than the spin Hilbert space [74, 76].

In Ref. [74] and Ref. [76] it was shown that one way to eliminate the additional dimension is to pair up the N spin sites, forming $\frac{N}{2}$ pairs. For each pair $\langle ij \rangle$ we take the operator $\gamma_i \gamma_j$ and fix its value to be $+i$ (or equivalently $-i$). Since these operators commute with each other and they all commute with the Hamiltonian, their eigenvalues are good quantum numbers and fixing them eliminates the extra $2^{\frac{N}{2}}$ dimensions. To see

this we note that the $\gamma_i\gamma_j$ operators for all the pairs are Z_2 variables whose eigenvalue can only take $\pm i$, and that the total number of constraints we apply is $\frac{N}{2}$. In Sec. 3.3.1 we will compare the SO(3) Majorana representation and the one-dimensional (1D) Jordan-Wigner transformation. From this we will see another way to eliminate the extra degrees of freedom in the Hilbert space. We will also discuss the origin of a Z_2 redundancy that always appears when we apply the SO(3) Majorana representation with $\frac{N}{2}$ constraints like these.

With these definitions at hand, one can start looking at spin Hamiltonians. Here, for the convenience of the discussion in later sections, we use the SO(3) Majorana representation to transform the Hamiltonian of the XXZ Heisenberg model, namely,

$$\mathcal{H}_{XXZ} = \sum_{ij} J_z \sigma_i^z \sigma_j^z + J_\pm(\sigma_i^+\sigma_j^- + h.c.). \tag{3.11}$$

First, using (3.9), we have the J_z term

$$J_z\sigma_i^z\sigma_j^z = J_z(2n_i - 1)(2n_j - 1), \tag{3.12}$$

which is a fermion density-density interaction. The XY part of the Hamiltonian is what we will focus on. With (3.7) and (3.8) we can rewrite the bilinear spin interaction terms of the XY Hamiltonian as the following

$$\sigma_i^+\sigma_j^- + \sigma_i^-\sigma_j^+ = \eta_i^z\eta_j^z(c_ic_j^\dagger + c_i^\dagger c_j), \tag{3.13}$$

and in terms of γ operators we have

$$\sigma_i^+\sigma_j^- + \sigma_i^-\sigma_j^+ = -(\gamma_i\gamma_j)(c_i^\dagger c_j + c_ic_j^\dagger). \tag{3.14}$$

Therefore we see that under the SO(3) Majorana representation, the XY Hamiltonian is transformed into a hopping of complex fermions (defined in Eq. (3.6)) coupled to link variables defined in terms of Majorana fermion η^z or the SO(3) singlet operator γ. With these results, we move on to discuss the relationship between the SO(3) Majorana representation and the Jordan-Wigner transformation in one and two dimensions.

3.1.2 Kitaev representation

To introduce the Kitaev representation [23] we first introduce four Majorana fermions for each spin operator. For the purpose of clearness, we follow the notation of the previous section and write them as $\eta_i^t, \eta_i^x, \eta_i^y, \eta_i^z$. The four Majorana fermions transform in the fundamental representation of SO(4) and they satisfy the *Clifford algebra* (from now on we use μ, ν to label index t, x, y, z)

$$\{\eta_i^\mu, \eta_j^\nu\} = 2\delta^{\mu\nu}\delta_{ij}, \qquad \mu, \nu = t, x, y, z. \tag{3.15}$$

In the Kitaev representation [23], the spin operator is given by a product of two Majorana fermions as

$$\sigma_i^\alpha = i\eta_i^t\eta_i^\alpha \qquad \alpha = x, y, z. \tag{3.16}$$

Note that comparing with Kitaev's original definition of the four Majorana fermions, we have the following equivalence $c_i \equiv \eta_i^t$, $b_i^x \equiv \eta_i^x$, $b_i^y \equiv \eta_i^y$, and $b_i^z \equiv \eta_i^z$. This Majorana representation of spins is overcomplete. In particular, the dimension of the Hilbert space of the Majorana fermions is 4 for each site, while this dimension is only 2 for the physical spin space. This means that the Majorana Hilbert space contains both physical and unphysical states. Thus it is necessary to project out the unphysical part in order to get the relevant physical information. It was proved by Kitaev [23] that the representation (3.16) satisfies the spin relation (3.1) under the constraint that

$$D_i = \eta_i^t\eta_i^x\eta_i^y\eta_i^z = 1 \qquad \text{for every physical state.} \tag{3.17}$$

To enforce the constraint (3.17) we define *chirality projection operator* as

$$P_{i,L} = \frac{1 + D_i}{2}, \tag{3.18}$$

for which the meaning of the subscript index "L" will become clear shortly. The physical states can now be written as $\prod_i P_{i,L}|\psi\rangle$, where $|\psi\rangle$ is a state in the extended Hilbert space of Majorana fermions. This procedure leads us to the definition of the third type of Majorana representation [78].

3.1.3 SO(4) chiral Majorana representation

Combining the Kitaev representation (3.16) and the chirality projector (3.18), we obtain another type of Majorana representation of spin,

$$\sigma_i^\alpha = P_{i,L}(i\eta_i^t\eta_i^\alpha) = \frac{i}{2}(\eta_i^t\eta_i^\alpha - \frac{1}{2}\epsilon^{\alpha\beta\gamma}\eta_i^\beta\eta_i^\gamma), \tag{3.19}$$

where $\alpha, \beta, \gamma = x, y, z$. Written out explicitly, Eq. (3.19) reads

$$\begin{aligned}
\sigma_i^x &= \frac{i}{2}(\eta_i^t\eta_i^x - \eta_i^y\eta_i^z), \\
\sigma_i^y &= \frac{i}{2}(\eta_i^t\eta_i^y - \eta_i^z\eta_i^x), \\
\sigma_i^z &= \frac{i}{2}(\eta_i^t\eta_i^z - \eta_i^x\eta_i^y).
\end{aligned} \tag{3.20}$$

It can be shown that this representation satisfies the spin relation (3.1) with the constraint (3.17). We will call this representation (3.19) the SO(4) chiral Majorana representation.

The spin operator defined in the SO(4) chiral representation (3.19) satisfies $[\sigma_i^\alpha, P_{i,L}] = 0$, which means that the projection onto the physical space has to be done only once, any spin terms acts on a physical state will give a physical state. However, to achieve this, we end up with a representation (3.20) much more complex than the simple Kitaev representation (3.16). Moreover, we note that in Ref.[78] the SO(4) chiral Majorana representation was introduced in a different way, there, the representation (3.20) was obtained as a complementary to the complex fermion representation using the Projective Symmetry Group (PSG) method [78]. Although the SO(4) chiral Majorana representation can be seen as a direct generalization of the Kitaev representation, we will treat it as another type of Majorana representation. To see the reason, we move on to discuss the Hilbert space of the four Majorana fermions defined in both Kitaev representation and SO(4) chiral Majorana representation. From that, we shall see that the SO(4) chiral Majorana representation has a direct correposdence to the familiar complex fermion representation and thus can be seen as a bridge connecting the Kitaev representation and the complex fermion representation [78].

Using representation (3.20), we have the spin raising and lowering operators

$$\begin{aligned}\sigma^+ &= \frac{1}{4}(\eta^z + i\eta^t)(\eta^x + i\eta^y),\\ \sigma^- &= \frac{1}{4}(\eta^x - i\eta^y)(\eta^z - i\eta^t).\end{aligned} \tag{3.21}$$

This invites us to define two complex fermions $f = \frac{1}{2}(\eta^z - i\eta^t), f^\dagger = \frac{1}{2}(\eta^z + i\eta^t)$ and $g = \frac{1}{2}(\eta^x - i\eta^y), g^\dagger = \frac{1}{2}(\eta^x + i\eta^y)$. For reasons which will become clear later, we may just label $f = f_\uparrow$ and $g = f_\downarrow^\dagger$, then we have the following relations

$$\begin{aligned}f_\uparrow &= \frac{1}{2}(\eta^z - i\eta^t),\ f_\uparrow^\dagger = \frac{1}{2}(\eta^z + i\eta^t),\\ f_\downarrow &= \frac{1}{2}(\eta^x + i\eta^y),\ f_\downarrow^\dagger = \frac{1}{2}(\eta^x - i\eta^y).\end{aligned} \tag{3.22}$$

Conversely, the Majorana fermions can be expressed in terms of these complex fermions as [78]

$$\begin{aligned}\eta^t &= i(f_\uparrow - f_\uparrow^\dagger),\\ \eta^x &= f_\downarrow + f_\downarrow^\dagger,\\ \eta^y &= i(f_\downarrow^\dagger - f_\downarrow),\\ \eta^z &= f_\uparrow + f_\uparrow^\dagger.\end{aligned} \tag{3.23}$$

Using (3.23), we can transform the spin raising and lowering operators expressed under the SO(4) chiral Majorana representation (3.21) into

$$\begin{aligned}\sigma^+ &= f_\uparrow^\dagger f_\downarrow,\ \sigma^- = f_\downarrow^\dagger f_\uparrow,\\ \sigma^z &= f_\uparrow^\dagger f_\uparrow - f_\downarrow^\dagger f_\downarrow.\end{aligned} \tag{3.24}$$

Eq.(3.24) shows that we have recovered the familiar complex fermion slave particle representation $\sigma^\alpha = f_\beta^\dagger(\tilde{\sigma}^\alpha)_{\beta\gamma} f_\gamma$, with $\tilde{\sigma}$ being the Pauli matrices and f_α being the complex slave particles called spinons. From (3.23) we have the relation $\eta^t\eta^x\eta^y\eta^z = -(1-2n_\uparrow)(1-2n_\downarrow)$, from which we can clearly see that the constraint (3.17) is equivalent to the constraint in the complex fermion representation that each site has only one fermion, i.e. $f_\uparrow^\dagger f_\uparrow + f_\downarrow^\dagger f_\downarrow = 1$.

From the mapping defined in (3.22) and (3.23) it is clear that the Hilbert space of the four Majorana fermions introduced in both Kitaev representation and the chiral Majorana representation can be mapped to the Hilbert space of the two complex fermions introduced in ordinary representation (3.24) locally. Moreover, the constraint (3.17) for the Majorana representations and the familiar one-fermion-per-site constraint [40] for the complex fermion representation are also mapped into each other. Therefore, the SO(4) chiral Majorana representation can be seen as exactly equivalent to the complex fermion representation and it is defined in the same Hilbert space as the Kitaev representation, thus it acts like a "bridge" to the two seemingly unrelated represetations.

In the following, to see the connection between the three types of Majorana representations, we will explore the Clifford algebra of the Majorana fermions in detail and link all the representations to the spinor representation of the SO(4) group and the Lorentz group.

3.2 The connection between three Majorana representations based on spinor representation of the SO(4) group

3.2.1 Representation of the Lorentz group

In order to see the relationship between the three types of Majorana representations of spin introduced above and the spinor representation of SO(4), we have to remind ourselves about the representation of the Lorentz group SO(1,3), which has almost identical structure but more familiar terminology. Strictly speaking the Lorentz group is not exactly the group SO(1,3) but in this thesis, we neglect such difference as long as no confusion is caused. We will follow and use the notations in Ref. [3] and define the space-time metric as $g_{\mu\nu} = \mathrm{diag}(1, -1, -1, -1)$. In the 4-vector representation, the Lorentz transformation is written as [3] $\Lambda_v = e^{i\theta_{\mu\nu}V^{\mu\nu}}$, in which $\theta_{\mu\nu}$ are the parameters charactering the transformation, and $V^{\mu\nu}$ are the generators of the Lorentz algebra. Due to symmetry, only six parameters of $\theta_{\mu\nu}$ are independent, three of them characterize the space rotation and the other three characterize the Lorentz boost. Taking this into account, the Lorentz elements in the 4-vector basis is also written as $\Lambda_v = e^{i\theta_i J_i + i\beta_i K_i}$, in which J_i are the generators of rotation and K_i are the generators of boost.

The Lie algebra of Lorentz group $\mathcal{L}(\mathrm{SO}(1,3)) = \mathrm{so}(1,3)$ can be decomposed into two commuting subalgebra $\mathrm{so}(1,3) = \mathrm{su}(2) \oplus \mathrm{su}(2)$, with the generators defined as $J_i^+ \equiv \frac{1}{2}(J_i + iK_i)$, $J_i^- \equiv \frac{1}{2}(J_i - iK_i)$. They satisfy two separate SU(2) Lie algebra,

$$\begin{aligned} [J_i^+, J_j^+] &= i\epsilon_{ijk} J_k^+, \\ [J_i^-, J_j^-] &= i\epsilon_{ijk} J_k^-, \\ [J_i^+, J_j^-] &= 0. \end{aligned} \tag{3.25}$$

Since the representation for a single SU(2) group is the angular momentum eigenstates, we can label the representation of the Lorentz group as (j_1, j_2), corresponding to the two su(2) subalgebra. The most fundamental but not trivial representation is $(\frac{1}{2}, 0)$ and $(0, \frac{1}{2})$, these are the *Weyl spinor representations*. The $(0, \frac{1}{2})$ is right-handed Weyl spinor, it transforms as $\psi_R \to e^{\frac{1}{2}(i\theta_i\sigma_i + \beta_i\sigma_i)}\psi_R$ under Lorentz group. The $(\frac{1}{2}, 0)$ is the left-handed Weyl spinor, it transforms as $\psi_L \to e^{\frac{1}{2}(i\theta_i\sigma_i - \beta_i\sigma_i)}\psi_L$ under Lorentz group. Again, we have used θ_i and β_i to characterize the space rotation and the boost.

The Weyl spinors are irreducible representations of the Lorentz group and they are the building blocks of the Dirac spinors, which are of fundamental importance to the elementary particle physics [3]. Dirac spinor lives in the representation $(\frac{1}{2}, 0) \oplus (0, \frac{1}{2})$, and normally it is written in terms of Weyl spinors as $\psi = (\psi_L, \psi_R)^T$. In order to study the Lorentz group in the Dirac spinor representation, it is necessary to introduce the γ-matrices, which were first used in the Dirac equations of relativistic quantum mechanics [3]. The γ-matrices are four 4×4 matrices satisfying the *Clifford algebra*

$$\{\gamma^\mu, \gamma^\nu\} = 2g^{\mu\nu}, \qquad \mu, \nu = 0, 1, 2, 3. \tag{3.26}$$

Using γ-matrices we can introduce the generators of the Lorentz group in the Dirac spinor representation as

$$S^{\mu\nu} = \frac{i}{4}[\gamma^\mu, \gamma^\nu]. \tag{3.27}$$

They satisfy the Lorentz algebra

$$[S^{\mu\nu}, S^{\rho\sigma}] = i(g^{\nu\rho}S^{\mu\sigma} - g^{\mu\rho}S^{\nu\sigma} - g^{\nu\sigma}S^{\mu\rho} + g^{\mu\sigma}S^{\nu\rho}). \tag{3.28}$$

A general Lorentz transformation in the Dirac spinor representation is written as $\Lambda_s =$

$\exp(i\theta_{\mu\nu}S^{\mu\nu})$. It is often useful to project a Dirac spinor to its left-handed or right-handed Weyl spinor component (called chirality projection). To do so, it is essential to introduce another matrix γ^5 defined as $\gamma^5 \equiv i\gamma^0\gamma^1\gamma^2\gamma^3$. The chirality projectors are thus given by $P_R = \frac{1+\gamma^5}{2}$ and $P_L = \frac{1-\gamma^5}{2}$. γ^5 matrix satisfies $\{\gamma^5, \gamma^\mu\} = 0$, and $(\gamma^5)^2 = 1$.

3.2.2 Three Types of Majorana Representation of Spin and the Spinor Representation of SO(4)

The Clifford algebra satisfied by the four Majorana fermions for each spin (3.15) differs from the Clifford algebra of γ matrices (3.26) only in the metric. Such difference in the metric is the source of the marginal difference of the group SO(4) and SO(1,3). Indeed, if we were to redefine the Majorana fermion $\eta^t \to i\eta^t$, the Clifford algebra of the Majorana fermions and the Clifford algebra of γ matrices would be the same. However for simplicity, there is no need for such redefinition.

Next we follow the steps of building the Dirac spinor representation of Lorentz group and define the objects

$$\mathcal{S}^{\mu\nu} \sim i[\eta^\mu, \eta^\nu] \tag{3.29}$$

according to (3.27). Such object $\mathcal{S}^{\mu\nu}$ satisfies the following algebra

$$[\mathcal{S}^{\mu\nu}, \mathcal{S}^{\rho\sigma}] = i(\delta^{\nu\rho}\mathcal{S}^{\mu\sigma} - \delta^{\mu\rho}\mathcal{S}^{\nu\sigma} - \delta^{\nu\sigma}\mathcal{S}^{\mu\rho} + \delta^{\mu\sigma}\mathcal{S}^{\nu\rho}) \tag{3.30}$$

and thus are the generators of the group SO(4) in some *Dirac-spinor-like representation*. The vector space this representation is acting on is the Hilbert space of the four Majorana fermions, we will explore it in more detail below. Although the four space-time directions t, x, y, z have identical footing in SO(4), it is more convenient for us to keep the terminology of the Lorentz group, which puts time direction in a special position.

From the definition 3.29, one can find that the components $\mathcal{S}^{0\alpha} \sim i[\eta^t, \eta^\alpha] \sim i\eta^t\eta^\alpha$ give exactly the Kitaev representation (3.16). In the Lorentz group terminology, $\mathcal{S}^{0\alpha}$ correspond to the generators of the "Lorentz boosts". On the other hand, the "space rotation" components, $\mathcal{S}^{\alpha\beta} \sim i[\eta^\alpha, \eta^\beta] \sim i\eta^\alpha\eta^\beta$, gives the SO(3) Majorana representation (3.3), if again we keep the same terminology. The Dirac spinor representation of SO(4)

can be decomposed into the left-handed and the right-handed Weyl spinor representation, just like the Lorentz group SO(1,3): $\mathrm{SO}(4) = \mathrm{SU}(2)_L \times \mathrm{SU}(2)_R$. Therefore we can still define the *chirality projection* operator in the Dirac-spinor-like representation

$$P_L = \frac{1 + \eta^t \eta^x \eta^y \eta^z}{2} \tag{3.31}$$

as in the Lorentz group. This leads us to intepret the projection defined in (3.18) as the projection to the left-chirality in the Dirac-spinor-like representation. Now the meaning of the definitions given in the previous section (such as the chirality of the Majorana representation etc) should become clear.

Therefore, we find that there is a clear connection between the three types of Majorana representation of spin and the Dirac-spinor-like representation of SO(4). In particular, we find that in a loose sense, the SO(3) Majorana representation (3.3) corresponds to the "space rotation" SO(3) subgroup of SO(4), the generators of which gives the spin relation automatically. The Kitaev representation (3.16), corresponding to the "Lorentz boost" part of SO(4), does not have the desired SO(3) structure. But once we project all the *states* to one of the chirality (say left), the Kitaev representation will satisfy the spin relation (3.1). On the other hand, the SO(4) chiral Majorana representation (3.19), as the projected Kitaev representation to the left-chirality, is the generators of $\mathrm{SU}(2)_L$ in the Dirac-spinor-like representation of SO(4). It has the desired spin commutator, but the constraint (3.17) is still needed to ensure the normalization $(\sigma^\alpha)^2 = 1$.

Now we examine the Hilbert space of the four Majorana fermion $\eta^t, \eta^x, \eta^y, \eta^z$, which is also the vector space the Dirac-spinor-like representation of SO(4) is acting on. From the discussion in the previous section, we see that this Hilbert space is 4-dimensional and is the same as the Hilbert space of the two complex fermions $f_\uparrow$, $f_\downarrow$, which has basis vectors $(|\uparrow\rangle, |\downarrow\rangle), (|0\rangle, |\uparrow\downarrow\rangle)$. This means that there is a one-to-one mapping between SO(4) Dirac spinor space and the Hilbert space of 2 complex fermions. A generalization of this statement for the mapping between Dirac spinor space of $\mathrm{SO}(2N)$ and the Hilbert space of N complex fermions where N is an integer has been proposed in high energy physics [85, 86] and later used in the description of non-Abelian Anyon [87, 88]. One can find detailed mathematical description of this mapping in these references. For our purpose of describing real spin in four space-time dimensions, the SO(4) group is

sufficient. Generalizations to higher SO($2N$) where $N > 2$ will involve spinor in higher dimensional space and thus are less interesting to condensed matter physics.

Although the mathematical discussion in this section is far from rigorous, it serves as a tool to help us think about the representations we have so far and compare them. From the discussion above, we see that the complex fermion representation might not be the most fundamental representation of spin as it seems; rather it can be understood as a part of a bigger class of representations, the Majorana fermion representation. Among the three types of Majorana fermion representation at hand, the SO(3) Majorana representation is special because it takes three Majorana fermions instead of four. The Hilbert space is thus not complete and well-defined for each site alone, and pairing of sites is required for proper definition of the Hilbert space [76]. In a sense, the Hilbert space defined in this way no longer possesses the properties discussed above and require further considerations to explore its nature. To understand the properties of the SO(3) Majorana representation better, we focus on its non-locality and disscuss its equivalence with the Jordan-Wigner transformation in both 1D and 2D spin models.

3.3 The SO(3) Majorana representation and the Jordan-Wigner transformation

As mentioned in the Introduction (Chapter 1), some types of spin representation define a non-local mapping between spin operators and fermionic (or possibly bosonic) operators. In particular, the *Jordan-Wigner transformation* [13, 89, 90] defines a one-dimensional (1D) mapping between spin operators in a spin chain to a fermion attached to a half-infinite string operator which creats a quantum kink. Using this transformation the one-dimensional quantum XY model is mapped into a free fermion hopping model, which is exactly solvable. The generalization of the Jordan-Wigner transformation to higher dimensions is also available [71]. In particular, the Jordan-Wigner transformation in two-dimensions (2D) involves Chern-Simons (CS) gauge theory [13, 91, 92], and thus it is often called *Chern-Simons Jordan-Wigner transformation*. Defining a mapping between spin operators and a fermion coupled to a string-operator of Chern-Simons gauge field [93], the 2D Jordan-Wigner transformation maps the quantum XY model in 2D into a model of complex fermion coupled to a Chern-Simons gauge theory (Some

details of the 2D Jordan-Wigner transformation are given in Appendix B). Besides the Jordan-Wigner (JW) transformation, another non-local representation of spin is the *SO(3) Majorana representation* which we introduced in this chapter [68, 69, 70, 71, 72, 73, 74, 75, 76, 77]. In the SO(3) Majorana representation, each spin operator is represented by three Majorana fermions. Because the number of Majorana fermions defined on each site is odd, it is not possible to establish the Majorana Hilbert space locally. Instead, we have to pair up sites and the Majorana fermions on them to define the Majorana Hilbert space [74, 76]. This pairing results in the non-local nature of the SO(3) Majorana representation of spin.

In this section, we focus on the properties of the SO(3) Majorana representation of spin. Knowing its non-local nature, our first question is whether there is any relation between the SO(3) Majorana representation and the Jordan-Wigner transformation in 1D and 2D. If there is such relation, what will it tell us about the properties of the SO(3) Majorana representation? To answer these questions, in Sec. 3.3.1 we discuss the relation between the SO(3) Majorana representation and the Jordan-Wigner transformation in the one-dimensional spin chain. We argue that under some specific conditions introduced to fix the Majorana Hilbert space, the SO(3) Majorana representation of spin can be mapped into the 1D Jordan-Wigner transformation. In the discussion, we also show that there should always be some Z_2 redundancy if we only impose $\frac{N}{2}$ (N is the total number of spins in the system) conditions to fix the Majorana Hilbert space. In Sec. 3.3.2, we analyze the relationship between the SO(3) Majorana representation and the Chern-Simons JW transformation in the two-dimensional XXZ Heisenberg model. With the proper definition of the lattice Chern-Simons gauge theory [94], we show that the SO(3) Majorana representation can be seen as an operator form of the Chern-Simons JW transformation due to the existence of anti-commuting link variables in both representations. Furthermore, we argue that the gauge field in the lattice Chern-Simons Jordan-Wigner transformation is *compact* (a concept which we will explain later) which leads to the quantization of the CS gauge connection. Such quantization further confirms the correspondence between the SO(3) Majorana representation and Chern-Simons Jordan-Wigner transformation. The correspondence we find in the specific models can be directly generalized to other spin models. It means that, except for some technical details which will be explained later, the application of

the SO(3) Majorana representation and the Jordan-Wigner transformation in one and two dimensions are equivalent to each other physically in any spin models.

3.3.1 Relation between the SO(3) Majorana representation of spin and the one-dimensional Jordan-Wigner Transformation

The Jordan-Wigner transformation defines a non-local transformation of a one-dimensional spin chain [89, 90, 13]. As we will see below, the non-local nature of the Jordan-Wigner transformation makes it directly comparable to the SO(3) Majorana representation of spin. Here, we emphasize again that although the SO(3) Majorana representation acts as a local transformation between spin and Majorana fermions (see (3.3) and (3.5)), the Hilbert space of the Majorana fermions can be defined only by pairing up the Majorana fermions non-locally because we have an odd number of Majorana fermions per site.

We start by considering a one-dimensional spin chain. For a spin chain, it is convenient to label the position of the spin sites as $i = 1, 2, 3, ..., N$ (throughout this section, we use N to denote the total number of spins in the spin chain). The Jordan-Wigner transformation in 1D takes the form [13, 89, 90]

$$\sigma_i^+ = c_i^\dagger e^{i\pi \sum_{j=1}^{i-1} c_j^\dagger c_j}, \qquad \sigma_i^- = c_i e^{-i\pi \sum_{j=1}^{i-1} c_j^\dagger c_j}. \tag{3.32}$$

Comparing with (3.7) and (3.8) one notice that the Majorana fermion operator η^z and γ in the SO(3) Majorana representation acts like the semi-infinite string operator in (3.32). This provides a guidance for us to discuss the correspondence between the SO(3) Majorana representation and the JW transformation in the 1D spin chain.

In order to establish the correspondence, our first task is to eliminate the extra dimensions (which is $2^{\frac{N}{2}}$ as discussed above) in the Majorana Hilbert space. This is achieved by enforcing a number of constraints on the Majorana Hilbert space. Specifically, let us denote the many-body physical space of η_i^x and η_i^y Majorana fermions as $\mathbb{H}_{\eta^x}$ and $\mathbb{H}_{\eta^y}$. The product space $\mathbb{H}_{xy} = \mathbb{H}_{\eta^x} \otimes \mathbb{H}_{\eta^y}$ has dimension 2^N. If we assign a single state from the many-body physical space of η^z, which we call $\mathbb{H}_{\eta^z}$, to each and every state in $\mathbb{H}_{xy}$, the resulting space $\mathbb{H}'_{xy}$, which is a subspace of $\mathbb{H}_{xyz} = \mathbb{H}_{\eta^x} \otimes \mathbb{H}_{\eta^y} \otimes \mathbb{H}_{\eta^z}$, will still have dimension 2^N and it is what we want. To make such assignment, one need some conditions or constraints. Here, following the definition of the SO(3) Majorana

representation in Sec. 3.1.1, we apply the following conditions

$$\eta^z_{2k-1} \sim (-1)^{\sum_{j=1}^{2k-1} n_j}, \qquad i\eta^z_{2k} \sim (-1)^{\sum_{j=1}^{2k} n_j}, \tag{3.33}$$

in which $k = 1, 2, 3, ...$ and we use $n_j = c_j^\dagger c_j$ to denote the number operator of the complex fermion c_j defined in (3.6). Using (3.10), we see that the mapping (3.33) corresponds to $\gamma_{2k-1} \sim -(-1)^{\sum_{j=1}^{2k-2} n_j}$ and $i\gamma_{2k} \sim -(-1)^{\sum_{j=1}^{2k-1} n_j}$. Comparing the definition of the SO(3) Majorana representation in (3.8) and the JW transformation (3.32), these conditions mean that the c fermion in SO(3) Majorana representation corresponds to the fermion in Jordan-Wigner transformation up to some extra phases; at sites $2k-1$, the phase is -1, at sites $2k$, the phase is $-i$. These extra phases have no influence on the definition of fermion number.

One may argue that the mapping in (3.33) is not mathematically rigorous because the left-hand-side is fermionic while the right-hand-side is bosonic. However, such discrepancy is not physical, all physical quantities must be functions of spin operators which come with the complex fermion operator c. After mutiplying the complex fermion operator, all the commutation relation (or algebra) of relevant operators is restored for the one-dimensional spin chain geometry. In this sense, there is no problem in (3.33). In physical applications, it is clearer to define an equivalent form of the mapping. Using the relation between γ and η^z (3.10) we see that the mapping (3.33) is equivalent to the following up to a global Z_2 degree of freedom,

$$i\eta^z_{2k-1}\eta^z_{2k} \sim (-1)^{n_{2k}}, \tag{3.34}$$

$$i\gamma_{2k}\gamma_{2k+1} \sim (-1)^{n_{2k}}, \tag{3.35}$$

in which $k = 1, 2, 3, ...$ Here in the mapping (3.34) and (3.35), both sides are bosonic operators.

To give a physical intepretation of the conditions (3.34) and (3.35), we pair up the Majorana fermions η^z_{2k-1} and η^z_{2k} and define complex fermion $d_{2k} = \frac{1}{2}(\eta^z_{2k-1} - i\eta^z_{2k})$ whose locations are defined on sites with an even number. Since we have $i\eta^z_{2k-1}\eta^z_{2k} = 1 - 2d^\dagger_{2k}d_{2k} = (-1)^{n_{d_{2k}}}$, the mapping (3.34) means that the number of d fermion on site $2k$ is equal to the number of c fermion (formed by η^x and η^y Majorana fermions) on

site $2k$. There are $\frac{N}{2}$ d fermions and so there are $\frac{N}{2}$ such conditions, which fix the state of the d fermion once the state of c fermion is defined. In this way, we have assigned a state in $\mathbb{H}_{\eta^z}$ to each and every state in $\mathbb{H}_{xy}$. Therefore the $\frac{N}{2}$ conditions in (3.34) are already sufficient to fix the dimension of the Hilbert space to be that of the spin space. But there is another $\frac{N}{2}$ constaints which take the form as (3.35). At first sight, the conditions (3.34) and (3.35) seem to be overcomplete.

To remedy this, we note that the extra $\frac{N}{2}$ constraints in (3.35) actually fix the remaining Z_2 gauge redundancy of the Majorana fermions. The SO(3) Majorana fermion representation involves bilinear form of Majorana fermions. Under the sign flip $\eta^\alpha \to -\eta^\alpha$ with $\alpha = x, y, z$, the original spin operator in (3.3) is invariant. After enforcing the conditions (3.34) there is still some Z_2 redundancy left. To see this, we note that the spin operator in the representation (3.3) and the conditions in (3.34) are invariant under simultaneous sign flipping $\eta^\alpha_{2k-1} \to -\eta^\alpha_{2k-1}$ and $\eta^\alpha_{2k} \to -\eta^\alpha_{2k}$ with k being an arbitrary integer and $\alpha = x, y, z$. Although the dimension of the Hilbert space is 2^N once the first $\frac{N}{2}$ constaints in (3.34) are enforced, the Hilbert space is still $2^{\frac{N}{2}}$ times larger than the spin space. Due to the remaining Z_2 gauge redundancy, for each state in the spin space, there are $2^{\frac{N}{2}}$ states in the corresponding Majorana Hilbert space $\mathbb{H}'_{xy}$. Once the other $\frac{N}{2}$ gauge fixing constaints of (3.35) are enforced, the remaining gauge redundancy is eliminated.

Therefore, the mapping (3.33) or (3.34) and (3.35) give a correspondence between the SO(3) Majorana representation and the 1D Jordan-Wigner transformation. The SO(3) Majorana representation (Eq. (3.7) and Eq. (3.8)) with some proper constraints (Eq. (3.34) and Eq. (3.35)) to fix the extra degrees of freedom will lead us to the same form as the 1D Jordan-Wigner transformation in (3.32). Throughout our discussion, we make no reference to the specific form of the spin Hamiltonian of the spin chain, thus the correspondence is between the two spin representations and can be applied to any one-dimensional spin Hamiltonian. On the other hand, the constraints in (3.34) and (3.35) take different form from the constrains that are previously discussed [74, 76], in which we pair up sites and demand that for each pair $\langle ij \rangle$, $\gamma_i \gamma_j = -i$. In general there are multiple ways to fix the extra degrees of freedom in the SO(3) Majorana representation. Different fixing will lead to different forms of the resulting theory.

It is important to emphasize that the complete elimination of extra degree of freedom

in Majorana Hilbert space is only achievable in one-dimensional spin chain. In 1D spin chain, after we pair up sites and enforce the first $\frac{N}{2}$ constraints to eliminate the extra dimension of the Majorana Hilbert space (like the ones in (3.34)), the rest of the link variables decouple and allow us to fix the extra Z_2 redundancy by introducing another set of constraints (like (3.35)). In higher dimensional space, the number of links connecting to each site is larger than two, it is generally impossible to define the second set of constraints. Without the extra gauge-fixing constraints like in (3.35), the original spin model is always mapped to some Z_2 gauge theory with complex fermion as its matter field. In Sec. 4.2 and Sec. 4.3, we study two spin models using the SO(3) Majorana representation, namely the quantum XY model on honeycomb lattice and the 90° compass model on the square lattice. We explicitly show that, if only $\frac{N}{2}$ constraints are enforced, both models can be mapped into some non-trivial Z_2 gauge theory. In our discussion, to get the $\frac{N}{2}$ constraints, we pair up sites of the lattice and demand that for each pair $\langle ij \rangle$, the product of the SO(3) singlets $\gamma_i \gamma_j = i$ (or $-i$). Due to the fact that all $\gamma_i \gamma_j$ commute with the spin Hamiltonian, we are able to transform these constraints into the form of standard Gauss law constraints in Z_2 gauge theory [13, 14], which commute with the Z_2 Hamiltonian by construction.

As another example, in Chapter 4 it is shown that the Kitaev honeycomb model [23] can be solved using SO(3) Majorana representation, the resulting solution takes the form of a Z_2 lattice gauge theory with standard Gauss law constraint. In other words, in the Kitaev model, due to the unique form of the Hamiltonian and the lattice geometry, it is possible to fix the Z_2 gauge without introducing any approximation. In this sense, the Kitaev model on 2D honeycomb lattice behaves like the 1D spin chain. The models we are considering in Sec. 4.2 and Sec. 4.3 do not have such property.

3.3.2 Relation between the SO(3) Majorana representation of spin and the two-dimensional Jordan-Wigner Transformation

There is a direct generalization of the Jordan-Wigner transformation to two-dimensional (2D) space with the aid of Chern-Simons gauge theory [91, 92, 93, 95, 96, 97]. The two-dimensional Jordan-Wigner transformation starts with the hard-core boson representation of spin [13, 91] (see Appendix B for a review). With the U(1) Chern-Simons

term, the statistics of the hard-core boson can be changed to fermionic. More generally, the statistics of particles in (2+1)D spacetime are not just bosonic and fermionic [98]. Particles in (2+1)D with exotic statistics are called *anyons* [13, 22, 23, 99]. The 2D Jordan-Wigner transformation maps the spin operator to a complex fermion attached to a half-infinite string operator of gauge field [91, 92, 93]. For a lattice spin model, applying the 2D Jordan-Wigner transformation (or Chern-Simons JW transformation) requires proper definition of U(1) Chern-Simons gauge theory on a lattice [92, 93, 94, 100, 101]. It is proved that the lattice Chern-Simons theory can only be defined on 2D lattices which have a one-to-one mapping between sites and plaquettes [94]. On 2D lattices with such property, the 2D Jordan-Wigner transformation maps a quantum XY model, whose Hamiltonian is given by

$$\mathcal{H}_{XY} = \sum_{ij} J_{\pm}(\sigma_i^+ \sigma_j^- + \text{h.c.}), \tag{3.36}$$

into a system of complex fermions c_i defined on lattice sites interacting with Chern-Simons gauge field A_{ij} defined on lattice bonds $\langle ij \rangle$ [13, 91],

$$\mathcal{H}_{XY} = \sum_{ij} J_{\pm} c_i^\dagger e^{iA_{ij}} c_j + \text{h.c.}. \tag{3.37}$$

To lay foundation of the discussion on the relationship between SO(3) Majorana representation and the 2D Jordan-Wigner transformation, we need to review the basics of the Chern-Simons gauge theory and the lattice Chern-Simons theory. We give such review in Appendix A following Ref. [13, 94]. In the following we will continue our discussion with the equations and conclusions from Appendix A. In order to discuss the relationship between the SO(3) Majorana representation of spin and the 2D Chern-Simons Jordan-Wigner transformation, we need one more element, which is the compactification of the lattice U(1) Chern-Simons gauge theory.

Compactification of U(1) Chern-Simons gauge theory on a lattice

As with other types of lattice gauge theories, the gauge field in the lattice Chern-Simons theory couples to the matter field by a Wilson line [13, 14, 92, 93],

$$\mathcal{H} \sim c_i^\dagger e^{iA_{ij}} c_j + \text{h.c.}, \tag{3.38}$$

in which A_{ij} is the lattice gauge field defined on the bond $\langle ij \rangle$. Throughout this section, we interchangably use $\langle ij \rangle$ (contains the start point and the end point of the bond) and e to label the bonds of the lattice. We note that the gauge field on the bond A_e actually corresponds to line integral of gauge field $\mathcal{A}_\mu$ in the continuous theory. The Wilson line on each bond e takes the form of $W_e = e^{iA_e}$, we call them the *Wilson link variables* (or Wilson links). The Wilson links are invariant under the addition of integer multiples of 2π to the gauge field on the link. This requires that the lattice Chern-Simons gauge field is defined in a compact manifold. The compactification of the gauge field A_e means that A_e and $A_e + 2n\pi$ are always equavilent when n is an integer. In other words, we have

$$A_e + 2\pi \equiv A_e. \tag{3.39}$$

From the discussion in Appendix A, we have that the commutator of the gauge field on a lattice is given by (A.19). It follows from (A.16) that

$$[A_e, A_{e'}] = -\frac{2\pi i}{k} K^{-1}_{e,e'} = \frac{2\pi i}{k}(\pm\frac{1}{2}) = \pm\frac{i\pi}{k}, \tag{3.40}$$

when e and e' share a vertex. For 2D Jordan-Wigner transformation, we are taking the level $k = 1$ (the corresponding theory is called $\text{U}(1)_1$ Chern-Simons gauge theory, see Appendix A for detailed definitions), so we have

$$[A_e, A_{e'}] = \begin{cases} \pm i\pi, & \text{if } e \text{ and } e' \text{ share a vertex,} \\ 0, & \text{otherwise.} \end{cases} \tag{3.41}$$

Now we suppose that $[A_e, A_{e'}] = i\pi$, which means that

$$[A_e, \frac{A_{e'}}{\pi}] = i. \tag{3.42}$$

Then, for an arbitrary variable θ, we have operator identity

$$e^{i\frac{A_{e'}}{\pi}\theta}A_e e^{-i\frac{A_{e'}}{\pi}\theta} = A_e + \theta. \tag{3.43}$$

Specifically when $\theta = 2\pi$, we have the following, using condition (3.39),

$$e^{2iA_{e'}}A_e e^{-2iA_{e'}} = A_e + 2\pi \equiv A_e. \tag{3.44}$$

To ensure this is an identity for all A_e we have to require that $e^{2iA_{e'}} = C$, where C is a constant. Eq. (3.44) implies that $|C|^2 = 1$, which means

$$e^{2iA_{e'}} = e^{i\phi_{e'}}, \tag{3.45}$$

in which $\phi_{e'}$ is a constant phase defined on bond e'.

On the other hand, if $[A_e, A_{e'}] = -i\pi$, we have $[A_e, -\frac{A_{e'}}{\pi}] = i$. This leads to

$$e^{-2iA_{e'}}A_e e^{2iA_{e'}} = A_e + 2\pi \equiv A_e. \tag{3.46}$$

Once again we arrive at the requirement (3.45). In summary, to compactify gauge field defined on bond e, we have to require that on all the bonds that share a vertex with it, the gauge field satisfies (3.45). Since the lattices we are interested in are always connected, all the bonds have some other neighbouring bonds, to compactify all the gauge field, we have to require that

$$e^{2iA_e} = e^{i\phi_e}, \quad \text{for all the links } e \text{ of the lattice.} \tag{3.47}$$

In (3.47), the constant ϕ_e can vary from bond to bond. On each bond, there are multiple solutions for (3.47) for each value of the constant phase ϕ_e, namely $A_e = \frac{1}{2}\phi_e + n\pi$, where n is an integer. If we restrict that $0 \leq \phi_e < 2\pi$, then there are two solutions for A_e satisfying $0 \leq A_e < 2\pi$, which are $A_e = \frac{1}{2}\phi_e$ and $A_e = \frac{1}{2}\phi_e + \pi$. For all values of ϕ_e, we see that under the condition of compactification (3.39), the lattice $\mathrm{U}(1)_1$ Chern-Simons gauge theory (see Appendix A for definition) naturally breaks down to a Z_2 theory whose Wilson link can only take eigenvalues $e^{i\frac{\phi_e}{2}}$ or $e^{i(\frac{1}{2}\phi_e+\pi)}$.

There is another intepretation of this result. The commutation relation of gauge

fields (3.41) means that the Hilbert space of the lattice gauge field A_e is not a "coordinate space", instead, it is a phase space containing both coordinate and momentum degrees of freedom. Consistency requires that this Hilbert space (or phase space) is defined in a compact manifold with finite volume. Quantization of a phase space with finite volume always results in a Hilbert space with finite dimension [18]. This is the origin of the quantization of the gauge field in the lattice $\mathrm{U}(1)_1$ Chern-Simons gauge theory.

With these results, we are ready to discuss the relationship between the SO(3) Majorana representation of spin and the compactified U(1) Chern-Simons Jordan-Wigner transformation.

SO(3) Majorana representation of spin as compactified Chern-Simons Jordan-Wigner transformation

In the Chern-Simons Jordan-Wigner transformation of spin in 2D, any spin Hamiltonian which is bilinear in spin operators is mapped to a lattice model of fermions intereacting with Chern-Simons gauge field. In particular the XY spin Hamiltonian is mapped according to

$$\sigma_i^+\sigma_j^- + \sigma_i^-\sigma_j^+ = c_i^\dagger e^{iA_{ij}} c_j + \text{h.c.}. \tag{3.48}$$

Based on the Baker-Hausdorff-Campbell formula (A.8), the Wilson link variables on the lattice $W_e = e^{iA_e}$, or $W_{ij} = e^{iA_{ij}}$ satisfy the following relation $W_e W_{e'} = W_{e'} W_e e^{-[A_e, A_{e'}]}$. Using the commutator (3.41) we arrive at the commutation relations between Wilson links on the lattice,

$$\begin{aligned} \left\{W_e, W_{e'}\right\} &= 0, \quad \text{if } e \text{ and } e' \text{ share a vertex,} \\ \left[W_e, W_{e'}\right] &= 0, \qquad\qquad \text{otherwise.} \end{aligned} \tag{3.49}$$

On the other hand, in the SO(3) Majorana representation of spin, the XY spin Hamiltonian is mapped according to Eq. (3.14), the link variables are $\gamma_i\gamma_j$ on link $\langle ij\rangle$. Following the commutation relation of Majorana fermions, these link variables satisfy the following commutation relations

$$\begin{aligned} \left\{\gamma_i\gamma_j, \gamma_j\gamma_k\right\} &= 0, \qquad\qquad \text{for } k \neq i, \\ \left[\gamma_i\gamma_j, \gamma_k\gamma_l\right] &= 0, \quad \text{for } k \neq i, j \text{ and } l \neq i, j. \end{aligned} \tag{3.50}$$

In other words, the link variables in the SO(3) Majorana representation of the spin model have the following commutation relation: two link variables anticommute if they share a vertex, otherwise they commute with each other. This is the same commutation relations as the Wilson links in the Chern-Simons Jordan-Wigner transformation of spin, which is given by (3.49). Based on this similarity and compare Eq. (3.14) and Eq. (3.48) we arrive at the following correspondence between the link variables in the SO(3) Majorana representation and the Wilson links in the lattice Chern-Simons JW transformation,

$$(-\gamma_i\gamma_j) \sim e^{iA_{ij}}, \tag{3.51}$$

The correspondence in (3.51) is not complete until we analyze the eigenvalues of the link variables in both representations. According to the compactification of the gauge field in lattice $\mathrm{U}(1)_1$ Chern-Simons gauge theory, its Wilson links can only take Z_2 values. Specifically, we have the Wilson links e^{iA_e} take values $e^{i\frac{\phi_e}{2}}$ or $e^{i(\frac{\phi_e}{2}+\pi)}$ for constant ϕ_e satisfying $0 \leq \phi_e < 2\pi$. If we take $\phi_e \equiv \pi$ for all the bonds e, then the Wilson links take values $e^{iA_e} = \pm i$. On the other hand, for the SO(3) Majorana representation of spin we also have $(-\gamma_i\gamma_j) = \pm i$. Therefore the link variables and the Wilson links in both sides of Eq. (3.51) can have the same eigenvalues. To clarify the physical meaning of the condition, $\phi_e \equiv \pi$ or $e^{2iA_e} \equiv -1$ for all bonds, we point out the following intepretation. Every time the gauge field changes by 2π on each bond, the wavefunction (of the whole system of fermions and gauge field) goes back to itself but acquire a phase $e^{i\pi} = -1$. This phase is identified as a *Berry phase* [102, 103, 104] since the gauge field is defined on a compact manifold.

In the discussion above, we have used the XXZ Heisenberg model (given by Eq. (3.11)) in 2D as an example to analyze the relation between the SO(3) Majorana representation and the Chern-Simons JW transformation. From the transformation of the XY part of the Hamiltonian, we find that the complex fermions in both representations (in SO(3) Majorana, complex fermion is defined by Eq. (3.6)) are identified with each other and the Chern-Simons Wilson links are identified with the link variables in SO(3) Majorana representation. In addition, we point out that the J_z part of the Hamiltonian under both representations are exactly the same four fermion interaction, given by Eq.

(3.12). These results can be directly generalized to other spin Hamiltonians in two dimensions, and the correspondence we find is between two spin representations without reference to specific spin models.

In summary of the discussion in this section, we conclude that the SO(3) Majorana representation of spin is equivalent to the Chern-Simons Jordan-Wigner transformation in two dimensions under the condition that the $U(1)_1$ Chern-Simons gauge field in the latter is compactified with a Berry phase $e^{i\pi}$. Such equivalence has several implications. Most importantly, from the equivalence (3.51) and the commutation relations (3.49), (3.50) we see that the key property of both representations is the *anticommuting link variables*. In previous studies of the Chern-Simons JW transformation [91, 92, 93], field theoretical approach was used to look for the saddle point of the gauge field configuration. Such approach neglects the anticommuting nature of the neighbouring link variables. In some sense it corresponds to a mean-field treatment of the anticommuting link variables. In the SO(3) Majorana representation, previous studies [75, 76, 77] also used mean-field approach to handle the link variables, which turns out to results in large discrepancies with the real physical states, as shown by Ref. [75]. In general, there is some difficulties in the treatment of anticommuting link variables. However, as we show in Sec. 3.3.1, it is possible to get rid of the anti-commuting link variables in one-dimensional systems due to the unique lattice geometry. Also, as a special two-dimensional case, in the solution of the Kitaev model using SO(3) Majorana representation [74] the anticommuting link variables are mapped out due to the specific form of spin Hamiltonian and lattice geometry. For general spin models in two dimensions and beyond, we do not expect such possibility.

Besides the similarities discussed previously, it is also important to note the subtleties in the correspondence between the SO(3) Majorana representation and the Chern-Simons Jordan-Wigner transformation (3.51). First, the definition of the Chern-Simons Jordan-Wigner transformation is restricted to two-dimensional space in which the Chern-Simons gauge theory exists. Specific to two-dimensional space, the proper definition of the 2D Jordan-Wigner transformation requires that the lattice has a one-to-one correspondence between its sites and plaquettes [94]. On the contrary, the SO(3) Majorana representation can be applied in any spatial dimension and in two-dimensional space specifically, it can be applied to any type of lattice. Moreover, due to the definition of

the SO(3) singlet γ in the SO(3) Majorana representation 3.4, the fermion operators defined on site i always anticommute with the link variables $\gamma_i\gamma_j$ that are connected to it. There is no such anticommuting relations in the Chern-Simons JW transformation. These discrepancies mean that the equivalence between the SO(3) Majorana representation and the 2D Jordan-Wigner transformation is *not mathematically rigorous*. We can understand it in the following way. Whenever the 2D Jordan-Wigner transformation can be applied to some spin model, the SO(3) Majorana representation can provide an alternative operator form for it. In general, the SO(3) Majorana representation can be applied to a broader range of models.

On the other hand, we should also mention the limitation of the theory. In particular, we note that there should always be a Maxwell term $S_M = -\frac{1}{4}\int d^3x \mathcal{F}^{\mu\nu}\mathcal{F}_{\mu\nu}$ (in which $\mathcal{F}^{\mu\nu}$ is the standard field strength tensor for the gauge field) coming along with the pure Chern-Simons term in the total continuous action (A.1). The Maxwell action will make sure that the Hamiltonian is bounded from below (i.e. there exists an minimum energy eigenvalue). After including the Maxwell action, the theory becomes a *Maxwell-Chern-Simons theory* [105, 106]. Specifically, the flux attachment constraint (A.5) and the commutator between gauge field (A.6) are modified accordingly, including the contribution from the electric field. In the continuum limit, the Chern-Simons term will give the gauge field a mass [105], making the interaction coming from the Maxwell term short-ranged, thus we can ignore the Maxwell part if we are only interested in long distances. However, things are different for the lattice version of the theory. Whether it is still possible to ignore the Maxwell term in the lattice Chern-Simons gauge theory is still an open question. If we include the Maxwell term in the lattice Chern-Simons theory, all the commutation relation discussed in this section will have to be modified significantly, including the compactification of gauge field. Exploration of the lattice Maxwell-Chern-Simons theory is beyond the scope of this work and left for future study.

Summarizing Sec. 3.3.1 and Sec. 3.3.2, we find that there is a correspondence between the SO(3) Majorana representation and the Jordan-Wigner transformation in both 1D and 2D under certain conditions. In Sec. 3.3.1 we see that under the SO(3) Majorana represetation general spin models will be mapped into a Z_2 gauge theory if only $\frac{N}{2}$ (N is the total number of spin in the system) fixing conditions are imposed. In Sec. 3.3.2 we see the importance of anticommuting link variables in both the SO(3)

Majorana representation and the Chern-Simons JW transformation.

To explore the application of the SO(3) Majorana representation, in Chapter 4 we will consider two spin models, namely the quantum XY model on the honeycomb lattice and the 90° compass model on the square lattice. We will map the two models into some lattice Z_2 gauge theories using the SO(3) Majorana representation. Our treatments of the two spin models is unique in that no approximation is introduced in obtaining the Z_2 gauge theory.

Chapter 4

Application of the SO(3) Majorana representation: Z_2 gauge theories for spin systems

Having discussed the three types of Majorana representation in Chapter 3, with an emphasize on the SO(3) Majorana representation, we now turn to demonstrate the application of the SO(3) Majorana representation in spin models. We will start with the Kitaev model which has exact solvability [74], then we will use the same strategy to study the quantum XY model on honeycomb lattice and 90° compass model on square lattice [79]. Our results map the three spin models to Z_2 lattice gauge theory of complex fermions. As mentioned in the Introduction (Chapter 1), our results differ from previous studies in that the Z_2 gauge theories we obtained are exact and can serve as a platform for further approximations.

4.1 The Kitaev model

The Kitaev model is a two-dimensional exactly solvable model of spin-1/2 degrees of freedom defined on honeycomb lattice [23]. To introduce the model, the bonds of the honeycomb lattice are categorized into three types which are labelled by x, y, and z, and denoted by $\langle ij \rangle_a$ where $a = x, y, z$. Spins interact with their nearest neighbours via an

anisotropic Ising-like interaction. In particular, on each type of bond only corresponding spin components are interacting (see Fig 4.1). The Hamiltonian of the model is given by,

$$\mathcal{H} = J_x \sum_{\langle ij \rangle_x} \sigma_i^x \sigma_j^x + J_y \sum_{\langle ij \rangle_y} \sigma_i^y \sigma_j^y + J_z \sum_{\langle ij \rangle_z} \sigma_i^z \sigma_j^z, \tag{4.1}$$

where J_x, J_y and J_z are the Ising coupling strengths on the x, y, and z bonds, respectively.

The Hamiltonian (4.1) can be solved exactly using the Kitaev representation of spins (3.16) [23]. The resulting theory is a Z_2 quantum spin liquid, which is either gapped or gapless depending on the values of J_x, J_y and J_z. Here we will not discuss Kitaev's original solution of the model, instead, we discuss some details about the Kitaev model and the solution by Kitaev [23] in Appendix C. As we discussed in Chapter 3, since the representation (3.16) is defined in the extended Hilbert space, every calculation of the model in Kitaev's original solution should be projected onto the physical space in each step. Such projection based on the chirality constraint (3.17) has been discussed in Refs. [23, 107, 108], where it has been explicitly shown that observables computed in the extended Hilbert space can be substantially different from the ones calculated in the physical space [107]. But in general the projection is hard to do, especially when the system size is small such that it is away from the thermodynamic limit [107]. Therefore, more systematic ways of obtaining the physical solution is desired to better understand the model and make reliable predictions. Some previous works have already made progress in this direction. In paticular, it has been shown that it is possible to achieve a solution of the model without using the slave-particle representation of spin, e.g., using Jordan-Wigner transformation [109, 110, 111]. Here in this section we will show that it is possible to obtain the solution of the Kitaev model using SO(3) Majorana representation of spin instead of the Kitaev representation. Without extending the Hilbert space, our solution is automatically physical.

4.1.1 Solution of the Kitaev model in SO(3) Majorana representation

In this section we show how the solution of the Kitaev model (4.1) can be obtained using the SO(3) Majorana representation. As described in Sec.3.1.1, we first introduce three Majorana fermions for each spin and label them as $\eta_i^x, \eta_i^y, \eta_i^z$. We then rewrite the

Hamiltonian (4.1) using representations (3.3) and (3.5) as following

$$\begin{aligned}\mathcal{H} &= \sum_{\langle ij\rangle_x} J_x(-i\eta_i^y\eta_i^z)(-i\eta_j^y\eta_j^z) + \sum_{\langle ij\rangle_y} J_y(-i\eta_i^z\eta_i^x)(-i\eta_j^z\eta_j^x) + \sum_{\langle ij\rangle_z} J_z(\gamma_i\eta_i^z)(\gamma_j\eta_j^z) \\ &= \sum_{\langle ij\rangle_x} J_x(\eta_i^y\eta_j^y)\eta_i^z\eta_j^z + \sum_{\langle ij\rangle_y} J_y(\eta_i^x\eta_j^x)\eta_i^z\eta_j^z + \sum_{\langle ij\rangle_z} J_z(-\gamma_i\gamma_j)\eta_i^z\eta_j^z.\end{aligned} \tag{4.2}$$

In particular, for all the z-bonds we use Eq. (3.5) to represent spins while for x-bonds and y-bonds we apply representation (3.3).

For the second step, we group the two sites belonging to every z-bond together and require that

$$\gamma_i\gamma_j = -i, \text{ for each } \langle ij\rangle_z \tag{4.3}$$

with i belonging to A sublattice. As discussed above, such pairing of honeycomb lattice sites and condition (4.3) eliminate all the extra degrees of freedom and the Hilbert space for $\eta_i^x, \eta_i^y, \eta_i^z$ is now the same as the spin space. With the condition (4.3), the Hamiltonian is transformed as

$$\mathcal{H}^{'} = \sum_{\langle ij\rangle_x} J_x(\eta_i^y\eta_j^y)\eta_i^z\eta_j^z + \sum_{\langle ij\rangle_y} J_y(\eta_i^x\eta_j^x)\eta_i^z\eta_j^z + \sum_{\langle ij\rangle_z} iJ_z\eta_i^z\eta_j^z. \tag{4.4}$$

Note that we have $[\eta_i^y\eta_j^y, \mathcal{H}^{'}] = 0$ for $\langle ij\rangle_x$ and $[\eta_i^x\eta_j^x, \mathcal{H}^{'}] = 0$ for $\langle ij\rangle_y$, therefore we are free to pick up eigenfunctions to solve the transformed Hamiltonian $\mathcal{H}^{'}$, one can choose $\eta_i^y\eta_j^y = \pm i$ for $\langle ij\rangle_x$ and $\eta_i^x\eta_j^x = \pm i$ for $\langle ij\rangle_y$. With this, the Hamiltonian is finally transformed to a free hopping Hamiltonian for η^z Majorana fermions,

$$\mathcal{H}^{''} = \sum_{\langle ij\rangle_x} (\pm i)J_x\eta_i^z\eta_j^z + \sum_{\langle ij\rangle_y} (\pm i)J_y\eta_i^z\eta_j^z + \sum_{\langle ij\rangle_z} iJ_z\eta_i^z\eta_j^z. \tag{4.5}$$

The Hamiltonian $\mathcal{H}^{''}$ has the same spectrum as the spectrum obtained in the Kitaev solution [23] but for η^z rather than for c Majorana fermions (or in our definition, η^t Majorana fermion). Note that in $\mathcal{H}^{''}$ the sign of the Majorana fermion η^z is not a local degree freedom. Now, for the physical space to be the same as the spin space we have to change the sign of two Majorana fermions on the end-points of a given z-bond

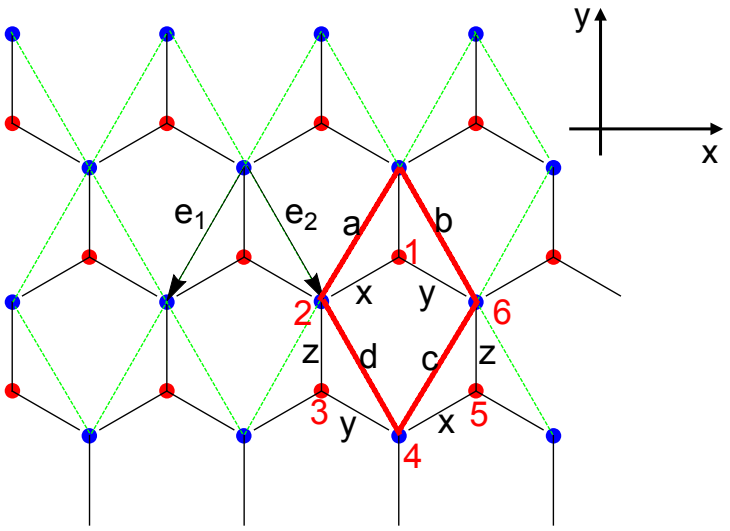

Figure 4.1: The Kitaev model on the honeycomb lattice. $\boldsymbol{e}_1 = a(-\frac{1}{2}, -\frac{\sqrt{3}}{2})$ and $\boldsymbol{e}_2 = a(\frac{1}{2}, -\frac{\sqrt{3}}{2})$ are the primitive translations, with a being the lattice constant. The two sublattices denoted in the main text by A and B are shown by blue and red dots, respectively. The sites of each of the two sublattices form a diamond lattice, as shown by the green dotted line for the A sublattice.

simultaneously. Mathematically, such transformation is given as $\eta_i^\alpha = \epsilon_{ij}\eta_i^\alpha, \eta_j^\alpha = \epsilon_{ij}\eta_j^\alpha$ for every z-bond $\langle ij\rangle_z$ with $\epsilon_{ij} = \pm 1$. We call this a *reduced Z_2 gauge redundancy*.

After the pairing of the two sites of each z-bond, we can define three complex fermions c_i^x, c_i^y, c_i^z for three flavors of Majorana fermions on every z-bond [76]. We use the honecomb site of A sublattice of the corresponding z-bond to label the real-space position of these complex fermions. Namely, we define

$$c_i^\alpha = \frac{1}{2}(\eta_i^\alpha + i\eta_j^\alpha), \qquad \alpha = x, y, z, \tag{4.6}$$

for z-bond $\langle ij\rangle_z$ with i in A sublattice and j in B sublattice. Conversely, the Majorana fermion operators are given by $\eta_i^\alpha = c_i^\alpha + c_i^{\alpha\dagger}$ for site i in the A sublattice, and $\eta_j^\alpha = -i(c_i^\alpha - c_i^{\alpha\dagger})$ for site j in B sublattice. The complex fermions live on the A sublattice of the honeycomb lattice and their positions form a diamond lattice, as shown by Fig.4.1.

By definition $\gamma_i = -i\eta_i^x\eta_i^y\eta_i^z$, thus for every z-bond the condition (4.3) can be written

as [76],

$$\gamma_i\gamma_j = i(2n_i^x - 1)(2n_i^y - 1)(2n_i^z - 1) = -i(-1)^{n_i^x+n_i^y+n_i^z}, \tag{4.7}$$

where n_i^x, n_i^y and n_i^z are the bond fermion numbers. Thus, the requirement that for every z-bond $\gamma_i\gamma_j = -i$ is equivalent to the requirement that the total fermion number is even on each z-bond, or on each site of the diamond sublattice. Now for each diamond lattice site, all the states can be represented as $|n^x, n^y, n^z\rangle = |000\rangle, |110\rangle, |101\rangle, |011\rangle$. These four states span exactly the spin Hilbert space of the z-bond: $|\uparrow\uparrow\rangle, \frac{1}{\sqrt{2}}(|\uparrow\downarrow\rangle + |\downarrow\uparrow\rangle), |\downarrow\downarrow\rangle$ and $\frac{1}{\sqrt{2}}(|\uparrow\downarrow\rangle - |\downarrow\uparrow\rangle)$. Thus our Hilbert space is settled to be the physical Hilbert space. The other condition for solving the Hamiltonian can also be written in terms of the c-fermions. Take x-bond condition $i\eta_i^y\eta_j^y = \pm 1$ as an example, we have

$$i\eta_i^y\eta_j^y = (c_i^y c_j^y + c_j^{y\dagger} c_i^{y\dagger}) + (c_i^{y\dagger} c_j^y + c_j^{y\dagger} c_i^y) = \pm 1. \tag{4.8}$$

With the complex fermion, one can obtain the energy spectrum of $\mathcal{H}''$ in Eq. 4.5, and show that it is the same as the Kitaev solution [23]. Details of this is given in Appendix C.3.

4.1.2 Z_2 Gauge Theory for Complex Fermions and Generalized Kitaev Model

The simple solution in the previous section suffers from the following fact. In the solution, we take the energy eigenstate to be eigenstate of operator $\gamma_i\gamma_j$ on each z-bond, $\eta_i^y\eta_j^y$ on each x-bond and $\eta_i^x\eta_j^x$ on each y-bond, but the three group of operators do not mutually commute. This means that the eigenstates found in this way are hardly the true eigenstates of the model itself. To treat this problem, we start from the Hamiltonian itself and try to map the Hamiltonian into some other forms which we are more familiar with. In doing so, we can see what the real eigenstates of the system look like and thus figure out how the solutions presented above are related to the real eigenstates.

Firstly, let's define a bond operator

$$T_{ij}^\alpha \equiv i\eta_i^\alpha\eta_j^\alpha = c_i^\alpha c_j^\alpha + c_j^{\alpha\dagger} c_i^{\alpha\dagger} + c_i^{\alpha\dagger} c_j^\alpha + c_j^{\alpha\dagger} c_i^\alpha, \tag{4.9}$$

where $\alpha = x, y, z$. Note that once we transform into complex fermions, the lattice is no longer a honeycomb lattice but a *diamond lattice*, with only x-bond and y-bond left, as shown in Fig 4.1. To obtain the solution of the Kitaev model we have required that on x-bond T^y_{ij} takes its eigenstates with eigenvalues ± 1 and on y-bond T^x_{ij} takes its eigenstates with eigenvalues ± 1.

Let us now give the complex fermions c^x or c^y a closer look. In the previous section we found that c^x and c^y are completely independent. For a given diamond site, the number of these fermions can be $n^x_i = 0, 1$ and $n^y_i = 0, 1$ independently. For a given y-bond ij on the diamond lattice, the Hilbert space can be defined by the occupation numbers $|n^x_i, n^x_j\rangle$, and there are four states $|00\rangle, |01\rangle, |10\rangle, |11\rangle$. The acting of the operator T^x_{ij} gives the following: $T^x_{ij}|00\rangle = |11\rangle$, $T^x_{ij}|01\rangle = |10\rangle$, $T^x_{ij}|10\rangle = |01\rangle$, and $T^x_{ij}|11\rangle = |00\rangle$. This is equivalent to say that the operator T^x_{ij} flips the occupation number of c^x fermion on both sites i and j, and flips it on each site independently. If we map this Hilbert space to some spin space and associate fermion occupation state $|1\rangle$ with spin state $|\tilde{\uparrow}\rangle$ and $|0\rangle$ with $|\tilde{\downarrow}\rangle$ on each site, the operator T^x_{ij} is equivalent to the operator $\tilde{\tau}^x_i \tilde{\tau}^x_j$, in which we use $\tilde{\tau}$ to label the new type of spin to avoid confusion with previous notations. Therefore we arrive to the following mapping

$$T^\alpha_{ij} \to \{\tilde{\tau}^x_i \tilde{\tau}^x_j\}^\alpha, \qquad \alpha = x, y, \tag{4.10}$$

which is actually changing from one bosonic operator to another bosonic operator acting on the Hilbert spaces of the same dimension.

With this mapping the problem of the original Kitaev model has been changed to the following: on each site of the diamond lattice there is one complex fermion c^z interacting with two flavors of spins, $\tilde{\tau}^\alpha_{1i}$ and $\tilde{\tau}^\alpha_{2i}$: one flavor of spin interacts with the c^z fermions only on x-bonds and the other flavor interacts with c^z only on y-bonds. Having performed this reformulation, we now write the Hamiltonian $\mathcal{H}'$ in Eq. (4.4) in terms of these new variables as (from now on we will sometimes use vector simbol $\boldsymbol{r}$ to

label sites of the diamond lattice)

$$\begin{aligned}\mathcal{H}' = &\sum_{\boldsymbol{r}\in A} -J_x(\tilde{\tau}^x_{2\boldsymbol{r}}\tilde{\tau}^x_{2,\boldsymbol{r}+\boldsymbol{e}_1})[(c^z_{\boldsymbol{r}}+c^{z\dagger}_{\boldsymbol{r}})(c^z_{\boldsymbol{r}+\boldsymbol{e}_1}-c^{z\dagger}_{\boldsymbol{r}+\boldsymbol{e}_1})] \\ &- J_y(\tilde{\tau}^x_{1\boldsymbol{r}}\tilde{\tau}^x_{1,\boldsymbol{r}+\boldsymbol{e}_2})[(c^z_{\boldsymbol{r}}+c^{z\dagger}_{\boldsymbol{r}})(c^z_{\boldsymbol{r}+\boldsymbol{e}_2}-c^{z\dagger}_{\boldsymbol{r}+\boldsymbol{e}_2})] \\ &+ J_z(2c^{z\dagger}_{\boldsymbol{r}}c^z_{\boldsymbol{r}}-1).\end{aligned} \tag{4.11}$$

Now we use a duality transformation from the site spins to the bond spins for the two quasi-one-dimensional spin chains along x and y-bonds of the diamond lattice:[13, 14]

$$\tilde{\tau}^x_i\tilde{\tau}^x_j \to \tilde{\sigma}^z_{ij},\ \tilde{\sigma}^x_{i-1,i}\tilde{\sigma}^x_{i,i+1} \to \tilde{\tau}^z_i. \tag{4.12}$$

Since the new spin variables $\tilde{\sigma}^z_{ij}$ are defined specifically on each type of the bonds and thus are independent by nature, we can drop the indices 1 and 2. Now the Hamiltonian is written as follows

$$\begin{aligned}\mathcal{H}' = &\sum_{\boldsymbol{r}\in A} -J_x(\tilde{\sigma}^z_{\boldsymbol{r},\boldsymbol{r}+\boldsymbol{e}_1})[(c^z_{\boldsymbol{r}}+c^{z\dagger}_{\boldsymbol{r}})(c^z_{\boldsymbol{r}+\boldsymbol{e}_1}-c^{z\dagger}_{\boldsymbol{r}+\boldsymbol{e}_1})] \\ &- J_y(\tilde{\sigma}^z_{\boldsymbol{r},\boldsymbol{r}+\boldsymbol{e}_2})[(c^z_{\boldsymbol{r}}+c^{z\dagger}_{\boldsymbol{r}})(c^z_{\boldsymbol{r}+\boldsymbol{e}_2}-c^{z\dagger}_{\boldsymbol{r}+\boldsymbol{e}_2})] \\ &+ J_z(2c^{z\dagger}_{\boldsymbol{r}}c^z_{\boldsymbol{r}}-1).\end{aligned} \tag{4.13}$$

This Hamiltonian describes a complex fermion on a diamond lattice interacting with a Z_2 gauge field defined on the bonds. Since topologically the diamond lattice is equivalent to a square lattice, the known results for Z_2 gauge theory on square lattice[13, 14] can be borrowed here.

However, this mapping is not complete until we consider the constraints. Recall that the original constraint is there is an even number of complex fermions on each diamond sites (see Eq. 4.7). The fermion occupation numbers n^x_i and n^y_i in terms of two flavors of spin $\tilde{\tau}_1$ and $\tilde{\tau}_2$ are given by

$$n^x_i = \frac{1}{2}(\tilde{\tau}^z_{1,i}+1), \qquad n^y_i = \frac{1}{2}(\tilde{\tau}^z_{2,i}+1). \tag{4.14}$$

Consequently, in terms of the new bond spins they are:

$$\begin{aligned} n^x_{\boldsymbol{r}} &= \frac{1}{2}(\tilde{\sigma}^x_{\boldsymbol{r}-\boldsymbol{e}_1,\boldsymbol{r}}\tilde{\sigma}^x_{\boldsymbol{r},\boldsymbol{r}+\boldsymbol{e}_1}+1), \\ n^y_{\boldsymbol{r}} &= \frac{1}{2}(\tilde{\sigma}^x_{\boldsymbol{r}-\boldsymbol{e}_2,\boldsymbol{r}}\tilde{\sigma}^x_{\boldsymbol{r},\boldsymbol{r}+\boldsymbol{e}_2}+1). \end{aligned} \tag{4.15}$$

Considering that the fermion occupation numbers can only be 0 and 1, the constraint that there is an even number of fermions per site can be written as

$$(-1)^{n^z_{\boldsymbol{r}}}\tilde{\sigma}^x_{\boldsymbol{r}-\boldsymbol{e}_1,\boldsymbol{r}}\tilde{\sigma}^x_{\boldsymbol{r},\boldsymbol{r}+\boldsymbol{e}_1}\tilde{\sigma}^x_{\boldsymbol{r}-\boldsymbol{e}_2,\boldsymbol{r}}\tilde{\sigma}^x_{\boldsymbol{r},\boldsymbol{r}+\boldsymbol{e}_2}=1, \tag{4.16}$$

which can be simplifed as $(-1)^{n^z_i}\prod_j \tilde{\sigma}^x_{ij}=1$, with j being the four nearest neighbour sites to i.

The Hamiltonian (4.13) and the constraints (4.16) define a model of complex matter fermion interacting with Z_2 gauge field. The fermion number measures the defects of *star operators* in the system (see Fig 4.2). In terms of lattice gauge theory Eq. (4.16) can also be intepreted as the Gauss law in the Z_2 gauge theory [13, 112].

From now on, we will drop the index z of the matter fermion whenever no confusion is caused. One important observation is that the operator in (4.16) commutes with the Hamiltonian $\mathcal{H}^{'}$ in (4.13), that is

$$[(-1)^{n_r}\tilde{\sigma}^x_{\boldsymbol{r}-\boldsymbol{e}_1,\boldsymbol{r}}\tilde{\sigma}^x_{\boldsymbol{r},\boldsymbol{r}+\boldsymbol{e}_1}\tilde{\sigma}^x_{\boldsymbol{r}-\boldsymbol{e}_2,\boldsymbol{r}}\tilde{\sigma}^x_{\boldsymbol{r},\boldsymbol{r}+\boldsymbol{e}_2},\mathcal{H}^{'}]=0. \tag{4.17}$$

To prove this, we use the fact that $\{(-1)^{n_r}, c_{\boldsymbol{r}}+c^\dagger_{\boldsymbol{r}}\}=0$, and $\{(-1)^{n_r}, c_{\boldsymbol{r}}-c^\dagger_{\boldsymbol{r}}\}=0$, and for spin variables, $\{\sigma^z,\sigma^x\}=0$. To make things clear, we define the operator as

$$\mathcal{D}_{\boldsymbol{r}}=(-1)^{n^z_{\boldsymbol{r}}}\tilde{\sigma}^x_{\boldsymbol{r}-\boldsymbol{e}_1,\boldsymbol{r}}\tilde{\sigma}^x_{\boldsymbol{r},\boldsymbol{r}+\boldsymbol{e}_1}\tilde{\sigma}^x_{\boldsymbol{r}-\boldsymbol{e}_2,\boldsymbol{r}}\tilde{\sigma}^x_{\boldsymbol{r},\boldsymbol{r}+\boldsymbol{e}_2}. \tag{4.18}$$

We have, from Eq. 4.17, $[\mathcal{D}_{\boldsymbol{r}},\mathcal{H}^{'}]=0$ and from the definition $[\mathcal{D}_{\boldsymbol{r}},\mathcal{D}_{\boldsymbol{r}'}]=0$, so the eigenstates of the Hamiltonian can be chosen as eigenstates of the operator $\mathcal{D}_{\boldsymbol{r}}$. Actually $\mathcal{D}_{\boldsymbol{r}}$ *generates the* Z_2 *local gauge transformation of the model at site* $\boldsymbol{r}$, so the condition (4.16) is actually equivalent to the gauge invariance of the physical states [13],

$$\mathcal{D}_{\boldsymbol{r}}|\psi\rangle_{\text{phys}}=|\psi\rangle_{\text{phys}}. \tag{4.19}$$

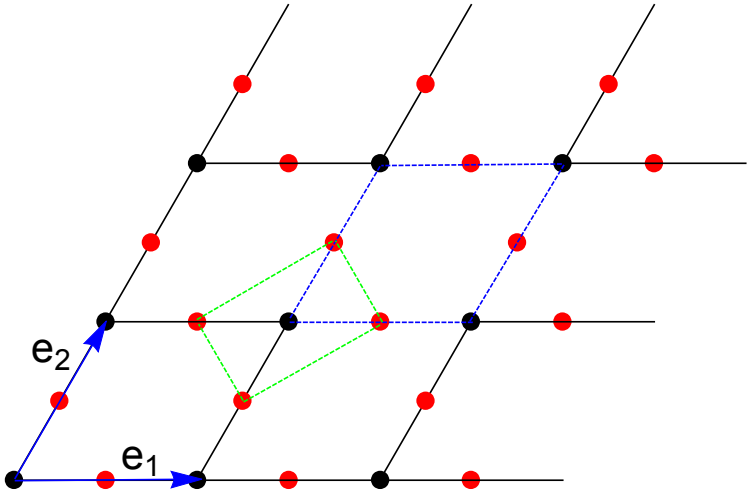

Figure 4.2: The diamond lattice corresponding to the original honecomb lattice, with unit vectors $\boldsymbol{e}_1, \boldsymbol{e}_2$. The matter (complex) fermion lives on the lattice sites, labelled by the black dots. The Z_2 gauge connection $\tilde{\sigma}^z$ lives on the bonds, labelled by the red dots. One of the *plaquettes* is shown by the blue dotted lines and one of the groups of sites involved in the constraint (4.16) is shown by the green dotted lines.

To make further progress, we add the pure gauge term to the Hamiltonian $\mathcal{H}'$ in the standard way [13, 14, 112]. We thus have the total Hamiltonian for the Z_2 gauge field interacting with matter fermion [14, 113],

$$\begin{aligned}\mathcal{H} =&\mathcal{H}^{'} + \mathcal{H}_g \\ =&\sum_{\boldsymbol{r}\in A} -J_x(\tilde{\sigma}^z_{\boldsymbol{r},\boldsymbol{r}+\boldsymbol{e}_1})[(c_{\boldsymbol{r}} + c^\dagger_{\boldsymbol{r}})(c_{\boldsymbol{r}+\boldsymbol{e}_1} - c^\dagger_{\boldsymbol{r}+\boldsymbol{e}_1})] \\ &- J_y(\tilde{\sigma}^z_{\boldsymbol{r},\boldsymbol{r}+\boldsymbol{e}_2})[(c_{\boldsymbol{r}} + c^\dagger_{\boldsymbol{r}})(c_{\boldsymbol{r}+\boldsymbol{e}_2} - c^\dagger_{\boldsymbol{r}+\boldsymbol{e}_2})] + J_z(2c^\dagger_{\boldsymbol{r}}c_{\boldsymbol{r}} - 1) \\ &- K\sum_P \prod_{\boldsymbol{r}\boldsymbol{r}'\in\partial P} \tilde{\sigma}^z_{\boldsymbol{r}\boldsymbol{r}'} - h\sum_{\boldsymbol{r}\boldsymbol{r}'} \tilde{\sigma}^x_{\boldsymbol{r}\boldsymbol{r}'}.\end{aligned} \tag{4.20}$$

In the equation above, P denotes the plaquettes in the two-dimensional lattice. The full Hamiltonian (4.20) together with the Gauss law condition (4.19) gives the effective theory of the Kitaev spin model in terms of Z_2 gauge fields interacting with complex matter fermions.

Now we move on to study the pure gauge sector of the Hamiltonian(4.20), $\mathcal{H}_g =$

$\mathcal{H}_P + \mathcal{H}_E$. The first term is the magnetic plaquette term

$$\mathcal{H}_P = -K \sum_P \prod_{\boldsymbol{r}\boldsymbol{r}' \in \partial P} \tilde{\sigma}^z_{\boldsymbol{r}\boldsymbol{r}'}, \tag{4.21}$$

which can be shown to be related to the plaquette operator $W_p = \sigma^x_1 \sigma^y_2 \sigma^z_3 \sigma^x_4 \sigma^y_5 \sigma^z_6$ defined in the original Kitaev model [23], see Fig 4.1. To see this correspondence, we note that the bond spin $\tilde{\sigma}^z_{ij}$ defined on the diamond lattice actually comes from the product of two Majorana fermions on the corresponding honecomb bond, in particular $\tilde{\sigma}^z_{\boldsymbol{r},\boldsymbol{r}+\boldsymbol{e}_1} = -i\eta^y_{\boldsymbol{r}+\boldsymbol{e}_1,A}\eta^y_{\boldsymbol{r},B}$, for x-bond; and $\tilde{\sigma}^z_{\boldsymbol{r},\boldsymbol{r}+\boldsymbol{e}_2} = -i\eta^x_{\boldsymbol{r}+\boldsymbol{e}_2,A}\eta^x_{\boldsymbol{r},B}$ for y-bond. (In these expressions, we again use $\boldsymbol{r}$ to label the sites of diamond lattice and $\boldsymbol{r}+\boldsymbol{e}_1, A$ and $\boldsymbol{r}, B$ denote the two sites of the x-bond of the honeycomb lattice belonging to A and B sublattice). Using this, we have for one plaquette operator (the labelling of the sites is shown in Fig 4.1 and the plaquette is shown explicitly in Fig 4.2),

$$\begin{aligned} \tilde{\sigma}^z_a \tilde{\sigma}^z_b \tilde{\sigma}^z_c \tilde{\sigma}^z_d &= (-i\eta^y_2\eta^y_1)(-i\eta^x_6\eta^x_1)(-i\eta^y_4\eta^y_5)(-i\eta^x_4\eta^x_3) \\ &= \sigma^z_1\sigma^y_2\sigma^x_3\sigma^z_4\sigma^y_5\sigma^x_6 = W_P. \end{aligned} \tag{4.22}$$

In this equation, we have used the condition that for every z-bond ij, $\gamma_i\gamma_j = -i$ and the representation for spin operators (3.3) and (3.5). Thus, the adding of plaquette term (4.21) is equivalent to adding a term of W_P in the original Hamiltonian,

$$-K \sum_P W_P \leftrightarrow \mathcal{H}_P. \tag{4.23}$$

It is noteworthy that this magnetic plaquette term has been considered in a generalized Kitaev model proposed in Ref. [114], in which the mean field theory is applied to study the quantum phases of the generalized Kitaev model.

For the electric part $\mathcal{H}_E = -h\sum_{\boldsymbol{r}\boldsymbol{r}'} \tilde{\sigma}^x_{\boldsymbol{r}\boldsymbol{r}'}$, it can be shown from lattice gauge theory that it corresponds to $\mathcal{H} = \frac{1}{2g}E^2$ term in the standard Electromagnetic Hamiltonian [112]. It is hard to find the spin correspondence for this form of electric Hamiltonian due to the complex mapping between bond gauge connection and the Majorana fermion. However, there are some other ways to write down $\mathcal{H}_E$, for example, Ref. [112] studies another form of the electric Hamiltonian given by the Kitaev star operator in the toric

code model, $\mathcal{H}_E = -h\sum_{\boldsymbol{r}}\prod_{\boldsymbol{r}'}\tilde{\sigma}^x_{\boldsymbol{r}\boldsymbol{r}'}$, with $\boldsymbol{r}'$ denoting the four sites adjacent to $\boldsymbol{r}$. This term, however, can be translated to a chemical potential term due to the Gauss-law constraint (4.16). It is then combined with the J_z term in Hamitonian (4.20) to give the total chemical potential term,

$$\begin{aligned} & J_z(2c^\dagger_{\boldsymbol{r}}c_{\boldsymbol{r}}-1) - h\sum_{\boldsymbol{r}}\prod_{\boldsymbol{r}'}\tilde{\sigma}^x_{\boldsymbol{r}\boldsymbol{r}'} \\ & \rightarrow (J_z+h)(2c^\dagger_{\boldsymbol{r}}c_{\boldsymbol{r}}-1) = \tilde{\mu}(2n_{\boldsymbol{r}}-1), \end{aligned} \tag{4.24}$$

in which $\tilde{\mu} = J_z + h$ is the effective chemical potential term.

4.1.3 Physical States of the Model

To describe the states of the pure Z_2 gauge theory without matter fermion, it is convenient to work in the σ^x basis [13], resulting in a geometric intepretation of the states in terms of loops. With matter fermion as in our model, it is more useful to work in the σ^z basis, which will have a close relationship with the Kitaev solution. First, we consider the model Hamiltonian (4.20) with $K = h = 0$. Without considering the Gauss-law condition (4.19), the *naive* eigenstates can be written as

$$|\psi\rangle = |\{\sigma^z_{\boldsymbol{r}\boldsymbol{r}'}\}\rangle \otimes |\phi_{\{\sigma^z\}}\rangle, \qquad \mathcal{H}|\psi\rangle = E|\psi\rangle, \tag{4.25}$$

in which $|\{\sigma^z_{\boldsymbol{r}\boldsymbol{r}'}\}\rangle$ denotes the product state of eigenstate of $\sigma^z_{\boldsymbol{r}\boldsymbol{r}'}$ on each bond. For every such distribution, $\mathcal{H}$ reduces to a free fermion Hamiltonian for complex fermion c, with eigenstate $|\phi_{\{\sigma^z\}}\rangle$ corresponding to the distribution $\{\sigma^z\}$. The Kitaev solution, although given in a different approach, is simply one of the states $|\psi\rangle$.

Now, we enforce the Gauss-law condition (4.19). We note again that the $\mathcal{D}_{\boldsymbol{r}}$ operators commute with each other and with the Hamiltonian and generates the local gauge transformation. Since $\mathcal{D}^2_{\boldsymbol{r}} = 1$, we have $(\mathcal{D}_{\boldsymbol{r}} - 1)\frac{1+\mathcal{D}_{\boldsymbol{r}}}{2}|\psi\rangle = 0$ and thus we can define the following projection of states from the eigenstates (4.25)

$$\hat{\mathcal{P}}|\psi\rangle = 2^{\frac{N-1}{2}}(\prod_{\boldsymbol{r}}\frac{1+\mathcal{D}_{\boldsymbol{r}}}{2})|\psi\rangle = \frac{1}{2^{\frac{N+1}{2}}}(\sum_{\{\boldsymbol{r}\}}\prod_{\boldsymbol{r}'\in\{\boldsymbol{r}\}}\mathcal{D}_{\boldsymbol{r}'})|\psi\rangle. \tag{4.26}$$

This projected state is given by equal superposition of all the states in the same gauge

sector as $|\psi\rangle$, and the prefactor $2^{\frac{N-1}{2}}$ is added to ensure the proper normalization of the states. This projected state satisfies two properties. First, since $\mathcal{D}_{\boldsymbol{r}}$ operator commutes with each other, we have $\mathcal{D}_{\boldsymbol{r}}\hat{\mathcal{P}}|\psi\rangle = \hat{\mathcal{P}}|\psi\rangle$, that is, the Gauss-law condition (4.19) is satisfied. Second, since $\mathcal{D}_{\boldsymbol{r}}$ operator commutes with $\mathcal{H}$, we have $\mathcal{H}\hat{\mathcal{P}}|\psi\rangle = \hat{\mathcal{P}}\mathcal{H}|\psi\rangle = E\hat{\mathcal{P}}|\psi\rangle$, which means that the projected state (4.26) is eigenstate of the Hamiltonian with the same energy as the unprojected one (4.25).

If the system has some periodic boundary condition, i.e. is defined on a torus, then the operation of performing gauge transformation for all the sites is important. For the operator $\hat{\mathcal{P}}$ to be non-zero, this operation has to have eigenvalue +1 instead of -1 for every physical state. This means that

$$\prod_{\boldsymbol{r}}(-1)^{n_{\boldsymbol{r}}}\prod_{\boldsymbol{r}'}\tilde{\sigma}^{x}_{\boldsymbol{r}\boldsymbol{r}'} = (-1)^{\sum_{\boldsymbol{r}} n_{\boldsymbol{r}}} = +1, \tag{4.27}$$

that is, the total number of fermion has to be an even number.

In order to calculate physical observables, we should use the projected states, which are the *physical states* of the model. However, the unprojected state $|\psi\rangle$ given by (4.25) can sometimes be useful as well. In terms of energy spectrum, they gives the same results as the projected states. Moreover, for other gauge invariant operators $\hat{\mathcal{O}}$, we have $[\hat{\mathcal{O}}, \hat{\mathcal{P}}] = 0$ from gauge invariance. So we have

$$\langle\hat{\mathcal{O}}\rangle = \langle\psi|\hat{\mathcal{P}}\hat{\mathcal{O}}\hat{\mathcal{P}}|\psi\rangle = \langle\psi|\hat{\mathcal{O}}\hat{\mathcal{P}}^2|\psi\rangle = 2^{\frac{N-1}{2}}\langle\psi|\hat{\mathcal{O}}\hat{\mathcal{P}}|\psi\rangle, \tag{4.28}$$

in which we use the fact that $\hat{\mathcal{P}}^2 = 2^{\frac{N-1}{2}}\hat{\mathcal{P}}$.

4.2 Quantum XY Model on Honeycomb Lattice

4.2.1 The model under SO(3) Majorana representation

Following our definition in Chapter 3, we now turn to study the quantum XY model on the honeycomb lattice (see Fig. 4.3) using the SO(3) Majorana representation. We introduce three types of Majorana fermions η^x, η^y, η^z on each site to represent spins in the model. For each site, we pair up Majorana fermion η^x and η^y to form complex fermion c according to Eq. (3.6). Then, based on Eq. (3.14), the Hamiltonian of

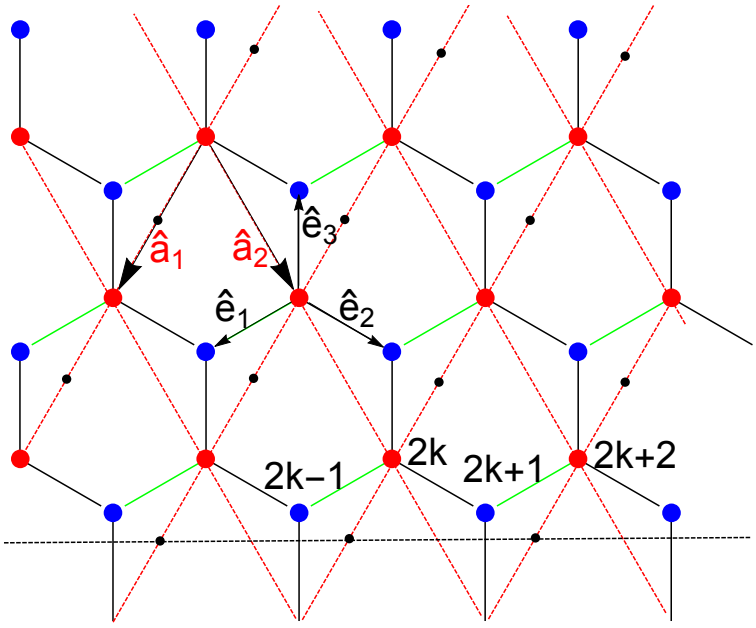

Figure 4.3: The honeycomb lattice and the diamond lattice. The original spins in the quantum XY model are defined on the sites of the honeycomb lattice, the three types of bonds are labelled by vectors $\hat{e}_1, \hat{e}_2$ and $\hat{e}_3$ respectively. The A sublattice of the honeycomb lattice is formed by the red dots which in turn form the diamond lattice, whose bonds are denoted by the red dashed lines. The unit vectors of the diamond lattice are $\hat{a}_1$ and $\hat{a}_2$. After defining the staggered fermion, the link variables form horizontal zig-zag chain. The sites in one of the chain are denoted by integer numbers $2k-1$, $2k$,..., with A sublattice sites labelled by even numbers. Link variables on each zig-zag chain are mapped into spin variables defined on the $\hat{a}_1$ bonds of the diamond lattice, labelled by black dots. Spins corresponding to the same zig-zag chain form a horizontal line, which is the black dashed line.

quantum XY model on honeycomb lattice under the SO(3) Majorana representation is given by

$$\mathcal{H} = J \sum_{\langle ij \rangle} (-\gamma_i \gamma_j)(c_i^\dagger c_j + c_i c_j^\dagger), \tag{4.29}$$

in which i and j are sites of the honeycomb lattice and $\langle ij \rangle$ denotes the bonds of the lattice. The three types of bonds of the honeycomb lattice are labelled by vectors $\hat{e}_1, \hat{e}_2, \hat{e}_3$ and the two primitive vectors are denoted by $\hat{a}_1, \hat{a}_2$, as shown in Fig. 4.3. The c_i fermions are formed by the Majorana fermion η_i^x and η_i^y according to (3.6), such definition leaves the η_i^z Majorana fermion unpaired at this stage. From now on and throughout this section, we use hatted symbol $\hat{i}$ to label the sites (and also the position vectors) of the honeycomb lattice belonging to the A sublattice (the red dots in Fig. 4.3). As discussed in Sec. 3.3.1, to fix the Hilbert space of the Majorana fermions, we have to introduce $\frac{N}{2}$ constraints. Here we choose to pair up each $\hat{e}_3$ bond (vertical bond in Fig. 4.3) and require that

$$\gamma_{\hat{i}} \gamma_{\hat{i}+\hat{e}_3} = -i, \tag{4.30}$$

in which $\gamma_{\hat{i}}$ is the SO(3) singlet of the Majorana representation defined in (3.4) and $\hat{i}$ belongs to the A sublattice. With (4.30) the Hamitonian (4.29) is transformed into

$$\begin{aligned}
\mathcal{H} &= J \sum_{\hat{i} \in \langle A \rangle} (-\gamma_{\hat{i}} \gamma_{\hat{i}+\hat{e}_3}) c_{\hat{i}}^\dagger c_{\hat{i}+\hat{e}_3} + (\eta_{\hat{i}}^z \eta_{\hat{i}+\hat{e}_1}^z) c_{\hat{i}}^\dagger c_{\hat{i}+\hat{e}_1} + \\
&\qquad (\eta_{\hat{i}}^z \eta_{\hat{i}+\hat{e}_2}^z) c_{\hat{i}}^\dagger c_{\hat{i}+\hat{e}_2} + \text{h.c.} \\
&= J \sum_{\hat{i} \in \langle A \rangle} (\eta_{\hat{i}}^z \eta_{\hat{i}+\hat{e}_1}^z)(c_{\hat{i}}^\dagger c_{\hat{i}+\hat{e}_1} + c_{\hat{i}} c_{\hat{i}+\hat{e}_1}^\dagger) + \\
&\qquad (\eta_{\hat{i}}^z \eta_{\hat{i}+\hat{e}_2}^z)(c_{\hat{i}}^\dagger c_{\hat{i}+\hat{e}_2} + c_{\hat{i}} c_{\hat{i}+\hat{e}_2}^\dagger) + \\
&\qquad i(c_{\hat{i}}^\dagger c_{\hat{i}+\hat{e}_3} + c_{\hat{i}} c_{\hat{i}+\hat{e}_3}^\dagger),
\end{aligned} \tag{4.31}$$

in which we have used the alternative form of XY spin interaction given by Eq. (3.13) for $\hat{e}_1$ bonds and $\hat{e}_2$ bonds.

For the next step, to simplify notation, we can pair up the complex fermions $c_{\hat{i}}$ and $c_{\hat{i}+\hat{e}_3}$ located on the two ends of each $\hat{e}_3$ bonds on the honeycomb lattice into a *staggered*

fermion

$$\psi_{\hat{i}} = \begin{pmatrix} c_{\hat{i}+\hat{e}_3} \\ c_{\hat{i}} \end{pmatrix}, \qquad \psi_{\hat{i}}^\dagger = \begin{pmatrix} c_{\hat{i}+\hat{e}_3}^\dagger & c_{\hat{i}}^\dagger. \end{pmatrix} \tag{4.32}$$

The positions of the staggered fermion are chosen to be the sites of the A sublattice. Using the staggered fermions we have that

$$\begin{aligned} c_{\hat{i}}^\dagger c_{\hat{i}+\hat{e}_3} + c_{\hat{i}} c_{\hat{i}+\hat{e}_3}^\dagger &= \psi_{\hat{i}}^\dagger \begin{pmatrix} 0 & -1 \\ 1 & 0 \end{pmatrix} \psi_{\hat{i}}, \\ c_{\hat{i}}^\dagger c_{\hat{i}+\hat{e}_1} + c_{\hat{i}} c_{\hat{i}+\hat{e}_1}^\dagger &= \psi_{\hat{i}}^\dagger \begin{pmatrix} 0 & 0 \\ 1 & 0 \end{pmatrix} \psi_{\hat{i}+\hat{a}_1} - \text{h.c.}, \\ c_{\hat{i}}^\dagger c_{\hat{i}+\hat{e}_2} + c_{\hat{i}} c_{\hat{i}+\hat{e}_2}^\dagger &= \psi_{\hat{i}}^\dagger \begin{pmatrix} 0 & 0 \\ 1 & 0 \end{pmatrix} \psi_{\hat{i}+\hat{a}_2} - \text{h.c.}. \end{aligned} \tag{4.33}$$

Using these relations, the Hamiltonian (4.31) can be transformed as

$$\begin{aligned} \mathcal{H} = J \sum_{\hat{i}\in\langle A\rangle} \Bigg[&\frac{1}{2} \psi_{\hat{i}}^\dagger \tilde{\sigma}_y \psi_{\hat{i}} + (\eta_{\hat{i}}^z \eta_{\hat{i}+\hat{e}_1}^z) \psi_{\hat{i}}^\dagger \begin{pmatrix} 0 & 0 \\ 1 & 0 \end{pmatrix} \psi_{\hat{i}+\hat{a}_1} \\ &+ (\eta_{\hat{i}}^z \eta_{\hat{i}+\hat{e}_2}^z) \psi_{\hat{i}}^\dagger \begin{pmatrix} 0 & 0 \\ 1 & 0 \end{pmatrix} \psi_{\hat{i}+\hat{a}_2} \Bigg] + \text{h.c.}, \end{aligned} \tag{4.34}$$

in which $\tilde{\sigma}_y$ is the Pauli matrix acting on the spin space of the staggered fermion.

The link variables $\eta_{\hat{i}}^z \eta_{\hat{i}+\hat{e}_1}^z$ and $\eta_{\hat{i}}^z \eta_{\hat{i}+\hat{e}_2}^z$ in Eq. (4.34) form a quasi-one-dimensional structure. In the honeycomb lattice, taking a horizontal zig-zag chain formed by $\hat{e}_1$ and $\hat{e}_2$, we see that there is a Majorana fermion η^z on each site of the zig-zag chain (see Fig. 4.3). In the Hamiltonian (4.34), Majorana fermions η^z on different zig-zag chains do not talk to each other. For one specific horizontal zig-zag chain we label the sites in the following way: for site $\hat{i}$ on the A sublattice, we assign an even integer $2k$ to it; the site $\hat{i} + \hat{e}_1$ is assigned an odd integer $2k-1$ and the site $\hat{i} + \hat{e}_2$ the number $2k+1$, as shown in Fig. 4.3. The Majorana fermions η^z on the zig-zag chain form a Kitaev chain [115]. Previously we paired up each $\hat{e}_3$ bonds to define the staggered fermion in terms of the complex fermions formed by η^x and η^y Majorana fermions, we can pair up the independent η^z Majorana fermions in a different way. Here, we choose to pair up the

Majorana fermions η^z on sites $2k-1$ and $2k$, in other words, sites $\hat{i}+\hat{e}_1$ and $\hat{i}$, and define complex fermion d, which we place on the middle point of the two paired sites, as

$$d_{2k-\frac{1}{2}} = \frac{1}{2}(\eta^z_{2k-1} - i\eta^z_{2k}), \quad d^\dagger_{2k-\frac{1}{2}} = \frac{1}{2}(\eta^z_{2k-1} + i\eta^z_{2k}), \tag{4.35}$$

in which we temporarily use the assigned integer number to label sites in the horizontal zig-zag chain (see Fig. 4.3).

To make further progress, for the horizontal (zig-zag) chain, we can perform the 1D Jordan-Wigner transformation (see Sec. 3.3.1) for complex fermion $d_{2k-\frac{1}{2}}$ in the following way:

$$\begin{aligned} d_{2k-\frac{1}{2}} &= \sigma^-_{2k-\frac{1}{2}} e^{i\pi \sum_{j=1}^{k-1} \frac{1}{2}(1+\sigma^z_{2j-\frac{1}{2}})}, \\ d^\dagger_{2k-\frac{1}{2}} &= \sigma^+_{2k-\frac{1}{2}} e^{-i\pi \sum_{j=1}^{k-1} \frac{1}{2}(1+\sigma^z_{2j-\frac{1}{2}})}, \end{aligned} \tag{4.36}$$

with Jordan-Wigner spins defined on sites numbered $2k-\frac{1}{2}$, which is the mid-point of two integer-numbered sites: site $2k-1$ and site $2k$. Using these definition, the link variables in (4.34), which in terms of d fermion read $i\eta^z_{2k-1}\eta^z_{2k} = 1 - 2d^\dagger_{2k-\frac{1}{2}} d_{2k-\frac{1}{2}}$ and $i\eta^z_{2k}\eta^z_{2k+1} = -(d_{2k-\frac{1}{2}} - d^\dagger_{2k-\frac{1}{2}})(d_{2k+\frac{3}{2}} + d^\dagger_{2k+\frac{3}{2}})$, can be transformed into

$$i\eta^z_{2k-1}\eta^z_{2k} \to -\sigma^z_{2k-\frac{1}{2}}, \quad i\eta^z_{2k}\eta^z_{2k+1} \to \sigma^x_{2k-\frac{1}{2}}\sigma^x_{2k+\frac{3}{2}}. \tag{4.37}$$

So far we have discussed only one chain, for other zig-zag chains we can pair up η^z Majorana fermions in the same way and put the d complex fermion and the Jordan-Wigner spins on the mid-points of all the $\hat{e}_1$ bonds.

After the pairing of sites $\hat{i}$ and $\hat{i}+\hat{e}_3$ in our definition of staggered fermion, the effective lattice for the staggered fermions has become a *diamond lattice* whose sites are the A sublattice points of the honeycomb lattice. In Fig. 4.3, the diamond lattice is formed by the red dots and we still use $\hat{i}$ to label the sites of the diamond lattice. The honeycomb bond $\langle\hat{i}, \hat{i}+\hat{e}_1\rangle$ effectively becomes diamond bond $\langle\hat{i}, \hat{i}+\hat{a}_1\rangle$. For the system of staggered fermions, we can effectively put the Jordan-Wigner spins on the diamond

lattice bonds $\langle\hat{i},\hat{i}+\hat{a}_1\rangle$. Using these notations, the mapping (4.37) becomes

$$i\eta^z_{\hat{i}+\hat{e}_1}\eta^z_{\hat{i}} \to -\sigma^z_{\hat{i}+\frac{1}{2}\hat{a}_1}, \quad i\eta^z_{\hat{i}}\eta^z_{\hat{i}+\hat{e}_2} \to \sigma^x_{\hat{i}+\frac{1}{2}\hat{a}_1}\sigma^x_{\hat{i}+\hat{a}_2-\frac{1}{2}\hat{a}_1}. \tag{4.38}$$

On the other hand, according to QED in dimension $(2+1)$, we define the *conjugate staggered fermion* $\bar{\psi}=\psi^\dagger\tilde{\sigma}_y$. Using (4.38) and the definition of conjugate spinor, we transform the Hamiltonian (4.34) into

$$\begin{aligned}\mathcal{H} =& J\sum_{\hat{i}}\left[\frac{1}{2}\bar{\psi}_{\hat{i}}\psi_{\hat{i}}+\sigma^z_{\hat{i}+\frac{1}{2}\hat{a}_1}\bar{\psi}_{\hat{i}}\begin{pmatrix}-1 & 0\\ 0 & 0\end{pmatrix}\psi_{\hat{i}+\hat{a}_1}\right.\\ &\left.+\sigma^x_{\hat{i}+\frac{1}{2}\hat{a}_1}\sigma^x_{\hat{i}+\hat{a}_2-\frac{1}{2}\hat{a}_1}\bar{\psi}_{\hat{i}}\begin{pmatrix}-1 & 0\\ 0 & 0\end{pmatrix}\psi_{\hat{i}+\hat{a}_2}\right]+\text{h.c.},\end{aligned} \tag{4.39}$$

in which the summation is over every diamond lattice site $\hat{i}$.

4.2.2 Z_2 gauge theory

In order to fix the Hilbert space of the Majorana fermion, we have to impose the constraint (4.30). To make further progress, we have to rewrite the constraint in terms of fermion operators. To this end, we use the relation (3.10) and the definition of the staggered fermion (4.32) to get the following relation

$$\gamma_{\hat{i}}\gamma_{\hat{i}+\hat{e}_3}=(-1)^{n_{\hat{i}}+n_{\hat{i}+\hat{e}_3}}\eta^z_{\hat{i}}\eta^z_{\hat{i}+\hat{e}_3}=(-1)^{\psi^\dagger_{\hat{i}}\psi_{\hat{i}}}\eta^z_{\hat{i}}\eta^z_{\hat{i}+\hat{e}_3}, \tag{4.40}$$

in which $n=c^\dagger c$ is the number of the complex fermion c. With this relation, the constraint can be rewritten as

$$(-1)^{\psi^\dagger_{\hat{i}}\psi_{\hat{i}}}\eta^z_{\hat{i}}\eta^z_{\hat{i}+\hat{e}_3}=-i. \tag{4.41}$$

In our previous discussion, we have taken the η^z Majorana fermion on each horizontal zig-zag edge to form a Kitaev chain and pair them up within the chain to form complex fermion d. In terms of the d fermion, the η^z Majorana fermion can be written as

$$\eta^z_{\hat{i}}=i(d_{\hat{i}+\frac{1}{2}\hat{a}_1}-d^\dagger_{\hat{i}+\frac{1}{2}\hat{a}_1}),\eta^z_{\hat{i}+\hat{e}_3}=(d_{\hat{i}-\frac{1}{2}\hat{a}_1}+d^\dagger_{\hat{i}-\frac{1}{2}\hat{a}_1}). \tag{4.42}$$

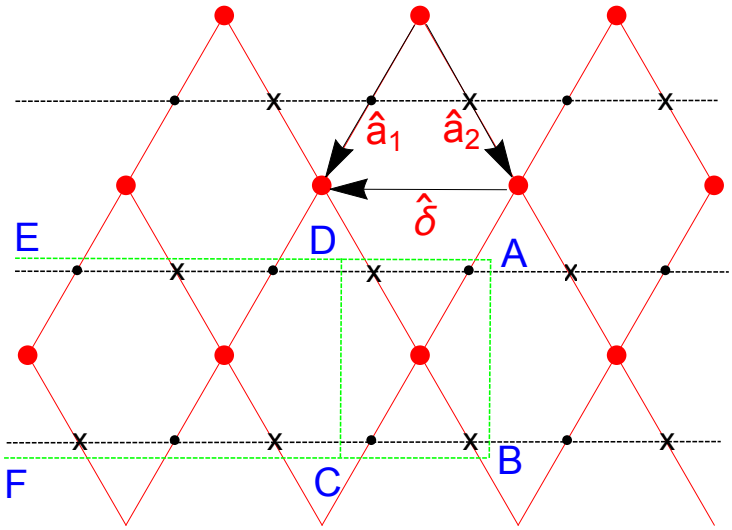

Figure 4.4: The diamond lattice, with unit vector $\hat{a}_1$ and $\hat{a}_2$. Vector $\hat{\delta}$ is defined to be $\hat{a}_1 - \hat{a}_2$. The spins from the link variables of the original honeycomb lattice are denoted by black dots in the $\hat{a}_1$ bonds. The original horizontal zig-zag chains in the honeycomb lattice become the horizontal black dashed lines. The treatment of the constraint (4.41) for site $\hat{i}$ in the middle of the (green dashed) block ABCD involves the spins in the half-infinite block CDEF. Duality transformation for each spin chain labelled by the black dashed line introduces new spin variables whose positions are denoted by black crosses. The Gauss-law constraint for the Z_2 gauge theory involves the staggered fermion and the four spin operators enclosed in ABCD.

We then performed 1D Jordan-Wigner transformation for the d complex fermion to define the spin variables on the middle points of the $\hat{a}_1$ bonds of the diamond lattice. In the Jordan-Wigner transformation, the spins (denoted by small black dots in Fig. 4.3) belonging to the same zig-zag edge form horizontal lines that cross the edges of the diamond lattice (the black dashed line in Fig 4.3 and Fig. 4.4). Based on the definition of the Jordan-Wigner transformation (4.36) and (4.42) we have, defining vector $\hat{\delta} = \hat{a}_1 - \hat{a}_2$,

$$\begin{aligned} \eta^z_{\hat{i}} &\to i(\sigma^-_{\hat{i}+\frac{1}{2}\hat{a}_1} - \sigma^+_{\hat{i}+\frac{1}{2}\hat{a}_1}) e^{i\pi \sum_{j\geq 1} \frac{1}{2}(1+\sigma^z_{\hat{i}+\frac{1}{2}\hat{a}_1+j\hat{\delta}})} \\ \eta^z_{\hat{i}+\hat{e}_3} &\to (\sigma^-_{\hat{i}-\frac{1}{2}\hat{a}_1} + \sigma^+_{\hat{i}-\frac{1}{2}\hat{a}_1}) e^{i\pi \sum_{j\geq 1} \frac{1}{2}(1+\sigma^z_{\hat{i}-\frac{1}{2}\hat{a}_1+j\hat{\delta}})}, \end{aligned} \tag{4.43}$$

here and hereafter we use j to denote an integer variable. Therefore we have

$$\eta^z_{\hat{i}} \eta^z_{\hat{i}+\hat{e}_3} = \sigma^y_{\hat{i}+\frac{1}{2}\hat{a}_1} \sigma^x_{\hat{i}-\frac{1}{2}\hat{a}_1} e^{i\pi \sum_{j\geq 1}[1+\frac{1}{2}(\sigma^z_{\hat{i}+\frac{1}{2}\hat{a}_1+j\hat{\delta}} + \sigma^z_{\hat{i}-\frac{1}{2}\hat{a}_1+j\hat{\delta}})]}. \tag{4.44}$$

To evaluate the phase factor in (4.44), we note that in Fig. 4.4, the σ^z operators appearing in the exponent in (4.44) are denoted as the black dots enclosed in the half-infinite region CDEF for the site $\hat{i}$ enclosed in the square ABCD. To make further progress, we have to make some assumptions about the boundary conditions. Let us suppose that the number of sites on the horizontal lines from the site $\hat{i} + \frac{1}{2}\hat{a}_1$ and $\hat{i} - \frac{1}{2}\hat{a}_1$ to the boundary are equal, which means that the boundary is parallel to vector $\hat{a}_1$. Under such assumption, we have the total number of σ^z operators enclosed in the region CDEF is an even number, which we call $2\tilde{N}$. Suppose that among these σ^z operators m of them take the value -1 (which implies that $2\tilde{N} - m$ σ^z operators take $+1$). Then the phase factor in (4.44) is $(-1)^{2\tilde{N}-m} = (-1)^m$. This means that under this specific boundary condition we have

$$\begin{aligned} & e^{i\pi \sum_{j\geq 1}[1+\frac{1}{2}(\sigma^z_{\hat{i}+\frac{1}{2}\hat{a}_1+j\hat{\delta}} + \sigma^z_{\hat{i}-\frac{1}{2}\hat{a}_1+j\hat{\delta}})]} \\ =& \prod_{j\geq 1} \sigma^z_{\hat{i}-\frac{1}{2}\hat{a}_1+j\hat{\delta}} \sigma^z_{\hat{i}+\frac{1}{2}\hat{a}_1+j\hat{\delta}}. \end{aligned} \tag{4.45}$$

Using (4.45) we map the constraint (4.41) into

$$(-1)^{\psi_{\hat{i}}^{\dagger}\psi_{\hat{i}}}\sigma^{z}_{\hat{i}+\frac{1}{2}\hat{a}_1}\sigma^{x}_{\hat{i}+\frac{1}{2}\hat{a}_1}\sigma^{x}_{\hat{i}-\frac{1}{2}\hat{a}_1}\prod_{j\geq 1}\sigma^{z}_{\hat{i}-\frac{1}{2}\hat{a}_1+j\hat{\delta}}\sigma^{z}_{\hat{i}+\frac{1}{2}\hat{a}_1+j\hat{\delta}}=1, \tag{4.46}$$

in which we rewrite σ^y operators as $i\sigma^z\sigma^x$ to facilitate further discussion.

To make further progress, we note that the Jordan-Wigner spins on the diamond lattice form horizontal spin chains, corresponding to the horizontal zig-zag edges of the original honeycomb lattice. In Fig. 4.4, the spin chains are denoted by black dashed lines. For each horizontal spin chain in the diamond lattice, we can perform a duality transformation among spins defined on the sites and spins defined on the bonds [14, 13]. Specifically, for a horizontal spin chain on the diamond lattice formed by sites $\hat{i}+\frac{1}{2}\hat{a}_1+j\hat{\delta}$ where j is an integer, we define a new set of spin variables τ on the mid-points of the two neighbouring sites of the original chain, formed by sites $\hat{i}+\frac{1}{2}\hat{a}_2+j\hat{\delta}$, in the following way

$$\begin{aligned}\tau^{z}_{\hat{i}+\frac{1}{2}\hat{a}_2}&=\sigma^{x}_{\hat{i}+\frac{1}{2}\hat{a}_1}\sigma^{x}_{\hat{i}+\frac{1}{2}\hat{a}_1-\hat{\delta}},\\ \tau^{x}_{\hat{i}+\frac{1}{2}\hat{a}_2}&=\prod_{j\geq 0}\sigma^{z}_{\hat{i}+\frac{1}{2}\hat{a}_1+j\hat{\delta}}.\end{aligned} \tag{4.47}$$

We emphasize that the new set of spin is located on the $\hat{a}_2$ bonds of the diamond lattice, they are labelled as black crosses in Fig. 4.4.

Under such duality mapping, the Hamiltonian (4.39) and the constraint (4.46) are both simplified significantly. The Hamiltonian becomes

$$\mathcal{H}=J\sum_{\hat{i}}\left[\frac{1}{2}\bar{\psi}_{\hat{i}}\psi_{\hat{i}}+\sigma^{z}_{\hat{i}+\frac{1}{2}\hat{a}_1}\bar{\psi}_{\hat{i}}\begin{pmatrix}-1&0\\0&0\end{pmatrix}\psi_{\hat{i}+\hat{a}_1}+\tau^{z}_{\hat{i}+\frac{1}{2}\hat{a}_2}\bar{\psi}_{\hat{i}}\begin{pmatrix}-1&0\\0&0\end{pmatrix}\psi_{\hat{i}+\hat{a}_2}\right]+\text{h.c.}. \tag{4.48}$$

It takes the form of a standard lattice gauge theory [13, 14, 112] in which the staggered fermion couples to Z_2 gauge field σ^z and τ^z. The constraint (4.46) becomes

$$(-1)^{\psi_{\hat{i}}^{\dagger}\psi_{\hat{i}}}\sigma^{x}_{\hat{i}+\frac{1}{2}\hat{a}_1}\sigma^{x}_{\hat{i}-\frac{1}{2}\hat{a}_1}\tau^{x}_{\hat{i}+\frac{1}{2}\hat{a}_2}\tau^{x}_{\hat{i}-\frac{1}{2}\hat{a}_2}=-1. \tag{4.49}$$

It takes the form of a standard Z_2 Gauss law [13].

Here let's move on and discuss the gauge symmetry of the problem. Most importantly we note that the Jordan-Wigner transformation and the duality transformation make the Z_2 gauge symmetry somewhat non-local. Specifically, the transformation $\psi_{\hat{i}} \to -\psi_{\hat{i}}$ in the matter field must accompany the following change in the σ gauge field: $\sigma^{x,y}_{\hat{i}+\frac{1}{2}\hat{a}_1-j\hat{\delta}} \to -\sigma^{x,y}_{\hat{i}+\frac{1}{2}\hat{a}_1-j\hat{\delta}}$, $\sigma^{y,z}_{\hat{i}+\frac{1}{2}\hat{a}_1} \to -\sigma^{y,z}_{\hat{i}+\frac{1}{2}\hat{a}_1}$ and $\sigma^{x,y}_{\hat{i}-\frac{1}{2}\hat{a}_1-j\hat{\delta}} \to -\sigma^{x,y}_{\hat{i}-\frac{1}{2}\hat{a}_1-j\hat{\delta}}$. $\sigma^{x,z}_{\hat{i}-\frac{1}{2}\hat{a}_1} \to -\sigma^{x,z}_{\hat{i}-\frac{1}{2}\hat{a}_1}$, in which integer $j = 1, 2, 3, ...$; and the corresponding transformation for τ spin can be deduced from Eq. (4.47). Although the gauge transformation involves half-infinite spin chains, the only relevant change that manifests in the Hamiltonian (4.48) is the following: $\psi_{\hat{i}} \to -\psi_{\hat{i}}$ and $\sigma^z_{\hat{i}\pm\frac{1}{2}\hat{a}_1} \to -\sigma^z_{\hat{i}\pm\frac{1}{2}\hat{a}_1}$, $\tau^z_{\hat{i}\pm\frac{1}{2}\hat{a}_2} \to -\tau^z_{\hat{i}\pm\frac{1}{2}\hat{a}_2}$, which is local. For all $\hat{i}$, the gauge transformation results in a sign change for even number of spins in the constraint (4.49), thus leaves it invariant.

Despite the simple form of the Z_2 Hamitonian (4.48) and the Gauss-law constraint (4.49), the model is still not solvable because the nontrivial relations between the Z_2 gauge fields (4.47), they are not independent from each other and thus we cannot fix the gauge in the usual way.

In order to discuss the physical states of the model, we first use the constraint (4.49) and define a projection operator for each site $\hat{i}$,

$$\mathcal{P}_{\hat{i}} = \frac{1}{2}[(-1)^{\psi^\dagger_{\hat{i}}\psi_{\hat{i}}}\sigma^x_{\hat{i}+\frac{1}{2}\hat{a}_1}\sigma^x_{\hat{i}-\frac{1}{2}\hat{a}_1}\tau^x_{\hat{i}+\frac{1}{2}\hat{a}_2}\tau^x_{\hat{i}-\frac{1}{2}\hat{a}_2} - 1]. \tag{4.50}$$

It can be proved that the projector on each site commutes with the Hamiltonian (4.48), $[\mathcal{P}_{\hat{i}}, \mathcal{H}] = 0$. This can be seen by noting that in the original definition of the constraint (4.30) the operators $\gamma_{\hat{i}}\gamma_{\hat{i}+\hat{e}_3}$ commute with the original spin Hamiltonian. The Hamiltonian (4.48) is defined in an enlarged Hilbert space. To get to the physical Hilbert space, we have to use the projection operator to project the state

$$|\psi_{\text{phys}}\rangle = \prod_{\hat{i}} \mathcal{P}_{\hat{i}}|\psi\rangle, \tag{4.51}$$

in which $|\psi\rangle$ is any state in the enlarged Hilbert space and the projected state $|\psi_{\text{phys}}\rangle$ is in the physical space.

Because the projectors commute with the Hamiltonian, if we manage to find the eigenvalues of the Hamitonian (4.48) in the enlarged Hilbert space, the true spectrum

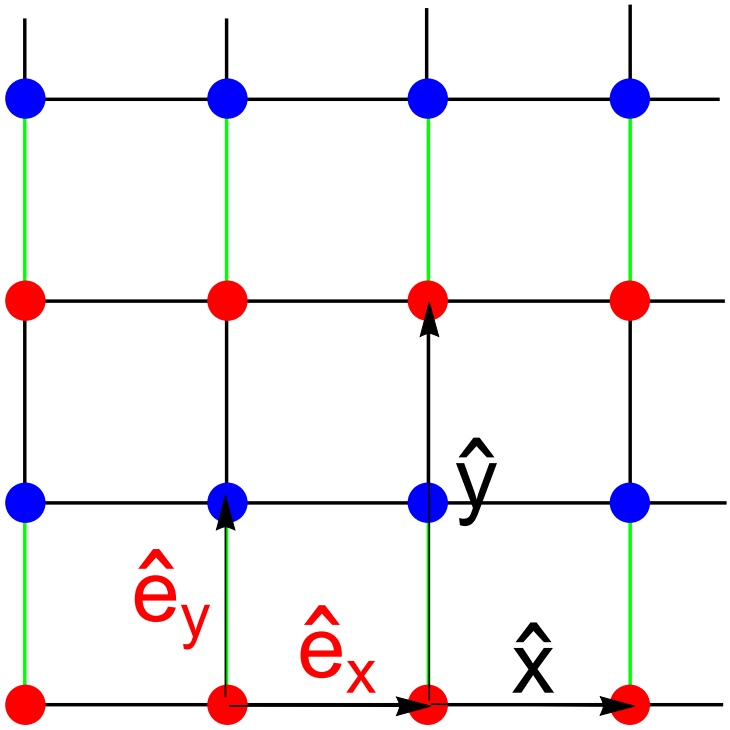

Figure 4.5: The square lattice, with unit vectors $\hat{e}_x$ and $\hat{e}_y$. Spins in the 90° compass are defined on the sites of the square lattice. Under SO(3) Majorana representation, we pair up the Majorana fermions on the two ends of the green bonds to form complex fermion. After the pairing, the lattice breaks into A sublattice labelled by the red dots, and B sublattice labelled by the blue dots. Complex fermion is defined on the A sublattice, which then forms a rectangle lattice. The unit vectors of the rectangle lattice are labelled by $\hat{x}$ and $\hat{y}$.

of the system will be the same. Unfortunately, as mentioned before, the spectrum of (4.48) is hard to find even in the enlarged Hilbert space because of the non-trivial relation of the gauge fields (4.47). The duality mapping (4.47) does not allow us to simply pick up a gauge like $\sigma^z = 1$ and $\tau^z = 1$ for all the bonds, therefore exact solution of the spectrum is unavailable.

4.3 The 90° Compass Model on Square Lattice

4.3.1 The model and SO(3) Majorana representation

The *compass models* refer to a group of frustrated lattice spin models in which the spin interaction is Ising-like and bond-dependent (for a review, see Ref. [116]). On the two-dimensional square lattice, the bonds can be categorized by its direction, as shown in Fig. 4.5, we call the horizontal bonds in the lattice *x-bonds* and vertical bonds *y-bonds*. In the 90° compass model on 2D square lattice [116, 117, 118], the spins are placed on each site of the square lattice and only the x-components are interacting on x-bonds and only y-components are interacting on the y-bonds. Correspondingly, the Hamiltonian is given by

$$\mathcal{H} = \sum_{\langle ij\rangle_x} J_1 \sigma_i^x \sigma_j^x + \sum_{\langle ij\rangle_y} J_2 \sigma_i^y \sigma_j^y, \tag{4.52}$$

in which $\langle ij\rangle_x$ denotes the x-bonds, and $\langle ij\rangle_y$ denotes the y-bonds, and J_1 and J_2 are the coupling strength on x-bonds and y-bonds respectively.

Following our discussion in Chapter 3, we can use the SO(3) Majorana representation to study this model. The first step is to use three Majorana fermions η_i^α with $\alpha = x, y, z$ to represent each spin operator. Using the definition of the SO(3) Majorana representation in Eq. (3.3), we have

$$\sigma_i^x \sigma_j^x = (\eta_i^y \eta_j^y)(\eta_i^z \eta_j^z), \quad \sigma_i^y \sigma_j^y = (\eta_i^z \eta_j^z)(\eta_i^x \eta_j^x). \tag{4.53}$$

According to the Hamiltonian (4.52), such decomposition into Majorana fermions implies that the η^x and η^y Majorana fermions only hop on y and x-bond, respectively and the η^z Majorana fermions hop on the entire lattice. Because the hopping of η^z Majorana fermion on x and y bonds mutually commute, it is expected that some kind of dimensional reduction exists in this model (which we do not discuss in detail) [116, 117, 118].

For the next step we pair up the sites and define complex fermion operators. Here we choose to pair the Majorana fermions on *half of the y-bonds*. In Fig. 4.5, the paired bonds are denoted by the green bonds. After the pairing, the lattice rotational symmetry is broken and the lattice contains two sublattices. The lower sites on the paired y-bonds are defined to be the A sublattice and the upper sites are the B sublattice. We then

pair up the Majorana fermions to form three flavors of complex fermion,

$$c_{\hat{i}}^{\alpha} = \frac{1}{2}(\eta_{\hat{i}}^{\alpha} - i\eta_{\hat{i}+\hat{e}_y}^{\alpha}), \quad c_{\hat{i}}^{\alpha\dagger} = \frac{1}{2}(\eta_{\hat{i}}^{\alpha} + i\eta_{\hat{i}+\hat{e}_y}^{\alpha}), \tag{4.54}$$

in which $\alpha = x, y, z$ and the position of these complex fermions is chosen to be on the A sublattice. Here and hereafter, we use hatted symbol $\hat{i}$ to label sites of the A sublattice of the original square lattice. Note that this definition of complex fermions is different from the one we used in Sec. 3.1.1 and Sec. 4.2. With this definition of pairing and complex fermions, the lattice is effectively transformed into a *rectangle lattice* in which only the A sublattice sites of the original square lattice are kept. The unit vectors of the original square lattice are labelled by $\hat{e}_x$ and $\hat{e}_y$, respectively. In the effective rectangle lattice, the unit vector of the y direction becomes $\hat{y} = 2\hat{e}_y$, while the unit vector on the x direction is $\hat{x} = \hat{e}_x$ (see Fig. 4.5). We will use $\hat{x}$ and $\hat{y}$ to label the unit vectors as well as bonds on the rectangle lattice.

In order to fix the Hilbert space of the Majorana fermions, we require that for each paired bond $\gamma_{\hat{i}}\gamma_{\hat{i}+\hat{e}_y} = i$, with $\gamma_{\hat{i}}$ being the SO(3) singlet in the Majorana representation defined in (3.4). In terms of the complex fermions, it reads

$$\begin{aligned} \gamma_{\hat{i}}\gamma_{\hat{i}+\hat{e}_y} &= -i(2c_{\hat{i}}^{x\dagger}c_{\hat{i}}^{x} - 1)(2c_{\hat{i}}^{y\dagger}c_{\hat{i}}^{y} - 1)(2c_{\hat{i}}^{z\dagger}c_{\hat{i}}^{z} - 1) \\ &= i(-1)^{n_{\hat{i}}^{x}+n_{\hat{i}}^{y}+n_{\hat{i}}^{z}} = i, \end{aligned} \tag{4.55}$$

in which we use $n_{\hat{i}}^{\alpha} = c_{\hat{i}}^{\alpha\dagger}c_{\hat{i}}^{\alpha}$ to denote the number of complex fermion of each flavor. The condition (4.55) implies that *there are even number of complex fermion on each site*.

Using the complex fermions (4.54) and decomposition (4.53), we can transform the Hamiltonian (4.52), which is first expressed as $\mathcal{H} = \mathcal{H}_x + \mathcal{H}_y$, in which $\mathcal{H}_x$ contains the spin interaction on $\hat{x}$-bonds and $\mathcal{H}_y$ contains spin interaction on $\hat{y}$-bonds. We have

$$\begin{aligned} \mathcal{H}_x &= \sum_{\hat{i}\in\langle A\rangle} J_1(\sigma_{\hat{i}}^{x}\sigma_{\hat{i}+\hat{e}_x}^{x} + \sigma_{\hat{i}+\hat{e}_y}^{x}\sigma_{\hat{i}+\hat{e}_x+\hat{e}_y}^{x}) \\ &= \sum_{\hat{i}} 2J_1[(c_{\hat{i}}^{y}c_{\hat{i}+\hat{x}}^{y} + c_{\hat{i}}^{y\dagger}c_{\hat{i}+\hat{x}}^{y\dagger})(c_{\hat{i}}^{z}c_{\hat{i}+\hat{x}}^{z} + c_{\hat{i}}^{z\dagger}c_{\hat{i}+\hat{x}}^{z\dagger}) \\ &\qquad + (c_{\hat{i}}^{y\dagger}c_{\hat{i}+\hat{x}}^{y} + c_{\hat{i}}^{y}c_{\hat{i}+\hat{x}}^{y\dagger})(c_{\hat{i}}^{z\dagger}c_{\hat{i}+\hat{x}}^{z} + c_{\hat{i}}^{z}c_{\hat{i}+\hat{x}}^{z\dagger})]. \end{aligned} \tag{4.56}$$

And

$$\begin{aligned}\mathcal{H}_y &= \sum_{\hat{i}\in\langle A\rangle} J_2(\sigma^y_{\hat{i}}\sigma^y_{\hat{i}+\hat{e}_y} + \sigma^y_{\hat{i}+\hat{e}_y}\sigma^y_{\hat{i}+2\hat{e}_y}) \\ &= \sum_{\hat{i}} J_2[(2c^{y\dagger}_{\hat{i}}c^y_{\hat{i}} - 1) \\ &\quad - (c^x_{\hat{i}} - c^{x\dagger}_{\hat{i}})(c^x_{\hat{i}+\hat{y}} + c^{x\dagger}_{\hat{i}+\hat{y}})(c^z_{\hat{i}} - c^{z\dagger}_{\hat{i}})(c^z_{\hat{i}+\hat{y}} + c^{z\dagger}_{\hat{i}+\hat{y}})].\end{aligned} \tag{4.57}$$

In the equations above, we have used the condition (4.55). In both (4.56) and (4.57), the summation is done for the sites on the retangle lattice, which coincide with the A sublattice of the original square lattice and thus are also labelled by $\hat{i}$.

Notice from Eq. (4.56) and Eq. (4.57) that the complex fermions c^x and c^y only hop within each individual chain of y-bonds and x-bonds respectively. Fermions on different chains don't talk to each other, which implies that the dynamics of the complex fermions c^x_i and c^y_i is *quasi-one-dimensional*. This invites us to perform 1D Jordan-Wigner transformation for fermions c^x_i and c^y_i.

4.3.2 Jordan-Wigner transformation for complex fermions and duality transformation

According to the one-dimensional Jordan-Wigner transformation (3.32), we can map a 1D chain of complex fermions c_i into a chain of spins σ_i. Specifically in our case, for each site $\hat{i}$ we have to define two sets of spin variables: one for the Jordan-Wigner transformation of $c^y_{\hat{i}}$ fermions on x-axis, which we call $\sigma_{\hat{i}}$; the other one for the Jordan-Wigner transformation of $c^x_{\hat{i}}$ fermions on y-axis, which we call $\tilde{\sigma}_{\hat{i}}$. (The c^z fermion and the Jordan-Wigner spin variables σ and $\tilde{\sigma}$ are located at sites of the rectangle lattice, labelled by red dots in Fig. 4.6.) Using (3.32) we have the Jordan-Wigner transformation on $\hat{x}$-bonds,

$$\begin{aligned} c^y_{\hat{i}}c^y_{\hat{i}+\hat{x}} + c^{y\dagger}_{\hat{i}}c^{y\dagger}_{\hat{i}+\hat{x}} &\to \frac{i}{2}(\sigma^y_{\hat{i}}\sigma^x_{\hat{i}+\hat{x}} + \sigma^x_{\hat{i}}\sigma^y_{\hat{i}+\hat{x}}) \\ c^{y\dagger}_{\hat{i}}c^y_{\hat{i}+\hat{x}} + c^y_{\hat{i}}c^{y\dagger}_{\hat{i}+\hat{x}} &\to \frac{i}{2}(\sigma^y_{\hat{i}}\sigma^x_{\hat{i}+\hat{x}} - \sigma^x_{\hat{i}}\sigma^y_{\hat{i}+\hat{x}}). \end{aligned} \tag{4.58}$$

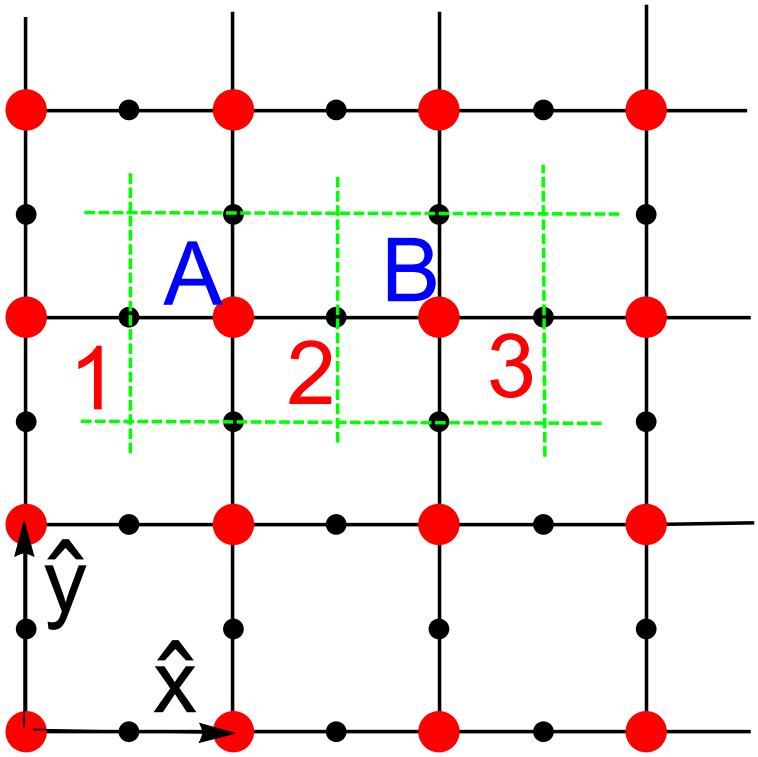

Figure 4.6: The rectangle lattice, with unit vectors $\hat{x}$ and $\hat{y}$, note that we have shrinked the length of $\hat{y}$ to half of its length to achieve a clearer look. The complex fermion lives on the sites of the rectangle lattice, denoted by the red dots. The spin variables τ are defined on the bonds of the lattice, which are the black dots. In the Z_2 gauge theory Hamiltonian (4.69), the hopping of complex fermions defined on sites A and B couples to the spins on sites 1, 2, and 3. The dual lattice can be defined by connecting the centers of plaquettes of the original lattice. Part of the dual lattice is shown by the green dashed lines.

The Jordan-Wigner transformation on $\hat{y}$-bonds reads,

$$(c^x_{\hat{i}} - c^{x\dagger}_{\hat{i}})(c^x_{\hat{i}+\hat{y}} + c^{x\dagger}_{\hat{i}+\hat{y}}) \to -\tilde{\sigma}^x_{\hat{i}}\tilde{\sigma}^x_{\hat{i}+\hat{y}}. \tag{4.59}$$

At this stage, it is important to consider the constraint (4.55) in the form of the Jordan-Wigner spin variables σ and $\tilde{\sigma}$. We have, based on the Jordan-Wigner transformation (3.32), that the number of fermion on each site is transformed according to

$$n_{\hat{i}} = c^\dagger_{\hat{i}} c_{\hat{i}} \to \sigma^+_{\hat{i}}\sigma^-_{\hat{i}} = \frac{1}{2}(1 + \sigma^z_{\hat{i}}). \tag{4.60}$$

Thus the condition that there are even number of fermions on each site (see Eq. (4.55)) is transformed into the following condition in terms of the number of the c^z fermions and the two Jordan-Wigner spins on each site,

$$2n^z_{\hat{i}} + \sigma^z_{\hat{i}} + \tilde{\sigma}^z_{\hat{i}} = \pm 2, \tag{4.61}$$

or in another form

$$(-1)^{n^z_{\hat{i}}}\sigma^z_{\hat{i}}\tilde{\sigma}^z_{\hat{i}} = 1. \tag{4.62}$$

Now we have two types of spin variables on each site. To simplify the problem we can apply a duality transformation of 1D spin system [13, 14] to transform the two types of spins on sites to spins on bonds.

To define the duality transformation, we introduce a new set of spin variables τ on the $\hat{x}$ and $\hat{y}$ bonds of the rectangle lattice. The new spin variables on $\hat{x}$-bonds $\tau_{\hat{i}+\frac{\hat{x}}{2}}$ are used to represent the $\sigma_{\hat{i}}$ variables and the new spin variables on $\hat{y}$-bonds $\tau_{\hat{i}+\frac{\hat{y}}{2}}$ are used to represent $\tilde{\sigma}_{\hat{i}}$ variables. In Fig. 4.6, the new spin variables τ are denoted by the small black dots on the bonds. Due to the distinction between the τ variables on x-bonds and y-bonds (in contrast to the σ and $\tilde{\sigma}$ variables which are located at the same site), there is no confusion in this transformation although we are using the same symbol to label all the new spin variables (for both σ and $\tilde{\sigma}$). The duality transformation [13, 14] can be defined subsequently; in particular, we have that the $\sigma_{\hat{i}}$ variables on x-bonds are transformed as

$$\sigma^z_{\hat{i}} = \tau^x_{\hat{i}-\frac{\hat{x}}{2}}\tau^x_{\hat{i}+\frac{\hat{x}}{2}}, \qquad \sigma^x_{\hat{i}} = \prod_{j\geq 1}\tau^z_{\hat{i}+\frac{\hat{x}}{2}-j\hat{x}}, \tag{4.63}$$

in which we use j to denote an integer variable. Therefore we have

$$\begin{aligned}\sigma^y_{\hat{i}}\sigma^x_{\hat{i}+\hat{x}} &= -i\sigma^z_{\hat{i}}\sigma^x_{\hat{i}}\sigma^x_{\hat{i}+\hat{x}} = -\tau^x_{\hat{i}-\frac{\hat{x}}{2}}\tau^y_{\hat{i}+\frac{\hat{x}}{2}},\\ \sigma^x_{\hat{i}}\sigma^y_{\hat{i}+\hat{x}} &= i\sigma^x_{\hat{i}}\sigma^x_{\hat{i}+\hat{x}}\sigma^z_{\hat{i}+\hat{x}} = -\tau^y_{\hat{i}+\frac{\hat{x}}{2}}\tau^x_{\hat{i}+\frac{3\hat{x}}{2}}.\end{aligned} \tag{4.64}$$

Similarly, the Jordan-Wigner spins on y axis are transformed as

$$\tilde{\sigma}^x_{\hat{i}}\tilde{\sigma}^x_{\hat{i}+\hat{y}} = \tau^z_{\hat{i}+\frac{\hat{y}}{2}}, \qquad \tau^x_{\hat{i}-\frac{\hat{y}}{2}}\tau^x_{\hat{i}+\frac{\hat{y}}{2}} = \tilde{\sigma}^z_{\hat{i}}. \tag{4.65}$$

With this duality transformation (4.64) and (4.65), the condition (4.55) (and further (4.62)) is transformed as

$$(-1)^{n_{\hat{i}}}\tau^x_{\hat{i}-\frac{\hat{x}}{2}}\tau^x_{\hat{i}+\frac{\hat{x}}{2}}\tau^x_{\hat{i}-\frac{\hat{y}}{2}}\tau^x_{\hat{i}+\frac{\hat{y}}{2}} \equiv 1. \tag{4.66}$$

4.3.3 Z_2 gauge theory

Using the bond spin operators, the two parts of the Hamiltonian (4.56) and (4.57) can be transformed. First, using Jordan-Wigner transformation on x-axis (4.58) and duality transformation (4.64) we have

$$\begin{aligned}\mathcal{H}_x \to \sum_{\hat{i}} 2J_1[&\frac{i}{2}\tau^y_{\hat{i}+\frac{\hat{x}}{2}}(-\tau^x_{\hat{i}-\frac{\hat{x}}{2}} - \tau^x_{\hat{i}+\frac{3\hat{x}}{2}})(c^z_{\hat{i}}c^z_{\hat{i}+\hat{x}} + c^{z\dagger}_{\hat{i}}c^{z\dagger}_{\hat{i}+\hat{x}})\\ &+ \frac{i}{2}\tau^y_{\hat{i}+\frac{\hat{x}}{2}}(-\tau^x_{\hat{i}-\frac{\hat{x}}{2}} + \tau^x_{\hat{i}+\frac{3\hat{x}}{2}})(c^{z\dagger}_{\hat{i}}c^z_{\hat{i}+\hat{x}} + c^z_{\hat{i}}c^{z\dagger}_{\hat{i}+\hat{x}})]\\ = \sum_{\hat{i}} J_1[&(\tau^x_{\hat{i}+\frac{\hat{x}}{2}}\tau^x_{\hat{i}-\frac{\hat{x}}{2}})\tau^z_{\hat{i}+\frac{\hat{x}}{2}}(c^z_{\hat{i}} + c^{z\dagger}_{\hat{i}})(c^z_{\hat{i}+\hat{x}} + c^{z\dagger}_{\hat{i}+\hat{x}})\\ &+ (\tau^x_{\hat{i}+\frac{\hat{x}}{2}}\tau^x_{\hat{i}+\frac{3\hat{x}}{2}})\tau^z_{\hat{i}+\frac{\hat{x}}{2}}(c^z_{\hat{i}} - c^{z\dagger}_{\hat{i}})(c^z_{\hat{i}+\hat{x}} - c^{z\dagger}_{\hat{i}+\hat{x}})].\end{aligned} \tag{4.67}$$

Here we have used the fact that $aA + bB = \frac{1}{2}[(a+b)(A+B) + (a-b)(A-B)]$ for any variables a, b and A, B. Similarly we can transfrom Eq. (4.57) as follows

$$\mathcal{H}_y \to \sum_{\hat{i}} J_2[\tau^x_{\hat{i}-\frac{\hat{x}}{2}}\tau^x_{\hat{i}+\frac{\hat{x}}{2}} + \tau^z_{\hat{i}+\frac{\hat{y}}{2}}(c^z_{\hat{i}} - c^{z\dagger}_{\hat{i}})(c^z_{\hat{i}+\hat{y}} + c^{z\dagger}_{\hat{i}+\hat{y}})], \tag{4.68}$$

in which we have used the following transformation coming from the Jordan-Wigner transformation and duality transformation mentioned above: $(2c_i^{y\dagger}c_i^y - 1) \rightarrow \sigma_i^z \rightarrow \tau^x_{i-\frac{\hat{x}}{2}}\tau^x_{i+\frac{\hat{x}}{2}}$.

Combining (4.67) and (4.68) we can see that now the Hamiltonian involves complex fermion $c^z_{\hat{i}}$ defined on the sites of the rectangle lattice and spin variables τ^α defined on the bonds of the rectangle lattice (see Fig. 4.6). The unphysical degrees of freedom are eliminated by the gauge condition (4.66) which takes the form of standard Z_2 Guass law [13, 74]. Although the form of the transformed Hamiltonian is simple, it is not the usual Z_2 gauge theory [112] in that the bond variables contain non-commuting τ^x and τ^z.

For the next step, we can safely drop the index z of the complex fermions without causing confusion since it is the only fermionic degree of freedom left. The total Hamiltonian is now given by

$$\begin{aligned}\mathcal{H} = \sum_{\hat{i}} J_1[&(\tau^x_{\hat{i}+\frac{\hat{x}}{2}}\tau^x_{\hat{i}-\frac{\hat{x}}{2}})\tau^z_{\hat{i}+\frac{\hat{x}}{2}}(c_{\hat{i}} + c^\dagger_{\hat{i}})(c_{\hat{i}+\hat{x}} + c^\dagger_{\hat{i}+\hat{x}}) \\ &+ (\tau^x_{\hat{i}+\frac{\hat{x}}{2}}\tau^x_{\hat{i}+\frac{3\hat{x}}{2}})\tau^z_{\hat{i}+\frac{\hat{x}}{2}}(c_{\hat{i}} - c^\dagger_{\hat{i}})(c_{\hat{i}+\hat{x}} - c^\dagger_{\hat{i}+\hat{x}})] \\ &+ J_2\tau^x_{\hat{i}-\frac{\hat{x}}{2}}\tau^x_{\hat{i}+\frac{\hat{x}}{2}} + J_2\tau^z_{\hat{i}+\frac{\hat{y}}{2}}(c_{\hat{i}} - c^\dagger_{\hat{i}})(c_{\hat{i}+\hat{y}} + c^\dagger_{\hat{i}+\hat{y}}).\end{aligned} \tag{4.69}$$

To see the Z_2 gauge symmetry, we note that the Hamiltonian (4.69) and the constraint (4.66) are invariant under the transformation: $c_{\hat{i}} \rightarrow -c_{\hat{i}}$ and $\tau^z_{\hat{i}\pm\frac{\hat{x}}{2}} \rightarrow -\tau^z_{\hat{i}\pm\frac{\hat{x}}{2}}$, $\quad \tau^z_{\hat{i}\pm\frac{\hat{y}}{2}} \rightarrow -\tau^z_{\hat{i}\pm\frac{\hat{y}}{2}}$, with all τ^x components unchanged.

From the condition (4.66) we can define a projector for each site $\hat{i}$,

$$\mathcal{P}_{\hat{i}} = \frac{1}{2}[(-1)^{n_{\hat{i}}}\tau^x_{\hat{i}-\frac{\hat{x}}{2}}\tau^x_{\hat{i}+\frac{\hat{x}}{2}}\tau^x_{\hat{i}-\frac{\hat{y}}{2}}\tau^x_{\hat{i}+\frac{\hat{y}}{2}} + 1]. \tag{4.70}$$

The projector (4.70) commutes with the Hamiltonian (4.69), $[\mathcal{P}_{\hat{i}}, \mathcal{H}] = 0$ following the fact that $\{(-1)^{n_i}, c_i\} = 0$ and $\{(-1)^{n_i}, c_i^\dagger\} = 0$. It can also be seen by noting that the operators $\gamma_{\hat{i}}\gamma_{\hat{i}+\hat{e}_y}$ that are picked to define the condition (4.55) commute with the original spin Hamiltonian. The Z_2 Hamiltonian (4.69) is defined in an enlarged Hilbert space, which contains the physical space as a subspace. The physical space is obtained by projection $|\psi_{\text{phys}}\rangle = \prod_{\hat{i}} \mathcal{P}_{\hat{i}}|\psi\rangle$, in which $|\psi\rangle$ is any state of the enlarged Hilbert space. As discussed in earlier sections, because we have $[\mathcal{P}_{\hat{i}}, \mathcal{H}] = 0$, if we manage to find the

eigenstate of $\mathcal{H}$, the physical state will have the same energy after projection. This allows us to focus on the Hamiltonian (4.69) first, find its eigenstates and its eigenvalues give the exact energy spectrum of the model.

Unfortunately the Z_2 Hamiltonian is highly non-trivial. In Fig. 4.6, we note that the hopping of complex fermions between sites A and B couples to Z_2 gauge fields on bonds 1, 2 and 3. In analogy to the U(1) lattice gauge theory [13], the τ^x operator acts like electric field while the τ^z operator acts like magnetic vector potential. The non-trivial form of Hamiltonian (4.69) means that the charge current in this Z_2 gauge theory couples non-trivially to the electric field. Another way to study the Hamiltonian is by going to the dual lattice which is defined by connecting the centers of all the plaquettes of the retangle lattice (in Fig. 4.6, part of the dual lattice is shown by green dashed lines). On the dual lattice, we perform the duality transformation of electrical and magnetric fields, i.e. define a new set of fields $\tilde{\tau}^z = \tau^x$ and $\tilde{\tau}^x = -\tau^z$ on the same sites of the original fields. The new set of gauge fields $\tilde{\tau}$ are still defined on the bonds of the dual lattice; however, the charges, which become the magnetic monopoles after the transformation, are located at the centers of the plaquettes of the dual lattice and the condition (4.66) becomes the flux attachment constraint to the magnetic monopole.

4.4 Discussion on the Z_2 gauge theories and the application of SO(3) Majorana representation in spin models

Applying the SO(3) Majorana representation, we study three spin models on 2D lattices, including the Kitaev model, the quantum XY model on honeycomb lattice and the 90° compass model on square lattice. For our solution of the Kitaev model in Sec 4.1, it is noteworthy that the physical solution we obtained is different from the previous works [107, 108] in that our results highlights the importance of the Z_2 gauge transformation in the relation between the physical state and the naive eigenstate of the Hamiltonian. Moreover, our results give an explicit formula to calculate the physical expectation of any observable, namely Eq. (4.28). This method is applicable to small systems away from the thermodynamic limit as well. Using this, one can obtain the physical observables such as the structural function and calculate the experimental response. In the quantum XY model on honeycomb lattice and the 90° compass model on square lattice, we show

how to use the SO(3) Majorana representation to exactly map these models into Z_2 lattice gauge theories. Specifically, we introduce $\frac{N}{2}$ constraints by pairing up sites and requiring that for each pair $\langle ij \rangle$, the value of the product of SO(3) singlets $\gamma_i \gamma_j$ is fixed. Due to the fact that these product operators commute with the spin Hamiltonian, we show that the conditions can be mapped into the standard form of Gauss law in the Z_2 gauge theories. Unfortunately, neither of the two models is exactly solvable and the resulting Z_2 gauge theories are non-trivial because we cannot simply pick up a gauge and determine the spectrum of the matter fields. To this end, further approximations are needed to treat these non-trivial Z_2 gauge theories. Here we give a brief discussion on the possible approximations that may be applied and make some remarks on future direction of study.

In the quantum XY model on honeycomb lattice, we obtain the exact Z_2 Hamiltonian (4.48) with Gauss-law constraint (4.49). If we ignore the non-trivial relation between gauge fields (4.47) and set $\sigma^z = 1$ and $\tau^z = 1$ for all the bonds, we can get an approximate spectrum of the fermion. For that, we have to return to the language of complex fermion c. Due to the form of the Hamiltonian (4.48) and the underlying lattice, the resulting spectrum is similar to that of graphene [119]. Adding a magnetic field to the model will corresponding to adding a chemical potential term to the complex fermion [93]. On the other hand, using the approximate spectrum we can study the possible phase transition in the quantum XY model with finite temperature [120].

In the 90° compass model on square lattice, the Z_2 Hamiltonian (4.69) and the condition (4.66) are exact results. To go further, we note that the link variables in (4.69) on the $\hat{x}$ direction are still anti-commuting to each other. Such property is rooted in the anti-commuting link variables in the original Hamiltonian under SO(3) Majorana representation which was discussed in Sec. 3.3.2. We can apply mean-field theory to treat them, and it is believed that proper mean-field treatment of (4.69) will lead to comparable results as the previous works [116], such as quantum phase transition near the point $J_1 = J_2$ [117].

In summary, our application of SO(3) Majorana representation in the three models in this chapter shows a new way to treat spin models. This method features a series of exact mapping and the results are always Z_2 gauge theories with standard Gauss law. The exact Z_2 gauge theories contain all the physics of the original spin model and serve

as the starting point of further approximations, if needed. At this stage, it is important to point out the limitation on the applicability of this method on spin models. As we seen in Sec. 3.1.1, in the SO(3) Majorana representation the z-component spin interaction is mapped into a four-fermion interaction (or density-density interaction), as shown in Eq. (3.12). There is considerable difficulty in treating such four-fermion interaction [21, 40]. Therefore, the mapping of spin models to exact Z_2 gauge theories is only applicable to the spin Hamiltonians which do not have the spin rotational symmetry. Otherwise the four-fermion interaction is included and the application of SO(3) Majorana representation holds no advantage over other representations. Specifically, there is no "$\sigma^z - \sigma^z$" interaction in either of the models considered here, and in the Kitaev model only one spin component is interacting on each bond [23]. However, the exact condition on the applicability of the method is still lacking and one should consider the application of SO(3) Majorana representation in each individual spin model separately.

Chapter 5

U(1) gauge theory of spin models from nonlocal spin representations

In previous chapters, we presented the study of spin models using various spin representations. In Chapter 2, we showed that the application of Abrikosov fermion representation on the mean-field level results in SU(2) gauge structure. We then focus on the SO(3) Majorana representation and demonstrated its application in three types of 2D spin models, which all resulted in exact Z_2 gauge theories (see Chapter 3 and Chapter 4). In this chapter, we will show the application of a special types of spin representation, the *nonlocal spin representation*. Unlike the previous discussed ones, in the non-local spin representation, the spinon operators are not defined on the same site as the spin. Such spin representation is generally useful for some special types of lattice geometries, such as the *pyrochlore* lattice and the *kagome* lattice. To illustrate this, we start with a review of the previous study of the *quantum spin ice*, a model in which spins live on the sites of a pyrochlore lattice. And then I will propose another nonlocal spin representation and discuss its possible application. As we will see, the resulting theory of the nonlocal spin representation usually has a U(1) gauge structure.

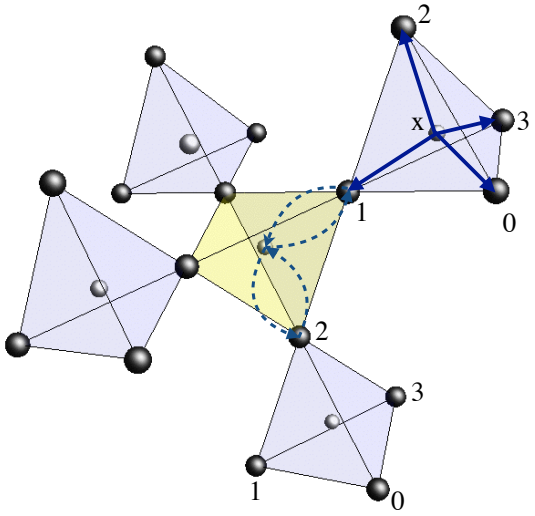

Figure 5.1: The pyrochlore lattice relevant for QSI materials. The centers of blue and yellow tetrahedra, labeled by $\boldsymbol{x}$, form the A and B sublattices of the diamond lattice, correspondingly. $\mu = 0, 1, 2, 3$ label the bonds of the diamond lattice. The spins, $S_{\boldsymbol{x},\mu}$, reside on the pyrochlore sites located on the middle of the bond μ. The dashed lines illustrate the electron hopping paths involved in the super-exchange processes that generate the spin Hamiltonian.

5.1 Quantum spin ice model and the U(1) gauge theory

In this section, we study a model quantum spin liquid (QSL), the quantum spin ice (QSI). Defined on the pyrochlore lattice, a network of corner-sharing tetrahedra (see Fig.5.1), this QSL emerges naturally from the classical spin ice limit [31, 32, 121]. In this limit, there are a macroscopic number of ground states characterized by the so-called "ice rule"; each tetrahedron must be in a two-in/two-out state [121]. Excitations about this manifold have three spins up and one down (or vice-versa) and can be separated at no energy cost [122]. As first shown by Ref. [80], adding transverse exchange induces quantum tunneling between different ice states. A sufficiently weak tunneling stabilizes a QSL ground state with an emergent U(1) gauge field and bosonic spinon excitations[32, 80, 81, 123, 124]. Much effort has been put forth to understand the nature of the QSI phase as well as its static and dynamic properties [80, 81, 123, 124, 125, 126, 127, 128, 129, 130, 131].

5.1.1 Spin Hamiltonian of the quantum spin ice

Before discussing the effective theories developed for the quantum spin ice, we first review the relevant anisotropic exchange models for the pertinent pyrochlore materials. In the candidate materials for QSI, the magnetic degrees of freedom originate from the rare-earth ions [32]. Although we are not per se confining ourselves to the details of the rare-earth ions that currently form the majority of the QSI materials, it is useful to set the stage and make some general observations about the spin Hamiltonian so far considered in the theoretical and experimental investigations of QSI systems [32].

In rare-earth ions, the atomic interactions dominate; the free-ion ground state is determined by following Hund's rules, first minimizing the Coulomb energy, followed by the spin-orbit energy. These free-ion states have well defined total angular momentum, J. In a crystalline environment, due to the electric fields from the surrounding ions, the remaining $2J+1$ degeneracy of this manifold is partially lifted. When J is a half-odd-integer, only Kramers' degeneracy remains and one has a series of doublets for the relevant D_{3d} site symmetry [132]. With respect to this symmetry, these doublets can transform either like spin-1/2 objects, a "pseudo-spin" doublet (as in $Yb_2Ti_2O_7$ or $Er_2Ti_2O_7$) [126], or like a more exotic "dipolar-octupolar" doublet [133] (as in $Dy_2Ti_2O_7$ and $Nd_2Zr_2O_7$). For integer J, Kramers' theorem does not apply and singlet states are possible. However, the D_{3d} site symmetry can allow a non-magnetic doublet, a so-called non-Kramers doublet (as, for example in $Ho_2Ti_2O_7$ or $Tb_2Ti_2O_7$) [132]. If well separated from the other crystal field levels, these crystal field doublets behave like an effective spin-1/2 degree of freedom. For this reason, we will refer to all of these states as a "spin" regardless of whether they are pseudo-spin-1/2, dipolar-octupolar or non-Kramers type.

To describe these doublets, we introduce the spin operators $\boldsymbol{S}_i$, defined in the local basis at each site [126]. For the dipolar-octupolar and non-Kramers doublets, only S_i^z contributes to the magnetic dipole moment with $\boldsymbol{\mu}_i = -g\mu_B S_i^z \hat{z}_i$, where $\hat{z}_i$ is the local [111] direction. For the pseudo-spin-1/2 case, both the $\hat{z}_i$ component and the components perpendicular to $\hat{z}_i$ contribute to the dipole moment. Since these three types of doublets transform quite differently under lattice symmetries [123, 133], the allowed exchange interactions are generally distinct. The most general nearest neighbor

anisotropic exchange model on the pyrochlore lattice can be written as [81, 126]:

$$\begin{aligned} H_{ex} = \sum_{\langle ij \rangle} [& J_{zz} S_i^z S_j^z - J_\pm \left(S_i^+ S_j^- + S_i^- S_j^+ \right) \\ & + J_{\pm\pm} \left(\gamma_{ij} S_i^+ S_j^+ + \text{H.c.} \right) + J_{z\pm} \left(\zeta_{ij} \left[S_i^z S_j^+ + S_i^+ S_j^z \right] + \text{H.c.} \right)], \end{aligned} \tag{5.1}$$

where the matrices $\zeta_{ij} = -\gamma_{ij}^*$ and γ_{ij} are defined in Appendix D. For the case of a pseudo-spin-1/2 doublet, all of these couplings are allowed. For a non-Kramers doublet, one has $J_{z\pm} = 0$ whereas for a dipolar-octupolar doublet, the phases are absent, i.e. $\gamma_{ij} = 1$ and $\zeta_{ij} = 1$ [133]. Microscopically, these kinds of short-range anisotropic interactions can be generated by various super-exchange mechanisms [134, 135]. If $J_{zz} > 0$ and $J_{\pm\pm} = J_\pm = J_{z\pm} = 0$, one recovers the model of classical spin ice. Here we are focusing on a nearest-neighbor description and exclude long-range dipolar interactions. Introducing a finite $J_\pm$ or $J_{\pm\pm}$ with $J_{zz} \gg J_\pm, J_{\pm\pm} \gg J_{z\pm}$ induces quantum tunneling between the ice states [80, 81], and stabilizes a QSI ground state [125, 127, 128, 129]. Note that finite $J_{z\pm}$, for a pseudo-spin-1/2 doublet, produces an ordered ferromagnetic state drawn from the ice manifold [81]. To obtain QSI, one can thus only include $J_{z\pm}$ in concern with $J_\pm$ or $J_{\pm\pm}$. For a dipolar-octupolar doublet, $J_{z\pm}$ is entirely innocuous and can be removed by a local redefinition of the doublet states. While in $Dy_2Ti_2O_7$ and $Ho_2Ti_2O_7$ one expects $J_\pm$ and $J_{\pm\pm}$ to be negligible [135], in other materials such as $Yb_2Ti_2O_7$, $Er_2Ti_2O_7$ or $Tb_2Ti_2O_7$, experiments strongly suggests that these couplings are significant [126, 136, 137, 138, 139]. Since we are interested in the spin ice limit, we shall restrict ourselves to cases where J_{zz} is dominant and is antiferromagnetic ($J_{zz} > 0$). In the remainder of the paper, we thus work with the dimensionless ratios

$$j_\pm = J_\pm / J_{zz}, \quad j_{z\pm} = J_{z\pm} / J_{zz}, \quad j_{\pm\pm} = J_{\pm\pm} / J_{zz}, \tag{5.2}$$

which we assume to be small such that we remain in the QSI phase.

5.1.2 U(1) gauge theory of scalar spinon

We now review the scalar slave-particle description of QSI [81], using the formulation introduced in Ref. [124]. In the following, we use the notation of Refs. [81, 124] and label the pyrochlore sites by a combined index $(\boldsymbol{x}, \mu)$, in which $\boldsymbol{x}$ denotes a diamond

lattice site (center of a tetrahedron) belonging to sublattice A and $\mu = 0, 1, 2, 3$ are the four nearest neighbors of the diamond site, as shown in Fig. 5.1. The spin at the center of the bond $\langle \boldsymbol{x}, \boldsymbol{x} + \boldsymbol{\mu} \rangle$ is then labeled as $\boldsymbol{S}_{\boldsymbol{x},\mu}$, with $\boldsymbol{\mu}$ being the vector connecting the two neighboring diamond sites shown in Fig. 5.1.

We study the exchange Hamiltonian, Eq. (5.1), in an enlarged Hilbert space containing both charge and spin degrees of freedom separately. We construct this by introducing a new Hilbert space for the charge operator $Q_{\boldsymbol{x}}$ on the diamond lattice sites independent of the spins on the pyrochlore sites. In terms of the spins, the charges are defined as

$$Q_{\boldsymbol{x}} = \begin{cases} +\sum_\mu S^z_{\boldsymbol{x},\mu}, & \boldsymbol{x} \in A, \\ -\sum_\mu S^z_{\boldsymbol{x}-\hat{\mu},\mu}, & \boldsymbol{x} \in B. \end{cases} \tag{5.3}$$

The charge operator $Q_{\boldsymbol{x}}$ characterizes violations of the ice rules: $Q_{\boldsymbol{x}} = 0$ being satisfied for a two-in/two-out state, while tetrahedra with three-in/one-out or three-out/one-in have $Q_{\boldsymbol{x}} = \pm 1$ and those with all-in/all-out have $Q_{\boldsymbol{x}} = \pm 2$.

Next, we enlarge the range of allowed charges from strictly $0, \pm 1$ and ± 2 to include all integers. Explicitly, if we define the physical Hilbert space as $\mathcal{H}_{phys} = \bigotimes_{\boldsymbol{x},\mu} \mathcal{H}_{1/2}$, where $\mathcal{H}_{1/2}$ is the spin Hilbert space, then the extended space is

$$\mathcal{H}_{ext} = \left[\bigotimes_{\boldsymbol{x},\mu} \mathcal{H}_{1/2} \right] \otimes \left[\bigotimes_{\boldsymbol{x}} \mathcal{H}_{O(2)} \right] \equiv \mathcal{H}_s \otimes \mathcal{H}_Q, \tag{5.4}$$

and where $\mathcal{H}_{O(2)}$ is the Hilbert space of an $O(2)$ rotor, defined at each diamond site and spanned by an infinite set of basis states that satisfy $Q_{\boldsymbol{x}} |q_{\boldsymbol{x}}\rangle = q_{\boldsymbol{x}} |q_{\boldsymbol{x}}\rangle$, where $q_{\boldsymbol{x}}$ is an integer. We define the physical subspace as the one in which the $Q_{\boldsymbol{x}}$ operators satisfy the constraint of Eq. (5.3).

In this extended space, one then introduces a phase $\theta_{\boldsymbol{x}}$, conjugate to the charge operators $Q_{\boldsymbol{x}}$ [81]. These two operators satisfy the canonical commutation relation

$$[\theta_{\boldsymbol{x}}, Q_{\boldsymbol{x}'}] = i \delta_{\boldsymbol{x},\boldsymbol{x}'}. \tag{5.5}$$

The quantization of $Q_{\boldsymbol{x}}$ implies the periodicity of $\theta_{\boldsymbol{x}}$. The operators $Q_{\boldsymbol{x}}$ and $\theta_{\boldsymbol{x}}$ allow us to introduce a spinon operator, $\psi_{\boldsymbol{x}}$, which is the basic element in a slave particle description of spin ice. To be precise, we define the raising and lowering operators

$\psi^\dagger_{\boldsymbol{x}} = e^{+i\theta_{\boldsymbol{x}}}$ and $\psi_{\boldsymbol{x}} = e^{-i\theta_{\boldsymbol{x}}}$, satisfying

$$[\psi^\dagger_{\boldsymbol{x}}, Q_{\boldsymbol{x}'}] = -\psi^\dagger_{\boldsymbol{x}}\delta_{\boldsymbol{x},\boldsymbol{x}'}, \qquad [\psi_{\boldsymbol{x}}, Q_{\boldsymbol{x}'}] = +\psi_{\boldsymbol{x}}\delta_{\boldsymbol{x},\boldsymbol{x}'}, \tag{5.6}$$

which thus increase or decrease the charge quantum number at diamond lattice site $\boldsymbol{x}$. We then interpret $Q_{\boldsymbol{x}}$ as the spinon number operator in the quantum theory, with $\psi^\dagger_{\boldsymbol{x}}$ and $\psi_{\boldsymbol{x}}$ being spinon creation and annihilation operators [81], living in the Hilbert space $\mathcal{H}_Q$.

For the $\mathcal{H}_s$ part of the extended Hilbert space, we define *new* auxiliary spin-1/2 operators, $\boldsymbol{s}_{\boldsymbol{x},\mu}$. The original physical spin-1/2 operators $\boldsymbol{S}_{\boldsymbol{x},\mu}$ can be expressed in terms of the $\boldsymbol{s}_{\boldsymbol{x},\mu}$, $\psi^\dagger_{\boldsymbol{x}}$ and $\psi_{\boldsymbol{x}}$ operators as

$$S^+_{\boldsymbol{x},\mu} = \psi^\dagger_{\boldsymbol{x}} s^+_{\boldsymbol{x},\mu}\psi_{\boldsymbol{x}+\hat{\mu}}, \tag{5.7a}$$

$$S^-_{\boldsymbol{x},\mu} = \psi^\dagger_{\boldsymbol{x}+\hat{\mu}} s^-_{\boldsymbol{x},\mu}\psi_{\boldsymbol{x}}, \tag{5.7b}$$

$$S^z_{\boldsymbol{x},\mu} = s^z_{\boldsymbol{x},\mu}. \tag{5.7c}$$

These combinations of operators are chosen such that the canonical commutation relations of the original spin-1/2 operators, $\boldsymbol{S}_{\boldsymbol{x},\mu}$, are preserved, and the physical constraint defined by Eq. (5.3) is also respected. If we were able to enforce these constraints exactly, Eqs. (5.3-5.7) would then constitute an exact reformulation of the original spin-1/2 problem of Eq. (5.1). While such an exact description is not feasible, this set of variables have nevertheless proven to be a useful starting point for describing the QSI phases of the anisotropic exchange model given in Eq. (5.1) [81, 124].

The enlargement of the Hilbert space implies a large degree of redundancy in this description. In particular, note that the mapping defined by Eq. (5.7) is invariant under the U(1) transformation

$$\psi_{\boldsymbol{x}} \to \psi_{\boldsymbol{x}} e^{i\alpha_{\boldsymbol{x}}}, \quad s^\pm_{\boldsymbol{x},\mu} \to s^\pm_{\boldsymbol{x},\mu} e^{\pm i(\alpha_{\boldsymbol{x}} - \alpha_{\boldsymbol{x}+\hat{\mu}})}, \tag{5.8}$$

for an arbitrary local phase $\alpha_{\boldsymbol{x}}$. This gauge redundancy can be made explicit by recasting the $\boldsymbol{s}_{\boldsymbol{x},\mu}$ operators in terms of an emergent gauge field, $A_{\boldsymbol{x},\mu}$, and an emergent

electric field, $E_{\boldsymbol{x},\mu}$, via

$$s^{\pm}_{\boldsymbol{x},\mu} = |s^{\pm}_{\boldsymbol{x},\mu}|e^{\pm iA_{\boldsymbol{x},\mu}}, \qquad s^{z}_{\boldsymbol{x},\mu} = E_{\boldsymbol{x},\mu}. \tag{5.9}$$

To simplify the problem, we replace the transverse components of the spin operator by their average values, with $|s^{\pm}_{\boldsymbol{x},\mu}| \approx \langle |s^{\pm}_{\boldsymbol{x},\mu}| \rangle$, and only keep the phase of $s^{\pm}_{\boldsymbol{x},\mu}$ as dynamical variable [30]. It is easy to check that the electric field and the gauge field satisfy the commutation relation

$$[A_{\boldsymbol{x},\mu}, E_{\boldsymbol{x}',\nu}] = i\delta_{\boldsymbol{x}\boldsymbol{x}'}\delta_{\mu\nu}. \tag{5.10}$$

By construction, these fields are compact given the redundancy built into the definition of $A_{\boldsymbol{x},\mu}$ and the periodicity of $\theta_{\boldsymbol{x}}$. This kind of mapping of an auxiliary spin-1/2 system to a gauge theory has been explored in many contexts; we refer the reader to the literature for further details [80, 128, 131].

Having performed this reformulation of the original spin degrees of freedom, we now rewrite H_{ex} in terms of these new variables. One finds

$$\begin{aligned}
H_{ex} &= \frac{1}{2}\sum_{\boldsymbol{x}} Q^2_{\boldsymbol{x}} \\
&- j_{\pm}\langle s^{\pm}\rangle^2 \sum_{\boldsymbol{x}\in\langle A\rangle}\sum_{\mu<\nu}\left[\psi^{\dagger}_{\boldsymbol{x}} e^{i(A_{\boldsymbol{x},\mu}-A_{\boldsymbol{x}+\hat{\mu}-\hat{\nu},\nu})}\psi_{\boldsymbol{x}+\hat{\mu}-\hat{\nu}} + \psi^{\dagger}_{\boldsymbol{x}+\hat{\mu}} e^{-i(A_{\boldsymbol{x},\mu}-A_{\boldsymbol{x},\nu})}\psi_{\boldsymbol{x}+\hat{\nu}} + \text{H.c.}\right] \\
&- j_{z\pm}\langle s^{\pm}\rangle \sum_{\boldsymbol{x}\in\langle A\rangle}\sum_{\mu\neq\nu}\left[E_{\boldsymbol{x},\mu}(\psi^{\dagger}_{\boldsymbol{x}} e^{iA_{\boldsymbol{x},\nu}}\psi_{\boldsymbol{x}+\hat{\nu}} + \psi^{\dagger}_{\boldsymbol{x}+\hat{\mu}-\hat{\nu}} e^{iA_{\boldsymbol{x}+\hat{\mu}-\hat{\nu},\nu}}\psi_{\boldsymbol{x}+\hat{\mu}})\zeta_{\mu\nu} + \text{H.c.}\right] \\
&- j_{\pm\pm}\langle s^{\pm}\rangle^2 \sum_{\boldsymbol{x}\in\langle A\rangle}\sum_{\mu<\nu}\left[(\psi^{\dagger}_{\boldsymbol{x}}\psi_{\boldsymbol{x}+\hat{\mu}}\psi^{\dagger}_{\boldsymbol{x}}\psi_{\boldsymbol{x}+\hat{\nu}} + \psi^{\dagger}_{\boldsymbol{x}+\hat{\mu}-\hat{\nu}}\psi_{\boldsymbol{x}+\hat{\mu}}\psi^{\dagger}_{\boldsymbol{x}}\psi_{\boldsymbol{x}+\hat{\mu}})\gamma_{\mu\nu} + \text{H.c.}\right].
\end{aligned} \tag{5.11}$$

Here we see that the J_{zz}- and $J_{\pm}$-parts of H_{ex} describe the spinon degrees of freedom, as well as their interaction with the gauge field A. Including finite $J_{z\pm}$ introduces further spinon-gauge couplings, while $J_{\pm\pm}$ produces direct four-spinon interactions. In the current work we consider only $J_{z\pm} = J_{\pm\pm} = 0$. Focusing on this limit has several advantages; aside from being theoretically simpler, this limit is common for the exchange models for all three types of microscopic degrees of freedom discussed in Sec. 5.1.1. In addition, there is no sign problem for the exchange model when $J_{\pm} > 0$ and $J_{\pm\pm} = J_{z\pm} = 0$. This would in principle allow validation of these results though direct numerical

simulation [125, 129]. However, in this thesis we pursue an analytical route.

As it stands, the reformulated model H_{ex} of Eq. (5.11) lacks any dynamics for the gauge fields at leading order. To remedy this, we follow Ref. [124] and add to the model

$$H_g \equiv \frac{U}{2} \sum_{\boldsymbol{x}\in\langle A\rangle,\mu} E^2_{\boldsymbol{x},\mu} - g \sum_{\hexagon} \cos\left(\sum_{\boldsymbol{x}\mu\in\hexagon} A_{\boldsymbol{x},\mu} \right), \tag{5.12}$$

to endow the gauge sector with its own dynamics. We denote the full model, with this additional gauge part, as

$$H_{\mathrm{QSI}} \equiv H_{ex} + H_g. \tag{5.13}$$

One should also include the constraint of Eq. (5.3) in addition to the Hamiltonian. Such constraints can be implemented by including a non-dynamical constraint field $\phi_{\boldsymbol{x}}$ into the problem [124]. This field induces a Coulomb interaction between the charges $Q_{\boldsymbol{x}}$ on different sites. Within low-density limit of the exclusive boson representation (to be introduced) these terms can be neglected. The final form can be inspired from the one of the effective Hamiltonian that arises when considering the effects of transverse exchange on the ground state spin-ice manifold [80]. The "ring"-exchange term, proportional to g in Eq. (5.12), appears first at third order in $j_\pm$ or at sixth order in $j_{\pm\pm}$ [80]. Such effective model has been analyzed in detail in Refs. [80, 128]. Here we have added it by hand to make up for some of the deficiencies in the slave-particle approach. In terms of $A_{\boldsymbol{x}\mu}$, the second term in Eq. 5.12 describes the "lattice curl" of the gauge field, while the first term penalizes large electric fields, as required for the mapping of the auxiliary spin-1/2 spins, $\boldsymbol{s}_{\boldsymbol{x}\mu}$, to a gauge theory. For our purposes, we will assume the compactness of the gauge field as innocuous; namely the effects of the gauge monopoles [14, 80] are not considered. Consistent with this assumption, we also take $A_{\boldsymbol{x},\mu} \ll 1$. Under such condition, H_g can be expanded to give [124, 128]

$$H_g = \sum_{\boldsymbol{x}\in\langle A\rangle,\mu} \left[\frac{U}{2} E^2_{\boldsymbol{x},\mu} + \frac{g}{2} B^2_{\boldsymbol{x},\mu} \right], \tag{5.14}$$

where the magnetic fluxes $B_{\boldsymbol{x},\mu}$ derive from the lattice curl of the gauge field $A_{\boldsymbol{x},\mu}$ [128]. In such a phenomenological description, the magnitudes of U and g must be set by comparison with more precise calculations within the full model, Eq. 5.13. For the

case of $j_{\pm\pm} = j_{z\pm} = 0$ they have been estimated to be on the order of $\sim j_\pm^3$ [124, 128]. More specifically, we use the values of Ref. [124], which are

$$g \simeq 24 j_\pm^3, \qquad U \simeq 2.16 j_\pm^3. \tag{5.15}$$

Because of the quantum rotor nature of the bosonic spinon ψ, it is nontrivial to handle the dynamics of the spinon in general. As proposed by Ref. [124], a specific bosonic many-body theory involving special representation of the ψ operators in terms of normal bosonic operators can be applied. Based on this theory, it is possible to calculate the Raman scattering response of the quantum spin ice material under some approximations, this process can be intepreted as the interaction between real U(1) gauge field (the light) and the effective (or artificial) U(1) gauge field in the QSI materials [140]. Details of these studies is beyond the scope of the thesis.

5.2 Staggered Abrikosov fermion representation and potential U(1) gauge theories for spin models

The nonlocal bosonic spin representation in Eq. 5.7 captures the collective dynamics of the spins around a certain tetrahedron by defining a bosonic spinon operator ψ located on the center of the tetrahedron. Such bosonic operator then becomes a new degree of freedom. However, the spin algebra cannot be reproduced with only the spinon operators, so an additional auxiliary "little-s" operator is necessary in Eq. 5.7. The physical meaning of the "little-s" operator is unclear and was treated on the mean-field level. In the effective theory discussed in previous section, the only physical degree of freedom that is left of the "little-s" operator is its phase flucturation. One then expects that the bosonic representation 5.7 can hardly capture all the physics of the quantum spin ice model.

This motivates me to propose another type of nonlocal spin representation for the quantum spin ice models (and some other model) based on the Abrikosov fermion representation. Such representation does not rely on unclearly defined degrees of freedom and is called *staggered Abrikosov fermion representation* due to its structure.

5.2.1 The represenation and its gauge structure

To introduce the staggered Abrikosov fermion representation, we start by considering a spin $\boldsymbol{\sigma}$ located on site $\boldsymbol{r}$ of a pyrochlore lattice (or kagome lattice, see below). One then introduce two complex fermions a and b, located at positions $\boldsymbol{r}+\delta\boldsymbol{r}$ and $\boldsymbol{r}-\delta\boldsymbol{r}$ respectively. Here the definition of the vector $\delta\boldsymbol{r}$ depends on the specific lattice and will be explained in detail later. The staggered Abrikosov fermion representation is given by

$$\sigma^+ = \frac{1}{2}(\sigma^x + i\sigma^y) \sim a^\dagger b; \qquad \sigma^- = \frac{1}{2}(\sigma^x - i\sigma^y) \sim b^\dagger a; \qquad \sigma^z \sim a^\dagger a - b^\dagger b. \tag{5.16}$$

At this stage, we omit the label of the position vectors for these operators, such labelling will be brought back when we discuss real models. More explicitly, we have

$$\sigma^x \sim a^\dagger b + b^\dagger a; \qquad \sigma^y \sim -i(a^\dagger b - b^\dagger a); \qquad \sigma^z \sim a^\dagger a - b^\dagger b. \tag{5.17}$$

From the Abrikosov fermion represenation, it can be shown that the representation (5.16) satisfies the spin relation automatically if we enforce the constraint that the number of fermion is one:

$$a^\dagger a + b^\dagger b = 1. \tag{5.18}$$

The name "staggered Abrikosov fermion representation" comes from the fact that this representation is nonlocal in that the positions of the fermionic spinons are not the same as the spin operator.

Before we move on, some discussions on its applicability is needed. First, let's consider the Hilbert space. The fermion Hilbert space has the same dimension as the spin space once the constraint is imposed. As with the Abrikosov fermion representation, the fermionic operators and the spin operators have the same algebric commutation relations. Thus, the Hilbert space of the nonlocal fermions and the spin Hilbert space have a one-to-one correspondence. Although the position of the fermionic spinons is not the same as the spin operators, the discrepancy has little influence in physical observables since the distance between them is on the scale of one lattice spacing and is small when macroscopic physics is being considered. The physics of the spin systems and the mapped fermionic spinon system is thus expected to be the same as long as

each operator is mapped according to (5.16) properly.

The representation does not change under phase rotation $a \to ae^{i\phi}, \quad b \to be^{i\phi}$, i.e. the two fermions on different sites rotate the same angles. According to the *gauge principle*, the gauge structure requires that the phases of the fermions on different sites can rotate separately and independently. Thus we enlarge the representation (5.16) by introducing a U(1) gauge connection on site $\boldsymbol{r}$, which is the site of the spin.

$$\sigma^+_{\boldsymbol{r}} \sim a^\dagger_{\boldsymbol{r}+\frac{\hat{\mu}}{2}} b_{\boldsymbol{r}-\frac{\hat{\mu}}{2}} e^{iA_{\boldsymbol{r}}}; \qquad \sigma^-_{\boldsymbol{r}} \sim b^\dagger_{\boldsymbol{r}-\frac{\hat{\mu}}{2}} a_{\boldsymbol{r}+\frac{\hat{\mu}}{2}} e^{-iA_{\boldsymbol{r}}}; \qquad \sigma^z_{\boldsymbol{r}} \sim a^\dagger_{\boldsymbol{r}+\frac{\hat{\mu}}{2}} a_{\boldsymbol{r}+\frac{\hat{\mu}}{2}} - b^\dagger_{\boldsymbol{r}-\frac{\hat{\mu}}{2}} b_{\boldsymbol{r}-\frac{\hat{\mu}}{2}}. \tag{5.19}$$

Such representation will be invariant under the local U(1) gauge transformation,

$$a_{\boldsymbol{r}+\frac{\hat{\mu}}{2}} \to a_{\boldsymbol{r}+\frac{\hat{\mu}}{2}} e^{i\phi_{\boldsymbol{r}+\frac{\hat{\mu}}{2}}}; \qquad b_{\boldsymbol{r}-\frac{\hat{\mu}}{2}} \to b_{\boldsymbol{r}-\frac{\hat{\mu}}{2}} e^{i\phi_{\boldsymbol{r}-\frac{\hat{\mu}}{2}}} \qquad A_{\boldsymbol{r}} \to A_{\boldsymbol{r}} + \phi_{\boldsymbol{r}+\frac{\hat{\mu}}{2}} - \phi_{\boldsymbol{r}-\frac{\hat{\mu}}{2}} \tag{5.20}$$

In the equations above, the meaning of the vector $\hat{\mu}$ will become clear later. Similarly with the case of quantum spin ice discussed in the previous section, the staggered complex fermion representation can be applied to spin models defined on the pyrochlore lattice (and the kagome lattice). The lattice structure will facilitate the interpretation of the fermionic spinon a and b as a charge operator on the lattice and it is thus possible to map the spin model to some kind of U(1) lattice gauge theory with the gauge structure 5.20. Contrary to the case we discussed for quantum spin ice in the previous section, in this case there is no need to introduce the "little s" operator whose physical meaning is vague. However, as we shall see later the price to pay is that the "spinon" now is fermionic and is potentially hard to handle.

For the next step, we will move on to discuss the application of the staggered complex fermion representation in the two models, namely the XXZ Heisenberg model on kagome lattice and the XXZ QSI model. Due to the similarity between the kagome lattice and the pyrochole lattice, the treatment of the two cases can be described in the same framework.

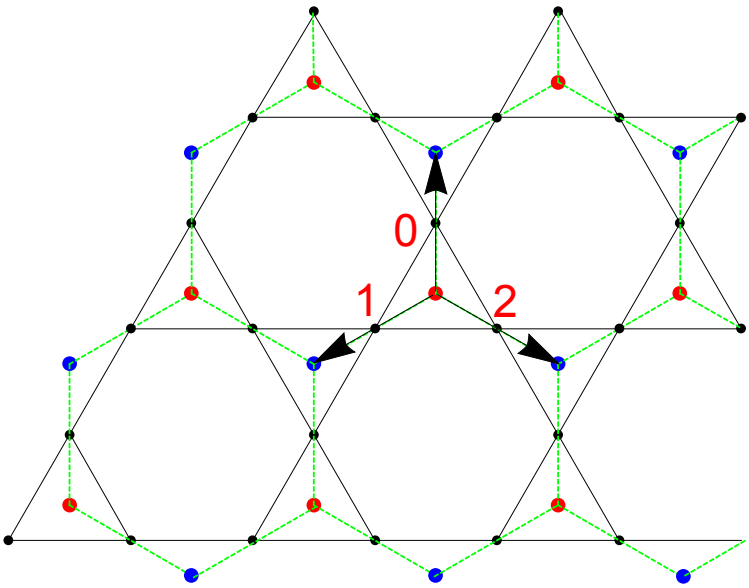

Figure 5.2: The kagome lattice where the XXZ Heisenberg model is defined on. The centers of triangles, labeled by the red and blue dots, form the A and B sublattices of the honeycomb lattice, correspondingly. $\mu = 0, 1, 2$ label the bonds of the underlying honeycomb lattice. The spins reside on the sites of the kagome lattice located on the middle of the honeycomb bond. The a and b-fermions reside on the A and B sublattice sites of the honeycomb lattice.

5.2.2 Application of the staggered Abrikosov fermion representation to the XXZ spin models on kagome and pyrochlore lattice

Let us now consider the XXZ Heisenberg spin interaction, the spin Hamiltonian is written as

$$\mathcal{H} = \sum_{\langle ij \rangle} J_z S_i^z S_j^z + J_{\pm}(S_i^+ S_j^- + S_i^- S_j^+). \tag{5.21}$$

When $J_{\pm} = 0$, this is the Ising model and when $J_z = 0$, it is the XY model. The kagome XXZ Heisenberg model and the XXZ quantum spin ice are very similar in this framework. The pyrochlore lattice and the kagome lattice both have A and B sublattices and we can thus place the a-fermions and b-fermions in the staggered complex fermion representation Eq. 5.16 on the A and B sublattices, respectively. For an illustration of the kagome lattice system, see Fig. 5.2.

For the kagome lattice, the lattice becomes honecomb lattice for the fermionic spinon after the mapping, each site of which has three a-fermions or three b-fermions (coming from the three spins around a certain triangle) on it. For pyrochlore lattice, the lattice for the fermionic spinons becomes diamond lattice (same as the previous section), each site of which has four a-fermions or four b-fermions, which come from the four spins around the tetrahedron, placed on it. We label these fermions by $a_{\boldsymbol{r}\mu}$ or $b_{\boldsymbol{r}\mu}$, in which μ denotes the position of the spin which the fermions are introduced to represent. On kagome lattice, $\mu = 0, 1, 2$ and on pyrochlore lattice, $\mu = 0, 1, 2, 3$. A simple comparison between Fig. 5.1 and Fig. 5.2 can clarify these statements. The spin Hamiltonian (5.21) can be written as, with the U(1) gauge field,

$$\begin{aligned}
\mathcal{H} = \sum_{\boldsymbol{r}\in A}\sum_{\mu\nu} \Big\{ & J_z(a^\dagger_{\boldsymbol{r}\mu}a_{\boldsymbol{r}\mu} - b_{\boldsymbol{r}+\hat{\mu},\mu}b_{\boldsymbol{r}+\hat{\mu},\mu})(a^\dagger_{\boldsymbol{r}\nu}a_{\boldsymbol{r}\nu} - b_{\boldsymbol{r}+\hat{\nu},\nu}b_{\boldsymbol{r}+\hat{\nu},\nu}) \\
& + J_{\pm}\left[(a^\dagger_{\boldsymbol{r}\mu}a_{\boldsymbol{r}\nu})b_{\boldsymbol{r}+\hat{\mu},\mu}b^\dagger_{\boldsymbol{r}+\hat{\nu},\nu}e^{i(A_{\boldsymbol{r}+\frac{\hat{\mu}}{2}} - A_{\boldsymbol{r}+\frac{\hat{\nu}}{2}})} + \text{H.c.}\right]\Big\} \\
+ \sum_{\boldsymbol{r}\in B}\sum_{\mu\nu} \Big\{ & J_z(a^\dagger_{\boldsymbol{r}+\hat{\mu},\mu}a_{\boldsymbol{r}+\hat{\mu},\mu} - b_{\boldsymbol{r}\mu}b_{\boldsymbol{r}\mu})(a^\dagger_{\boldsymbol{r}+\hat{\nu},\nu}a_{\boldsymbol{r}+\hat{\nu},\nu} - b_{\boldsymbol{r},\nu}b_{\boldsymbol{r},\nu}) \\
& + J_{\pm}\left[(b_{\boldsymbol{r}\mu}b^\dagger_{\boldsymbol{r}\nu})a^\dagger_{\boldsymbol{r}+\hat{\mu},\mu}a_{\boldsymbol{r}+\hat{\nu},\nu}e^{i(A_{\boldsymbol{r}+\frac{\hat{\mu}}{2}} - A_{\boldsymbol{r}+\frac{\hat{\nu}}{2}})} + \text{H.c.}\right]\Big\}.
\end{aligned} \tag{5.22}$$

As stated above, for the kagome lattice (honecomb lattice), we have $\mu, \nu = 0, 1, 2$ and for

the pyrochlore lattice (diamond lattice) we have $\mu, \nu = 0, 1, 2, 3$. The vector $\hat{\mu}$ denote the lattice vectors (connecting A and B sublattices) of the underlying diamond lattice on the pyrochlore lattice and the underlying honeycomb lattice of the kagome lattice (see Fig. 5.1 and Fig. 5.2 for an illustration). The summation $\sum_{\mu\nu}$ is understood as taken over all possible *combinations* of $\mu\nu$, it is not summed over μ and ν independently. The constraint on the fermionic Hilbert space is written as (on both the kagome and pyrochlore lattices)

$$n^a_{\boldsymbol{r}\mu} + n^b_{\boldsymbol{r}+\hat{\mu},\mu} = 1, \tag{5.23}$$

in which we define $n^a_{\boldsymbol{r}\mu} = a^\dagger_{\boldsymbol{r}\mu} a_{\boldsymbol{r}\mu}$ as the number of a-fermion on A sublattice corresponding to bond μ and $n^b_{\boldsymbol{r}+\hat{\mu},\mu}$ being the number of b-fermion on B sublattice correspondingly.

For the next step we focus on the J_z term in the Hamiltonian 5.22. We have

$$\begin{aligned}
&\sum_{\boldsymbol{r}\in A}\sum_{\mu\nu}(a^\dagger_{\boldsymbol{r}\mu}a_{\boldsymbol{r}\mu} - b_{\boldsymbol{r}+\hat{\mu},\mu}b_{\boldsymbol{r}+\hat{\mu},\mu})(a^\dagger_{\boldsymbol{r}\nu}a_{\boldsymbol{r}\nu} - b_{\boldsymbol{r}+\hat{\nu},\nu}b_{\boldsymbol{r}+\hat{\nu},\nu}) \\
&= \sum_{\boldsymbol{r}\in A}\sum_{\mu\nu}(n^a_{\boldsymbol{r}\mu} - n^b_{\boldsymbol{r}+\hat{\mu},\mu})(n^a_{\boldsymbol{r}\nu} - n^b_{\boldsymbol{r}+\hat{\nu},\nu}) \\
&= \sum_{\boldsymbol{r}\in A}\sum_{\mu\nu}(2n^a_{\boldsymbol{r}\mu} - 1)(2n^a_{\boldsymbol{r}\nu} - 1) \\
&= \sum_{\boldsymbol{r}\in A}\sum_{\mu\nu} 4n^a_{\boldsymbol{r}\mu}n^a_{\boldsymbol{r}\nu} - 2n^a_{\boldsymbol{r}\mu} - 2n^a_{\boldsymbol{r}\nu} + 1.
\end{aligned} \tag{5.24}$$

We note that for both kagome and pyrochlore lattices, using the fact that the number of fermion n can only be 1 or 0 we have

$$(\sum_\mu n^a_{\boldsymbol{r}\mu})^2 = \sum_\mu n^a_{\boldsymbol{r}\mu} + 2\sum_{\mu\nu} n^a_{\boldsymbol{r}\mu}n^a_{\boldsymbol{r}\nu}. \tag{5.25}$$

Again, the summation $\sum_{\mu\nu}$ is understood as taken over all possible combinations of $\mu\nu$. This invites us to define

$$Q^a_{\boldsymbol{r}} \equiv \sum_\mu n^a_{\boldsymbol{r}\mu}, \tag{5.26}$$

which is the total number of the a-fermion on each site of the A sublattice. Similar definition applies for the b-fermion on each B sublattice site. With this definition we

have,

$$\begin{aligned} \sum_{\mu\nu} n^a_{\boldsymbol{r}\mu} + n^a_{\boldsymbol{r}\nu} &= 3Q^a_{\boldsymbol{r}} \qquad \text{for pyrochlore lattice} \\ \sum_{\mu\nu} n^a_{\boldsymbol{r}\mu} + n^a_{\boldsymbol{r}\nu} &= 2Q^a_{\boldsymbol{r}} \qquad \text{for kagome lattice.} \end{aligned} \tag{5.27}$$

Therefore the initial J_z term in the Hamiltonian 5.22 can be written as

$$\begin{aligned} \sum_{\boldsymbol{r}\in A}\sum_{\mu\nu} 4n^a_{\boldsymbol{r}\mu}n^a_{\boldsymbol{r}\nu} - 2n^a_{\boldsymbol{r}\mu} - 2n^a_{\boldsymbol{r}\nu} + 1 &= \sum_{\boldsymbol{r}\in A}[2Q^{a2}_{\boldsymbol{r}} - 8Q^a_{\boldsymbol{r}} + 1] \qquad \text{for pyrochlore lattice} \\ \sum_{\boldsymbol{r}\in A}\sum_{\mu\nu} 4n^a_{\boldsymbol{r}\mu}n^a_{\boldsymbol{r}\nu} - 2n^a_{\boldsymbol{r}\mu} - 2n^a_{\boldsymbol{r}\nu} + 1 &= \sum_{\boldsymbol{r}\in A}[2Q^{a2}_{\boldsymbol{r}} - 6Q^a_{\boldsymbol{r}} + 1] \qquad \text{for kagome lattice.} \end{aligned} \tag{5.28}$$

With these definitions and transformations, the Hamiltonian for XXZ model on pyrochlore lattice is written as,

$$\begin{aligned} &\mathcal{H} = \\ &\sum_{\boldsymbol{r}\in A}\left\{J_z[2Q^{a2}_{\boldsymbol{r}} - 8Q^a_{\boldsymbol{r}} + 1] + \sum_{\mu\nu} J_\pm\left[(a^\dagger_{\boldsymbol{r}\mu}a_{\boldsymbol{r}\nu})b_{\boldsymbol{r}+\hat{\mu},\mu}b^\dagger_{\boldsymbol{r}+\hat{\nu},\nu}e^{i(A_{\boldsymbol{r}+\frac{\hat{\mu}}{2}} - A_{\boldsymbol{r}+\frac{\hat{\nu}}{2}})} + h.c.\right]\right\} \\ &+\sum_{\boldsymbol{r}\in B}\left\{J_z[2Q^{b2}_{\boldsymbol{r}} - 8Q^b_{\boldsymbol{r}} + 1] + \sum_{\mu\nu} J_\pm\left[(b_{\boldsymbol{r}\mu}b^\dagger_{\boldsymbol{r}\nu})a^\dagger_{\boldsymbol{r}+\hat{\mu},\mu}a_{\boldsymbol{r}+\hat{\nu},\nu}e^{i(A_{\boldsymbol{r}+\frac{\hat{\mu}}{2}} - A_{\boldsymbol{r}+\frac{\hat{\nu}}{2}})} + h.c.\right]\right\}. \end{aligned} \tag{5.29}$$

And the Hamiltonian for XXZ model on kagome lattice can be written simply by replacing the J_z term using Eq. 5.28. In both pyrochlore and kagome systems, the system is completely classical for $J_\pm = 0$. The ground state for the pyrochlore model is captured by equation $Q^a_{\boldsymbol{r}} = Q^b_{\boldsymbol{r}} = 2$. This is exactly the "two-in-two-out" ice rule condition for spin ice materials discussed in the previous section. For the kagome system on the other hand, the naive classical ground state is given by $Q^a_{\boldsymbol{r}} = Q^b_{\boldsymbol{r}} = \frac{3}{2}$ which cannot be satisfied. The true ground state is thus expected to be a distribution of $Q_{\boldsymbol{r}} = 1$ or $Q_{\boldsymbol{r}} = 2$ on the entire lattice. Such distribution has macroscopic degeneracy and thus implies frustration and possible spin liquid behavior.

For the next step, let us briefly discuss the possible ways to treat the Hamiltonian 5.29. It is clear from the four-fermion interaction term in the Hamiltonian 5.29 that the systems are not exactly solvable, therefore some kinds of approximation are necessary.

As we can see, the four-fermion interaction terms contain two fermions of the same kind (a-fermion or b-fermion) on the same site of the lattice, while the term containing the other kind of fermion describes a hopping within the same sublattice. This invites us to apply a mean-field theory. To this end, one can define the Hubbard-Stranovich fields

$$\langle a^\dagger_{\boldsymbol{r}\mu} a_{\boldsymbol{r}\nu}\rangle = \tilde{\gamma}^{\mu\nu}_{\boldsymbol{r}}, \qquad \langle b^\dagger_{\boldsymbol{r}\mu} b_{\boldsymbol{r}\nu}\rangle = -\gamma^{\mu\nu}_{\boldsymbol{r}}. \tag{5.30}$$

They satisfy $\gamma^{\mu\nu *}_{\boldsymbol{r}} = \gamma^{\nu\mu}_{\boldsymbol{r}}$. With these, the Hamiltonian Eq. 5.29 (for pyrochlore system) is transformed into

$$\begin{aligned}\mathcal{H} = &\sum_{\boldsymbol{r}\in A}\sum_{\mu\nu}\left\{J_z[2Q^{a2}_{\boldsymbol{r}} - 8Q^a_{\boldsymbol{r}} + 1] + J_\pm\left[\tilde{\gamma}^{\mu\nu}_{\boldsymbol{r}} b_{\boldsymbol{r}+\hat{\mu},\mu} b^\dagger_{\boldsymbol{r}+\hat{\nu},\nu} e^{i(A_{\boldsymbol{r}+\frac{\hat{\mu}}{2}} - A_{\boldsymbol{r}+\frac{\hat{\nu}}{2}})} + h.c.\right]\right\} \\ &+ \sum_{\boldsymbol{r}\in B}\sum_{\mu\nu}\left\{J_z[2Q^{b2}_{\boldsymbol{r}} - 8Q^b_{\boldsymbol{r}} + 1] + J_\pm\left[\gamma^{\nu\mu}_{\boldsymbol{r}} a^\dagger_{\boldsymbol{r}+\hat{\mu},\mu} a_{\boldsymbol{r}+\hat{\nu},\nu} e^{i(A_{\boldsymbol{r}+\frac{\hat{\mu}}{2}} - A_{\boldsymbol{r}+\frac{\hat{\nu}}{2}})} + h.c.\right]\right\}.\end{aligned} \tag{5.31}$$

The mean-field Hamiltonian 5.31 describes a U(1) lattice gauge theory. The theory actually consists of two parts on the two sublattices, the a-fermion only hopps on the A-sublattice and the b-fermion only hopps on the B sublattice. The connection between the two parts is through the mean-field parameter γ. The theory is not easy to solve because of various constraints. Firstly, the single fermion constraint 5.18 should be taken into account; and secondly, the consistency of the mean-field definition 5.30 should also be considered. Possible ways to treat the model Hamiltonian 5.31 is to apply computer simulation. Detailed subsequent studies in this direction is left for the future.

Chapter 6

Conclusion and Discussion

In this dissertation, I have explored the gauge theory description of spin models, an approach rooted in the study of quantum spin liquid states. The starting point of this approach is to write the spin operator in terms of slave-particle operators, which are often called spinons. After such mapping the original spin model Hamiltonian becomes an interacting Hamiltonian of spinons. Because there is usually redundancy in the spin representations, the resulting theories always possess gauge symmetry. In this regard, I started with a review of the traditional Abrikosov fermion representation and discussed its application in spin models with Heisenberg interaction. Because the resulting spinon Hamiltonian contains four-fermion interaction terms, a mean-field approach is applied and the resulting theory is a SU(2) gauge theory with spinon doublet as its matter field. As we pointed out, this approach has a number of difficulties in its application. Most importantly the assumptions of the mean-field approach are not always valid and it is usually hard to correctly pick up the mean-field parameters for each specific model. Moreover, the representation itself requires a "single-occupation" constraint to reproduce the correct spin algebra, such constraint is brought into the effective gauge theory in terms of a auxiliary Lagrange multiplier field, which makes the theory more complicated.

Other types of spin representation exist without the difficulties of the traditional Abrikosov fermion representation. In this regard, we discussed the Majorana representation in Chapter 3 and Chapter 4. We discussed three types of Majorana represenation,

namely the SO(3) Majorana representation, the SO(4) chiral representation and the Kitaev representation, which Kitaev applied in his solution to an exactly solvable spin model on honeycomb lattice (called the Kitaev model). We started with a discussion on the relationship between the three types of Majorana representation, and we pointed out that these three types of representation could be understood in the same framework by refering to the spinor representation of the SO(4) group. Among the three types, the SO(3) Majorana represenation stands out because it does not require any additional constraints to reproduce the spin algebra, which implies potential advantage over the other types of slave-particle spin representations. In light of this, we focused on the SO(3) Majorana representation and explored more properties of it. Importantly, due to its nonlocal nature, we argued that it is equivalent to the Jordan-Wigner transformation in both 1D and 2D spin models. We also pointed out that the SO(3) Majorana representation might have broader application than the Jordan-Wigner transformation because it is better defined, especially in the 2D case.

To apply the SO(3) Majorana representation in real systems, we discussed three 2D spin models. We started with the Kitaev model and obtained the equivalent solution to it using the SO(3) Majorana representation. Our solution takes the form of a standard Z_2 gauge theory with standard Gauss law constraint. Comparing with Kitaev's original solution, our solution shows how to get to the physical space in a systematic way. We then consider further application in two other spin models which do not has exact solvability, namely the quantum XY model on honeycomb lattice and the 90° compass model on square lattice. In these two models we used the same strategy as the solution of the Kitaev model. The resulting theories are Z_2 lattice gauge theories with some non-trivial features. Although the Z_2 theories themselves are not integrable, they are still different from previous studies using the SO(3) Majorana representation in that no approximation was brought in. In other words, the Z_2 gauge theories we obtained contain the same *physical* information as the original spin models. For the next step, approximation has to be introduced to the Z_2 gauge theories to acquire more physical properties of the model. In this regard, the Z_2 lattice gauge theories can serve as a new platform for the study of these spin models.

Besides the local spin representations, the specific lattice geometries of the spin model may facilitate the definition of a special type of spin representation, the nonlocal

spin representation. In this regard, the quantum spin ice (QSI) model stands out. In the QSI model the spins are located on the sites of the pyrochlore lattice which consists of corner-sharing tetrahedra. In this specific lattice one can place the spinon operator on the center of each tetrahedron and each spin is representated by a *dipole* of spinon. As we discussed in detail in Chapter 5, previous studies constructed such a theory in terms of bosonic spinon which results in a U(1) lattice gauge theory. The theory has a number of difficulties, including a "little-s" operator whose physical meaning was unclear and had to be treated on the mean-field level. To resolve this problem, I proposed a similar nonlocal representation based on the Abrikosov fermion representation, in which each spin of the QSI model is represented by a *fermionic dipole*. Due to the similarities of lattice geometry with the pyrochlore lattice, I pointed out that such representation can be used for XXZ Heisenberg model on the kagome lattice as well. Because of the redundancy, the resulting theory is a U(1) gauge theory.

In all the cases disscussed in this dissertation, the spin models are mapped into lattice gauge theories of various gauge group. Such gauge theories are expected to possess part of (or all of) the physics of the original spin models. To further explore the properties of such theories, we can certainly borrow the concepts of the gauge theory in particle physics. Some concepts such as *confinement* transition has already been used in the discussion of the physics of the quantum spin liquid phases. Due to various limitations, such an explaination is far from well-established so far. Further consideration is needed to clarify these issues. Specifically, in this dissertation we have identified some clear directions for future studies.

Firstly, in our application of the SO(3) Majorana representation in the three spin models, future work will be directed to explore more physical properties of the models based on the Z_2 gauge theories. In particular, for the Kitaev model, it is possible to study the edge modes as well as thermal transport properties using our solution. For the quantum XY model on honeycomb lattice and the 90° compass model on square lattice, we will have further discussion on the further approximation needed to treat the Z_2 gauge theories and their implications on the physical properties of the models. It is believed that, although the present Z_2 gauge theories are not exactly solvable, the discrete nature of the gauge group will bring opportunities for us to have a better controlled way to study them. On the other hand, in future studies one could explore

the application of the SO(3) Majorana representation in other types of spin models, such as other types of compass models. Another important direction for future study is to apply the SO(3) Majorana representation in three-dimensional spin models.

As for the nonlocal spin representations for the QSI model, further treatment is needed to explore the physics based on the staggered Abrikosov fermion representation. In this regard, mean-field studies can be applied. Also, it would be an interesting direction to find other possible spin representations for the specific lattice geometry.

To conclude, due to the interesting features of the quantum spin systems, I believe that it will remain a major area in modern condensed matter physics. And the gauge theory description of the spin systems will continue to be an interesting direction of research.

References

[1] R. P. Feynman, R. B. Leighton, and M. Sands. *The Feynman Lectures on Physics, Vol. I: Mainly Mechanics, Radiation, and Heat*. The Feynman Lectures on Physics. Addison-Wesley, 1964.

[2] M. E. Peskin and D. V. Schroeder. *An Introduction To Quantum Field Theory*. Frontiers in Physics. Westview Press, 1995.

[3] M. D. Schwartz. *Quantum Field Theory and the Standard Model*. Quantum Field Theory and the Standard Model. Cambridge University Press, 2014.

[4] Q. Ho-Kim and X. Y. Pham. *Elementary Particles and Their Interactions: Concepts and Phenomena*. Springer Berlin Heidelberg, 2013.

[5] T. P. Cheng and L. F. Li. *Gauge Theory of Elementary Particle Physics*. Oxford science publications. Clarendon Press, 1984.

[6] W. Pauli. *Theory of Relativity*. Dover Books on Physics. Dover Publications, 1981.

[7] J. Polchinski. *String Theory: Volume 1, An Introduction to the Bosonic String*. Cambridge Monographs on Mathematical Physics. Cambridge University Press, 1998.

[8] N. W. Ashcroft and N. D. Mermin. *Solid State Physics*. HRW international editions. Holt, Rinehart and Winston, 1976.

[9] L. D. Landau and E. M. Lifshitz. *Statistical Physics*. Course of theoretical physics. Butterworth-Heinemann, 2013.

[10] E. M. Lifshitz and L. P. Pitaevskii. *Statistical Physics: Theory of the Condensed State*. Course of theoretical physics. Butterworth-Heinemann, 2013.

[11] P. W. Anderson. More is different. *Science*, 177(4047):393–396, 1972, http://science.sciencemag.org/content/177/4047/393.full.pdf.

[12] A. Altland and B. D. Simons. *Condensed Matter Field Theory*. Cambridge books online. Cambridge University Press, 2010.

[13] Eduardo Fradkin. *Field Theories of Condensed Matter Physics*. Cambridge University Press, second edition, 2013.

[14] John B. Kogut. An introduction to lattice gauge theory and spin systems. *Rev. Mod. Phys.*, 51:659–713, Oct 1979.

[15] J. Bardeen, L. N. Cooper, and J. R. Schrieffer. Theory of superconductivity. *Phys. Rev.*, 108:1175–1204, Dec 1957.

[16] A. J. Leggett. Superfluidity. *Rev. Mod. Phys.*, 71:S318–S323, Mar 1999.

[17] D. J. Thouless, M. Kohmoto, M. P. Nightingale, and M. den Nijs. Quantized hall conductance in a two-dimensional periodic potential. *Phys. Rev. Lett.*, 49:405–408, Aug 1982.

[18] David Tong. Lectures on the quantum Hall effect. *arXiv:1606.06687*, 2016.

[19] A. Auerbach. *Interacting Electrons and Quantum Magnetism*. Graduate Texts in Contemporary Physics. Springer-Verlag New York, 1994.

[20] A.A. Abrikosov, L.P. Gorkov, I.E. Dzyaloshinski, and I.E. Dzyaloshinski *Methods of Quantum Field Theory in Statistical Physics*. Dover Books on Physics Series. Dover Publications, 1975.

[21] R. Shankar. Renormalization-group approach to interacting fermions. *Rev. Mod. Phys.*, 66:129–192, Jan 1994.

[22] A. Yu. Kitaev. Fault-tolerant quantum computation by anyons. *Annals of Physics*, 303(1):2 – 30, 2003.

[23] Alexei Kitaev. Anyons in an exactly solved model and beyond. *Annals of Physics*, 321(1):2 – 111, 2006.

[24] Lawrence Schulman. A path integral for spin. *Phys. Rev.*, 176:1558–1569, Dec 1968.

[25] P. B. Wiegmann. Superconductivity in strongly correlated electronic systems and confinement versus deconfinement phenomenon. *Phys. Rev. Lett.*, 60:821–824, Feb 1988.

[26] Eduardo Fradkin and Michael Stone. Topological terms in one- and two-dimensional quantum heisenberg antiferromagnets. *Phys. Rev. B*, 38:7215–7218, Oct 1988.

[27] Fedor Levkovich-Maslyuk. The bethe ansatz. *Journal of Physics A: Mathematical and Theoretical*, 49(32):323004, Jul 2016.

[28] T. Holstein and H. Primakoff. Field dependence of the intrinsic domain magnetization of a ferromagnet. *Phys. Rev.*, 58:1098–1113, Dec 1940.

[29] P. W. Anderson. Resonating valence bonds: A new kind of insulator? *Mat. Res. Bull*, 8(2):153 – 160, 1973.

[30] Xiao-Gang Wen. Quantum orders and symmetric spin liquids. *Phys. Rev. B*, 65:165113, Apr 2002.

[31] Leon Balents. Spin liquids in frustrated magnets. *Nature*, 464(7286):199–208, 2010.

[32] M. J. P. Gingras and P. A. McClarty. Quantum spin ice: a search for gapless quantum spin liquids in pyrochlore magnets. *Reports on Progress in Physics*, 77(5):056501, 2014.

[33] Lucile Savary and Leon Balents. Quantum spin liquids: a review. *Reports on Progress in Physics*, 80(1):016502, 2017.

[34] Yi Zhou, Kazushi Kanoda, and Tai-Kai Ng. Quantum spin liquid states. *Rev. Mod. Phys.*, 89:025003, Apr 2017.

[35] P. Fazekas and P. W. Anderson. On the ground state properties of the anisotropic triangular antiferromagnet. *Phil. Mag.*, 30(2):423–440, 1974.

[36] V. Kalmeyer and R. B. Laughlin. Equivalence of the resonating-valence-bond and fractional quantum Hall states. *Phys. Rev. Lett.*, 59:2095–2098, Nov 1987.

[37] X. G. Wen. Topological orders in rigid states. *International Journal of Modern Physics B*, 04(02):239–271, 1990, https://doi.org/10.1142/S0217979290000139.

[38] X. G. Wen. Mean-field theory of spin-liquid states with finite energy gap and topological orders. *Phys. Rev. B*, 44:2664–2672, Aug 1991.

[39] X. G. Wen. *Quantum Field Theory of Many-Body Systems: From the Origin of Sound to an Origin of Light and Electrons*. Oxford Graduate Texts. Oxford, 2004.

[40] Patrick A. Lee, Naoto Nagaosa, and Xiao-Gang Wen. Doping a Mott insulator: Physics of high-temperature superconductivity. *Rev. Mod. Phys.*, 78:17–85, Jan 2006.

[41] S. Liang, B. Doucot, and P. W. Anderson. Some new variational resonating-valence-bond-type wave functions for the spin-1/2 antiferromagnetic Heisenberg model on a square lattice. *Phys. Rev. Lett.*, 61:365–368, Jul 1988.

[42] Daniel S. Rokhsar and Steven A. Kivelson. Superconductivity and the quantum hard-core dimer gas. *Phys. Rev. Lett.*, 61:2376–2379, Nov 1988.

[43] Piers Coleman. New approach to the mixed-valence problem. *Phys. Rev. B*, 29:3035–3044, Mar 1984.

[44] G. Baskaran, Z. Zou, and P.W. Anderson. The resonating valence bond state and high-Tc superconductivity - A mean field theory. *Solid State Communications*, 63(11):973 – 976, 1987.

[45] Andrei E. Ruckenstein, Peter J. Hirschfeld, and J. Appel. Mean-field theory of high-T_c superconductivity: The superexchange mechanism. *Phys. Rev. B*, 36:857–860, Jul 1987.

[46] Menke U. Ubbens and Patrick A. Lee. Flux phases in the t-J model. *Phys. Rev. B*, 46:8434–8439, Oct 1992.

[47] Michael Hermele. SU(2) gauge theory of the Hubbard model and application to the honeycomb lattice. *Phys. Rev. B*, 76:035125, Jul 2007.

[48] Michael Hermele, T. Senthil, and Matthew P. A. Fisher. Algebraic spin liquid as the mother of many competing orders. *Phys. Rev. B*, 72:104404, Sep 2005.

[49] J. Brad Marston and Ian Affleck. Large-n limit of the Hubbard-Heisenberg model. *Phys. Rev. B*, 39:11538–11558, Jun 1989.

[50] Ian Affleck and J. Brad Marston. Large-n limit of the Heisenberg-Hubbard model: Implications for high-T_c superconductors. *Phys. Rev. B*, 37:3774–3777, Mar 1988.

[51] Ryuichi Shindou and Tsutomu Momoi. $SU(2)$ slave-boson formulation of spin nematic states in $s = \frac{1}{2}$ frustrated ferromagnets. *Phys. Rev. B*, 80:064410, Aug 2009.

[52] F. J. Burnell and Chetan Nayak. SU(2) slave fermion solution of the Kitaev honeycomb lattice model. *Phys. Rev. B*, 84:125125, Sep 2011.

[53] G. Baskaran, Saptarshi Mandal, and R. Shankar. Exact results for spin dynamics and fractionalization in the Kitaev model. *Phys. Rev. Lett.*, 98:247201, Jun 2007.

[54] G. Jackeli and G. Khaliullin. Mott insulators in the strong spin-orbit coupling limit: From Heisenberg to a quantum compass and Kitaev models. *Phys. Rev. Lett.*, 102:017205, Jan 2009.

[55] Yogesh Singh and P. Gegenwart. Antiferromagnetic Mott insulating state in single crystals of the honeycomb lattice material Na_2IrO_3. *Phys. Rev. B*, 82:064412, Aug 2010.

[56] Yogesh Singh, S. Manni, J. Reuther, T. Berlijn, R. Thomale, W. Ku, S. Trebst, and P. Gegenwart. Relevance of the Heisenberg-Kitaev model for the Honeycomb Lattice Iridates A_2IrO_3. *Phys. Rev. Lett.*, 108:127203, Mar 2012.

[57] Feng Ye, Songxue Chi, Huibo Cao, Bryan C. Chakoumakos, Jaime A. Fernandez-Baca, Radu Custelcean, T. F. Qi, O. B. Korneta, and G. Cao. Direct evidence of a zigzag spin-chain structure in the honeycomb lattice: A neutron and x-ray diffraction investigation of single-crystal Na_2IrO_3. *Phys. Rev. B*, 85:180403, May 2012.

[58] Sae Hwan Chun, Jong-Woo Kim, Jungho Kim, H. Zheng, Constantinos C. Stoumpos, C. D. Malliakas, J. F. Mitchell, Kavita Mehlawat, , Yogesh Singh, Y. Choi, T. Gog, A. Al-Zein, M. Moretti Sala, M. Krisch, J. Chaloupka, G. Jackeli, G. Khaliullin, and B. J. Kim. Direct evidence for dominant bond-directional interactions in a honeycomb lattice iridate Na_2IrO_3. *Nat Phys*, 10:1038, 2015.

[59] S. C. Williams, R. D. Johnson, F. Freund, Sungkyun Choi, A. Jesche, I. Kimchi, S. Manni, A. Bombardi, P. Manuel, P. Gegenwart, and R. Coldea. Incommensurate counterrotating magnetic order stabilized by Kitaev interactions in the layered honeycomb α-Li_2IrO_3. *Phys. Rev. B*, 93:195158, May 2016.

[60] K. W. Plumb, J. P. Clancy, L. J. Sandilands, V. Vijay Shankar, Y. F. Hu, K. S. Burch, Hae-Young Kee, and Young-June Kim. $\alpha - RuCl_3$: A spin-orbit assisted Mott insulator on a honeycomb lattice. *Phys. Rev. B*, 90:041112, Jul 2014.

[61] J. A. Sears, M. Songvilay, K. W. Plumb, J. P. Clancy, Y. Qiu, Y. Zhao, D. Parshall, and Young-June Kim. Magnetic order in $\alpha-RuCl_3$: A honeycomb-lattice quantum magnet with strong spin-orbit coupling. *Phys. Rev. B*, 91:144420, Apr 2015.

[62] R. D. Johnson, S. C. Williams, A. A. Haghighirad, J. Singleton, V. Zapf, P. Manuel, I. I. Mazin, Y. Li, H. O. Jeschke, R. Valentí, and R. Coldea. Monoclinic crystal structure of $\alpha - RuCl_3$ and the zigzag antiferromagnetic ground state. *Phys. Rev. B*, 92:235119, Dec 2015.

[63] K. Kitagawa, T. Takayama, Y. Matsumoto, A. Kato, R. Takano, Y. Kishimoto, R. Dinnebier, G. Jackeli, and H. Takagi. Quantum liquid of Kramers doublets on a honeycomb lattice. *Nature*, 2018.

[64] William Witczak-Krempa, Gang Chen, Yong Baek Kim, and Leon Balents. Correlated quantum phenomena in the strong spin-orbit regime. *Annu. Rev. Condens. Matter Phys.*, 5(1):57–82, 2014.

[65] Jeffrey G. Rau, Eric Kin-Ho Lee, and Hae-Young Kee. Spin-orbit physics giving rise to novel phases in correlated systems: Iridates and related materials. *Annual Review of Condensed Matter Physics*, 7:195, 2015.

[66] Simon Trebst. Kitaev Materials. *arXiv:1701.07056*, 2017.

[67] M. Hermanns, I. Kimchi, and J. Knolle. Physics of the Kitaev model: Fractionalization, dynamical correlations, and material connections. *Annual Review of Condensed Matter Physics*, 9(1):17, 2018, https://doi.org/10.1146/annurev-conmatphys-033117-053934.

[68] F. A. Berezin and M. S. Marinov. Classical spin and Grassmann algebra. *Sov. Phys. JETP Lett.*, 21:320, 1975.

[69] F. A. Berezin and M. S. Marinov. Particle spin dynamics as the Grassmann variant of classical mechanics. *Ann. Phys.*, 104:336, 1977.

[70] A. M. Tsvelik. New fermionic description of quantum spin liquid state. *Phys. Rev. Lett.*, 69:2142–2144, Oct 1992.

[71] Alexei M. Tsvelik. *Quantum Field Theory in Condensed Matter Physics*. Cambridge University Press, second edition, 2003.

[72] Alexander Shnirman and Yuriy Makhlin. Spin-spin correlators in the Majorana representation. *Phys. Rev. Lett.*, 91:207204, Nov 2003.

[73] W. Mao, P. Coleman, C. Hooley, and D. Langreth. Spin dynamics from Majorana fermions. *Phys. Rev. Lett.*, 91:207203, Nov 2003.

[74] Jianlong Fu, Johannes Knolle, and Natalia B. Perkins. Three types of representation of spin in terms of Majorana fermions and an alternative solution of the Kitaev honeycomb model. *Phys. Rev. B*, 97:115142, Mar 2018.

[75] B. Sriram Shastry and Diptiman Sen. Majorana fermion representation for an antiferromagnetic spin- chain. *Phys. Rev. B*, 55:2988–2994, Feb 1997.

[76] Rudro R. Biswas, Liang Fu, Chris R. Laumann, and Subir Sachdev. SU(2)-invariant spin liquids on the triangular lattice with spinful Majorana excitations. *Phys. Rev. B*, 83:245131, Jun 2011.

[77] Tim Herfurth, Simon Streib, and Peter Kopietz. Majorana spin liquid and dimensional reduction in Cs_2CuCl_4. *Phys. Rev. B*, 88:174404, Nov 2013.

[78] Gang Chen, Andrew Essin, and Michael Hermele. Majorana spin liquids and projective realization of SU(2) spin symmetry. *Phys. Rev. B*, 85:094418, Mar 2012.

[79] Jianlong Fu. Properties and application of SO(3) majorana representation of spin: Equivalence with Jordan-Wigner transformation and exact Z_2 gauge theories for spin models. *Phys. Rev. B*, 98:214432, Dec 2018.

[80] Michael Hermele, Matthew P. A. Fisher, and Leon Balents. Pyrochlore photons: The $U(1)$ spin liquid in a $s = \frac{1}{2}$ three-dimensional frustrated magnet. *Phys. Rev. B*, 69:064404, Feb 2004.

[81] Lucile Savary and Leon Balents. Coulombic quantum liquids in spin-1/2 pyrochlores. *Phys. Rev. Lett.*, 108:037202, Jan 2012.

[82] Elbio Dagotto, Eduardo Fradkin, and Adriana Moreo. SU(2) gauge invariance and order parameters in strongly coupled electronic systems. *Phys. Rev. B*, 38:2926–2929, Aug 1988.

[83] Ian Affleck, Z. Zou, T. Hsu, and P. W. Anderson. SU(2) gauge symmetry of the large-u limit of the hubbard model. *Phys. Rev. B*, 38:745–747, Jul 1988.

[84] S. E. Barnes. New method for the Anderson model. *Journal of Physics F: Metal Physics*, 6(7):1375–1383, Jul 1976.

[85] R. N. Mohapatra and B. Sakita. SO($2n$) grand unification in an SU(N) basis. *Phys. Rev. D*, 21:1062–1066, Feb 1980.

[86] Frank Wilczek and A. Zee. Families from spinors. *Phys. Rev. D*, 25:553–565, Jan 1982.

[87] Chetan Nayak and Frank Wilczek. 2n-quasihole states realize 2^{n-1}-dimensional spinor braiding statistics in paired quantum Hall states. *Nuclear Physics B*, 479:529, 1996.

[88] André Ahlbrecht, Lachezar S. Georgiev, and Reinhard F. Werner. Implementation of Clifford gates in the Ising-anyon topological quantum computer. *Phys. Rev. A*, 79:032311, Mar 2009.

[89] P. Jordan and E. Wigner. Über das paulische äquivalenzverbot. *Zeitschrift für Physik*, 47(9):631–651, Sep 1928.

[90] Elliott Lieb, Theodore Schultz, and Daniel Mattis. Two soluble models of an antiferromagnetic chain. *Annals of Physics*, 16(3):407 – 466, 1961.

[91] Eduardo Fradkin. Jordan-Wigner transformation for quantum-spin systems in two dimensions and fractional statistics. *Phys. Rev. Lett.*, 63:322–325, Jul 1989.

[92] Ana Lopez, A. G. Rojo, and Eduardo Fradkin. Chern-Simons theory of the anisotropic quantum Heisenberg antiferromagnet on a square lattice. *Phys. Rev. B*, 49:15139–15158, Jun 1994.

[93] Krishna Kumar, Kai Sun, and Eduardo Fradkin. Chern-Simons theory of magnetization plateaus of the spin-$\frac{1}{2}$ quantum XXZ Heisenberg model on the kagome lattice. *Phys. Rev. B*, 90:174409, Nov 2014.

[94] Kai Sun, Krishna Kumar, and Eduardo Fradkin. Discretized Abelian Chern-Simons gauge theory on arbitrary graphs. *Phys. Rev. B*, 92:115148, Sep 2015.

[95] Y. R. Wang. Ground state of the two-dimensional antiferromagnetic Heisenberg model studied using an extended Wigner-Jordon transformation. *Phys. Rev. B*, 43:3786–3789, Feb 1991.

[96] J. Ambjørn and G.W. Semenoff. Fermionized spin systems and the boson-fermion mapping in (2+1)-dimensional gauge theory. *Physics Letters B*, 226(1):107 – 112, 1989.

[97] Mohamed Azzouz. Interchain-coupling effect on the one-dimensional spin-1/2 antiferromagnetic Heisenberg model. *Phys. Rev. B*, 48:6136–6140, Sep 1993.

[98] Frank Wilczek. Magnetic flux, angular momentum, and statistics. *Phys. Rev. Lett.*, 48:1144–1146, Apr 1982.

[99] Chetan Nayak, Steven H. Simon, Ady Stern, Michael Freedman, and Sankar Das Sarma. Non-Abelian anyons and topological quantum computation. *Rev. Mod. Phys.*, 80:1083–1159, Sep 2008.

[100] D. Eliezer and G. W. Semenoff. Anyonization of lattice Chern-Simons theory. *Annals of Physics*, 217(1):66 – 104, 1992.

[101] D. Eliezer and G. W. Semenoff. Intersection forms and the geometry of lattice Chern-Simons theory. *Physics Letters B*, 286(1):118 – 124, 1992.

[102] M. V. Berry. Quantal phase factors accompanying adiabatic changes. *Proc. R. Soc. London, Ser. A*, 392(1802):45–57, 1984.

[103] Di Xiao, Ming-Che Chang, and Qian Niu. Berry phase effects on electronic properties. *Rev. Mod. Phys.*, 82:1959–2007, Jul 2010.

[104] Y. Aharonov and J. Anandan. Phase change during a cyclic quantum evolution. *Phys. Rev. Lett.*, 58:1593–1596, Apr 1987.

[105] R. Jackiw and Erick J. Weinberg. Self-dual Chern-Simons vortices. *Phys. Rev. Lett.*, 64:2234–2237, May 1990.

[106] M. C. Diamantini, P. Sodano, and C. A. Trugenberger. Topological excitations in compact Maxwell-Chern-Simons theory. *Phys. Rev. Lett.*, 71:1969–1972, Sep 1993.

[107] Fabio L. Pedrocchi, Stefano Chesi, and Daniel Loss. Physical solutions of the Kitaev honeycomb model. *Phys. Rev. B*, 84:165414, Oct 2011.

[108] Fabian Zschocke and Matthias Vojta. Physical states and finite-size effects in Kitaev's honeycomb model: Bond disorder, spin excitations, and NMR line shape. *Phys. Rev. B*, 92:014403, Jul 2015.

[109] Han-Dong Chen and Zohar Nussinov. Exact results of the kitaev model on a hexagonal lattice: spin states, string and brane correlators, and anyonic excitations. *Journal of Physics A: Mathematical and Theoretical*, 41(7):075001, 2008.

[110] G. Kells, J. K. Slingerland, and J. Vala. Description of Kitaev's honeycomb model with toric-code stabilizers. *Phys. Rev. B*, 80:125415, Sep 2009.

[111] Balázs Dóra and Roderich Moessner. Gauge field entanglement in Kitaev's honeycomb model. *Phys. Rev. B*, 97:035109, Jan 2018.

[112] Christian Prosko, Shu-Ping Lee, and Joseph Maciejko. Simple Z_2 lattice gauge theories at finite fermion density. *Phys. Rev. B*, 96:205104, Nov 2017.

[113] T. Senthil and M. P. A. Fisher. Z_2 gauge theory of electron fractionalization in strongly correlated systems. *Phys. Rev. B*, 62:7850, 2000.

[114] Robert Schaffer, Subhro Bhattacharjee, and Yong Baek Kim. Quantum phase transition in Heisenberg-Kitaev model. *Phys. Rev. B*, 86:224417, Dec 2012.

[115] A. Yu Kitaev. Unpaired Majorana fermions in quantum wires. *Physics-Uspekhi*, 44(10S):131, 2001.

[116] Zohar Nussinov and Jeroen van den Brink. Compass models: Theory and physical motivations. *Rev. Mod. Phys.*, 87:1–59, Jan 2015.

[117] Han-Dong Chen, Chen Fang, Jiangping Hu, and Hong Yao. Quantum phase transition in the quantum compass model. *Phys. Rev. B*, 75:144401, Apr 2007.

[118] Zohar Nussinov, Cristian D. Batista, and Eduardo Fradkin. Intermediate symmetries in electronic systems: Dimensional reduction, order out of disorder, dualities, and fractionalization. *Int. J. Mod. Phys. B*, 20(30n31):5239–5249, 2006.

[119] A. H. Castro Neto, F. Guinea, N. M. R. Peres, K. S. Novoselov, and A. K. Geim. The electronic properties of graphene. *Rev. Mod. Phys.*, 81:109–162, Jan 2009.

[120] H.-Q. Ding and M. S. Makivić. Kosterlitz-Thouless transition in the two-dimensional quantum XY model. *Phys. Rev. B*, 42:6827–6830, Oct 1990.

[121] Steven T Bramwell and Michel JP Gingras. Spin ice state in frustrated magnetic pyrochlore materials. *Science*, 294(5546):1495–1501, 2001.

[122] C. Castelnovo, R. Moessner, and S. L. Sondhi. Magnetic monopoles in spin ice. *Nature*, 451:42–45, 2008.

[123] SungBin Lee, Shigeki Onoda, and Leon Balents. Generic quantum spin ice. *Phys. Rev. B*, 86:104412, Sep 2012.

[124] Zhihao Hao, Alexandre G. R. Day, and Michel J. P. Gingras. Bosonic many-body theory of quantum spin ice. *Phys. Rev. B*, 90:214430, Dec 2014.

[125] Argha Banerjee, Sergei V. Isakov, Kedar Damle, and Yong Baek Kim. Unusual liquid state of hard-core bosons on the pyrochlore lattice. *Phys. Rev. Lett.*, 100:047208, Jan 2008.

[126] Kate A. Ross, Lucile Savary, Bruce D. Gaulin, and Leon Balents. Quantum excitations in quantum spin ice. *Phys. Rev. X*, 1:021002, Oct 2011.

[127] Nic Shannon, Olga Sikora, Frank Pollmann, Karlo Penc, and Peter Fulde. Quantum ice: A quantum Monte Carlo study. *Phys. Rev. Lett.*, 108:067204, Feb 2012.

[128] Owen Benton, Olga Sikora, and Nic Shannon. Seeing the light: Experimental signatures of emergent electromagnetism in a quantum spin ice. *Phys. Rev. B*, 86:075154, Aug 2012.

[129] Yasuyuki Kato and Shigeki Onoda. Numerical evidence of quantum melting of spin ice: Quantum-to-classical crossover. *Phys. Rev. Lett.*, 115:077202, Aug 2015.

[130] P. A. McClarty, O. Sikora, R. Moessner, K. Penc, F. Pollmann, and N. Shannon. Chain-based order and quantum spin liquids in dipolar spin ice. *Phys. Rev. B*, 92:094418, Sep 2015.

[131] M. P. Kwasigroch, B. Douçot, and C. Castelnovo. Semi-classical approach to quantum spin ice. *arXiv:1609.03079*, 2016.

[132] Jason S. Gardner, Michel J. P. Gingras, and John E. Greedan. Magnetic pyrochlore oxides. *Rev. Mod. Phys.*, 82:53–107, Jan 2010.

[133] Yi-Ping Huang, Gang Chen, and Michael Hermele. Quantum spin ices and topological phases from dipolar-octupolar doublets on the pyrochlore lattice. *Phys. Rev. Lett.*, 112:167203, Apr 2014.

[134] Shigeki Onoda and Yoichi Tanaka. Quantum fluctuations in the effective pseudospin-$\frac{1}{2}$ model for magnetic pyrochlore oxides. *Phys. Rev. B*, 83:094411, Mar 2011.

[135] Jeffrey G. Rau and Michel J. P. Gingras. Magnitude of quantum effects in classical spin ices. *Phys. Rev. B*, 92:144417, Oct 2015.

[136] Lucile Savary, Kate A. Ross, Bruce D. Gaulin, Jacob P. C. Ruff, and Leon Balents. Order by quantum disorder in $Er_2Ti_2\mathbf{O}_7$. *Phys. Rev. Lett.*, 109:167201, Oct 2012.

[137] M. E. Zhitomirsky, M. V. Gvozdikova, P. C. W. Holdsworth, and R. Moessner. Quantum order by disorder and accidental soft mode in $Er_2Ti_2\mathbf{O}_7$. *Phys. Rev. Lett.*, 109:077204, Aug 2012.

[138] J. Robert, E. Lhotel, G. Remenyi, S. Sahling, I. Mirebeau, C. Decorse, B. Canals, and S. Petit. Spin dynamics in the presence of competing ferromagnetic and antiferromagnetic correlations in $Yb_2Ti_2O_7$. *Phys. Rev. B*, 92:064425, Aug 2015.

[139] H. Takatsu, S. Onoda, S. Kittaka, A. Kasahara, Y. Kono, T. Sakakibara, Y. Kato, B. Fåk, J. Ollivier, J. W. Lynn, T. Taniguchi, M. Wakita, and H. Kadowaki. Quadrupole order in the frustrated pyrochlore $Tb_{2+x}Ti_{2-x}O_{7+y}$. *Phys. Rev. Lett.*, 116:217201, May 2016.

[140] Jianlong Fu, Jeffrey G. Rau, Michel J. P. Gingras, and Natalia B. Perkins. Fingerprints of quantum spin ice in Raman scattering. *Phys. Rev. B*, 96:035136, Jul 2017.

[141] Jeffrey G. Rau, Eric Kin-Ho Lee, and Hae-Young Kee. Generic spin model for the honeycomb Iridates beyond the Kitaev limit. *Phys. Rev. Lett.*, 112:077204, Feb 2014.

Appendix A

Basics of U(1) Chern-Simons gauge theory and lattice Chern-Simons theory

A.1 U(1) Chern-Simons gauge theory

The definition of Chern-Simons (CS) term relies on the existence of the total anti-symmetrized tensor $\epsilon_{\mu\nu\rho}$ in (2+1)-dimensions. The definition of U(1) CS action with interaction with matter current is given by

$$S_{CS} + S_{int} = \int d^3x (\frac{k}{4\pi} \epsilon^{\mu\nu\rho} \mathcal{A}_\mu \partial_\nu \mathcal{A}_\rho - J^\mu \mathcal{A}_\mu), \tag{A.1}$$

in which $\mathcal{A}_\mu$ is the Chern-Simons gauge field and matter current is given by J^μ, all the indices $\mu, \nu, \rho = 0, 1, 2$. Throughout this paper, we use $\mathcal{A}$ to label Chern-Simons gauge field in continuum and use A to denote Chern-Simons gauge field on a lattice. The pure Chern-Simons term

$$S_{CS} = \frac{k}{4\pi} \int d^3x \epsilon^{\mu\nu\rho} \mathcal{A}_\mu \partial_\nu \mathcal{A}_\rho. \tag{A.2}$$

is gauge invariant under local gauge transformation. In particular, under gauge transformation $\mathcal{A}_\mu \to \mathcal{A}_\mu - \partial_\mu \phi$, the action change to

$$S_{CS} \to S_{CS} - \frac{k}{4\pi} \int d^3x \partial_\mu (\epsilon^{\mu\nu\rho} \phi \partial_\nu \mathcal{A}_\rho), \tag{A.3}$$

which vanishes because it is a total derivative. In the prefactor $\frac{k}{4\pi}$, the k is called the *level* of the Chern-Simons theory, it can be proved that k can only take integer values under the requirement that the Chern-Simons term (A.2) is gauge invariant at finite temperature [13].

The time component of $\mathcal{A}$ does not have any dynamics, to see this we have to write the action (A.1) in the following way [13]

$$S_t = \int d^3x [(\frac{k}{2\pi} \mathcal{A}_0 \mathcal{B} - J_0 \mathcal{A}_0) - \frac{k}{4\pi} \epsilon_{ij} \mathcal{A}_i \partial_t \mathcal{A}_j - J_i \mathcal{A}_i], \tag{A.4}$$

in which magnetic field $\mathcal{B}$ is defined by $\mathcal{B} = \epsilon_{ij} \partial_i \mathcal{A}_j$. We can see that the $\mathcal{A}_0$ field acts like a Lagrange mutiplier. Upon intergrating out $\mathcal{A}_0$ in the path integral, we have the constraint that $\frac{k}{2\pi} \mathcal{B} - J_0 = 0$. In the canonical formalism, it should be understood as the operator on the left hand side acting on the physical states gives zero [13, 94], i.e.

$$[\frac{k}{2\pi} \mathcal{B}(\boldsymbol{x}) - J_0(\boldsymbol{x})] |\text{Phys}\rangle = 0. \tag{A.5}$$

This is a requirement that the charge carried by the complex fermion c must come with a magnetic flux. Due to the Aharonov-Bohm effect, the attachment of magnetic flux to charged particles results in exotic statistics of particles [13, 99].

The CS term (A.2) has an important property, the canonical momentum conjugate to the gauge field is the gauge field itself. This results in the following non-trivial commutation relation

$$[\mathcal{A}_i(\boldsymbol{x}), \mathcal{A}_j(\boldsymbol{y})] = i \frac{2\pi}{k} \epsilon_{ij} \delta(\boldsymbol{x} - \boldsymbol{y}). \tag{A.6}$$

On the other hand, this property also results in the fact that the Hamiltonian of the pure Chern-Simons term (A.2) vanishes $\mathcal{H}_{CS} = 0$.

The line integral of gauge field plays important roles in gauge theories, the commutation relation (A.6) results in non-trivial commutation between line integrals. For two

arbitrary lines $\mathcal{C}$ and $\mathcal{C}'$ (with directions defined) we have

$$\left[\int_{\mathcal{C}} \mathcal{A}, \int_{\mathcal{C}'} \mathcal{A}\right] = i\frac{2\pi}{k}\nu[\mathcal{C}, \mathcal{C}'], \tag{A.7}$$

in which $\nu[\mathcal{C}, \mathcal{C}']$ is the number of oriented intersections between two lines [94]. If $\mathcal{C}$ and $\mathcal{C}'$ are closed loops, $\nu[\mathcal{C}, \mathcal{C}']$ is topologically invariant; besides, if any of $\mathcal{C}$ and $\mathcal{C}'$ can be contracted into a point, $\nu[\mathcal{C}, \mathcal{C}'] = 0$. The line integral of gauge field can be used to construct the *Wilson line* operators and the *Wilson loop* operators. In general the Wilson line operator is defined as $W_L = \exp(i \int_L \mathcal{A} \cdot d\boldsymbol{x})$.

Now we explore the non-trivial commutation relations between Wilson lines in Chern-Simons gauge theory. To do this, it turns out that the Baker-Hausdorff-Campbell (BHC) formula is useful; it states that for any operators X and Y, if commutator $[X, Y]$ is a number then we have

$$e^X e^Y = e^{X+Y+\frac{1}{2}[X,Y]} = e^Y e^X e^{[X,Y]}. \tag{A.8}$$

For two lines $\mathcal{C}$ and $\mathcal{C}'$, we define the Wilson line operators

$$W_{\mathcal{C}} = e^{i\int_{\mathcal{C}} \mathcal{A}}, \qquad W_{\mathcal{C}'} = e^{i\int_{\mathcal{C}'} \mathcal{A}}. \tag{A.9}$$

Using the BHC formula, we have

$$W_{\mathcal{C}} W_{\mathcal{C}'} = W_{\mathcal{C}'} W_{\mathcal{C}} e^{-[\int_{\mathcal{C}} \mathcal{A}, \int_{\mathcal{C}'} \mathcal{A}]} = W_{\mathcal{C}'} W_{\mathcal{C}} e^{-i\frac{2\pi}{k}\nu[\mathcal{C}, \mathcal{C}']}. \tag{A.10}$$

Now we focus on some special situations. In the 2D Jordan-Wigner transformation we take the level $k = 1$ [13, 91] (see Appendix B for details), the corresponding CS theory is called the $\mathrm{U}(1)_1$ Chern-Simons theory. In the $\mathrm{U}(1)_1$ Chern-Simons theory we have $e^{-i\frac{2\pi}{k}\nu[\mathcal{C}, \mathcal{C}']} = 1$, therefore

$$[W_{\mathcal{C}}, W_{\mathcal{C}'}] = 0. \tag{A.11}$$

This means that the Wilson lines in the $\mathrm{U}(1)_1$ Chern-Simons gauge theory all commute with each other. This is the result for Chern-Simons theory in the continuum. The lattice version of the Chern-Simons theory has different results for Wilson lines [94], which we will discuss in the next section.

A.2 Lattice U(1) Chern Simons gauge theory

The lattice discretization of the U(1) Chern-Simons gauge theory has been discussed on square lattice [92, 100, 101] and kagome lattice [93]. A general discussion on the conditions for lattice Chern-Simons theory has also been done [94]. Here, we follow Ref. [94] and give a brief review of some general results of lattice U(1) Chern-Simons theory, and we will focus on the situation where the level $k = 1$.

From the standard way to define lattice gauge theories [14], we place the paricle operators on the sites of the lattice and the gauge field operators on the bonds of the lattice. To discretize the U(1) CS theory (A.2) on a lattice, it is proved that a key condition is that there is a one-to-one mapping between sites and plaquettes of the lattice. If a graph or lattice has such mapping, one can find a way to pair up the sites and plaquettes. Once the pairing is determined, the lattice CS theory will attach the gauge flux in the plaquette to the particle defined on the corresponding site. For any given 2D lattice, the three types of elements are sites (or vertices), labelled by v; bonds (or edges), labelled by e; and plaquettes (or faces) labelled by f. For a lattice with one-to-one correspondence between sites and plaquettes, we have the action of the lattice CS theory,

$$S_{CS} = \frac{k}{2\pi} \int dt \sum_{v,f,e,e'} \left[A_v M_{v,f} \Phi_f - \frac{1}{2} A_e K_{e,e'} \dot{A}_{e'} \right], \tag{A.12}$$

in which the sum is over all sites, faces and edges of the lattice. Specifically, the flux operator Φ_f is defined by $\Phi_f = \sum_e \xi_{f,e} A_e$, in which $\xi_{f,e} = \pm 1$ if and only if e is an edge of face f, otherwise $\xi_{f,e} = 0$. The sign of $\xi_{f,e}$ is determined by the orientation of the bond. The Φ_f defined in this way is the lattice version of the flux. Also, in (A.12) the $M_{v,f}$ and $K_{e,e'}$ are two matrices. In particular, the matrix element $M_{v,f}$ picks up the site that is paired up with each face; in other words, its element is non-zero if and only if v is paired up with f; the $K_{e,e'}$ matrix is defined in the following way:

$$\begin{aligned} &K_{e,e'} = \pm\frac{1}{2}, \quad \text{if } e \text{ and } e' \text{ belong to the same face,} \\ &K_{e,e'} = 0, \quad \text{for all other cases.} \end{aligned} \tag{A.13}$$

The sign of non-vanishing elements of $K_{e,e'}$ is determined by the orientation of the bonds and their relative positions in the face, the details of which is not important for our

purpose (see Ref. [94] for a detailed description).

The gauge transformation in the lattice is defined by

$$A_v \to A_v - \partial_t \tilde{\phi}_v, \qquad A_e \to A_e - D_{v,e}\tilde{\phi}_v, \tag{A.14}$$

in which $\tilde{\phi}_v$ is an arbitrary real function defined on the sites and $D_{v,e} = \pm 1$ if and only if v is one of the end points of edge e, otherwise it is zero. As defined above, $\xi_{f,e}$ represents a lattice curl and $D_{v,e}$ represents a lattice gradient. It can be shown that the key condition for the lattice theory to be gauge invariant is that [94]

$$\sum_f M_{v,f}\xi_{f,e} = \sum_{e'} K_{e,e'} D_{v,e'}. \tag{A.15}$$

It can be proved that this condition is indeed satisfied by the construction described above [94].

One key property for the lattice satisfying the one-to-one correspondence between sites and faces is the existance of a dual lattice. To get the dual lattice, one simply reverses the definition of face and vertices. We put a vertex v^* in each face of the original graph and connect two v^* vertices if in the original graph the two faces share an edge, and thus we get the dual edge e^*. Obviously, we have the duality of each element as $v^* = f$, $e^* = e$ etc [94]. In the dual lattice the dual Chern-Simons theory can be defined according to (A.12). The $K_{e,e'}$ matrix in the dual theory becomes $K^*_{e^*,e'^*}$. Due to the correpondence between edges e and e^*, this can also be denoted as $K^*_{e,e'}$, its definition in the original edge indicies reads

$$\begin{aligned} &K^*_{e,e'} = \pm\frac{1}{2}, \quad \text{if e and } e' \text{ share a vertex,} \\ &K^*_{e,e'} = 0, \quad \text{otherwise.} \end{aligned} \tag{A.16}$$

It can be shown that the K^* matrix is actually related to the inverse of the K matrix,

$$K^* = -K^{-1}. \tag{A.17}$$

so that the $K_{e,e'}$ matrix is non-singular [94].

In the canonical formalism, the commutator between gauge fields on edges follows

directly from the Lagrangian, which is the integrand in (A.12). From Eq. A.12 one can read off the canonical conjugate variables to gauge fields, which results in the following commutation relation,

$$[A_e, \frac{k}{2\pi} K_{e',e''} A_{e''}] = i\delta_{e,e'}. \tag{A.18}$$

Since the K matrix can be inverted, we have

$$[A_e, A_{e'}] = -\frac{2\pi i}{k} K^{-1}_{e,e'}. \tag{A.19}$$

The flux attachment on the lattice work similarly as in the continous case, we place charge density J^0_v on each vertex v and couple it to A_v. We thus have the constraint

$$[\frac{k}{2\pi} M_{v,f} \Phi_f - J^0_v] |\text{Phys}\rangle = 0. \tag{A.20}$$

With these results at hand, we have a consistent theory of lattice Chern-Simons gauge theory.

Appendix B

Jordan-Wigner Transformation in 2D Using Chern-Simons Flux Attachment

Spin can be viewed as hard-core boson which behaves like bosonic operator but under the constraint that the number of boson on each site can only be 0 or 1 [13]. Here we start with a system of hard-core bosons and study its properties.

Suppose for each site i we have a hard-core boson a_i. For any ordinary bosonic operator b_i, we have the commutation relation $[b_i, b_j^\dagger] = \delta_{ij}$. However, this is not the commutation relation for hard-core boson a_i, for which we have to require that on each site there can only be 0 or 1 boson, in other words,

$$a_i^2 = 0; \qquad a_i^{\dagger 2} = 0. \tag{B.1}$$

The Hilbert space for each hard-core boson is restricted to be spanned by two basis states $|0\rangle$ and $|1\rangle$. For an ordinary bosonic operator b_i, to go to this two-dimensional subspace of the original Hilbert space (which has inifinite dimension), a projection is needed. Let's call it $\hat{P}_i$. We have that the hard-core boson operator a_i is obtained from the ordinary bosonic operator b_i by $a_i = \hat{P}_i b_i \hat{P}_i$; $a_i^\dagger = \hat{P}_i b_i^\dagger \hat{P}_i$. Due to the fact that $[\hat{P}_i, b_i] \neq 0$, one can see the hard-core boson as *dressed boson*.

The hard-core boson has the following commutation relations

$$\begin{aligned} &\{a_i, a_i^\dagger\} = 1; \qquad \text{and} \\ &[a_i, a_j] = [a_i, a_j^\dagger] = [a_i^\dagger, a_j^\dagger] = 0 \qquad \text{for } i \neq j. \end{aligned} \tag{B.2}$$

There is a one-to-one mapping between the Hilbert space of hard-core boson and the spin space, using the commutation relations of the hard-core boson operator (B.2), we have the following mapping between spin operator and hard-core boson operator,

$$\begin{aligned} \sigma_i^+ &= \frac{1}{2}(\sigma_i^x + i\sigma_i^y) = a_i^\dagger, \\ \sigma_i^- &= \frac{1}{2}(\sigma_i^x - i\sigma_i^y) = a_i; \\ \sigma_i^z &= 2a_i^\dagger a_i - 1. \end{aligned} \tag{B.3}$$

Next we follow Ref. [13, 91, 92, 93] to give a brief review of the 2D Jordan-Wigner transformation using the Chern-Simons gauge theory. We start with a simple two-dimensional quantum XY model, which according to (B.3) can be written in terms of hard-core boson as

$$\mathcal{H}_a = \sum_{ij} a_i^\dagger a_j + \text{h.c.}. \tag{B.4}$$

Here we assume the coupling constant $J = 1$. Due to the exotic commutation relation of the hard-core boson (B.2), it can be seen as an anyonic operator.

To see this, we start with a fermionic system coupled to Chern-Simons gauge field. The fermions reside on the sites of the lattice while the gauge field is defined on the bonds or edges of the lattice. The Hamiltonian is, setting coupling constant to unity,

$$\mathcal{H}_f = \sum_{ij} c_i^\dagger e^{iA_{ij}} c_j + \text{h.c.}. \tag{B.5}$$

The gauge field A_{ij} is subject to Chern-Simons action (A.12), which results in a constraint (A.20). Classically one can solve the configuation of the gauge field classically according to the charge distribution of fermion c on a certain lattice using the constraint [13, 91, 93, 95]. To this end, if we define an operator

$$\tilde{a}_i = e^{-i\phi_i} c_i, \tag{B.6}$$

in which operator ϕ_i is a functional of the density of the fermion $n_i = c_i^\dagger c_i$. Such functional form will lead to nontrivial commutation relation between operator $e^{-i\phi_i}$ and operator c_i. This will result in the exotic commutation relation of the anyonic operator $\tilde{a}_i$

$$\tilde{a}_i \tilde{a}_j^\dagger = \delta_{ij} - e^{i\delta} \tilde{a}_j^\dagger \tilde{a}_i, \tag{B.7}$$

in which $\delta = \frac{\pi}{k}$ is a constant, with k being the level of the Chern-Simons theory in (A.12) and (A.1). If the level $k = 1$, then $\delta = \pi$ and the commutation relation of anyon $\tilde{a}$ becomes bosonic. Further more, it satisfies the hard-core condition (B.1) following from its definition (B.6). Therefore when $k = 1$, the anyonic operator $\tilde{a}$ is identified to be a hard-core boson.

Under the condition that $k = 1$, it can also be shown that using (B.6), the fermionic Hamiltonian (B.5) can be transformed to hard-core boson Hamiltonian (B.4) which itself is the quantum XY spin Hamiltonian. In this way, we obtain the 2D Jordan-Wigner transformation.

Appendix C

Some details of the solving of the Kitaev model

C.1 The original solution of the Kitaev model

In this section, I will briefly review the original solution of the Kitaev model based on Ref. [23] and the material realization of the model. The Hamiltonian of the Kitaev model is given by Eq. (4.1), it has a conserved plaquette operator defined by

$$W_p = \sigma_1^x \sigma_2^y \sigma_3^z \sigma_4^x \sigma_5^y \sigma_6^z, \tag{C.1}$$

it satisfies the following equation $[W_p, \mathcal{H}] = 0$ for every plaquette in the lattice. This can be checked simply by applying the relation between Pauli matrices:

$$\sigma^i \sigma^j = \delta_{ij} + i\epsilon_{ijk}\sigma^k. \tag{C.2}$$

As discussed in Chapter 3, Kitaev proposed a Majorana fermion representation of spins [23], in which he used four type of Majorana fermions c_i and b_i^x, b_i^y, b_i^z for each site i. Being Majorana fermion operators, they satisfy $c = c^\dagger$ and $b = b^\dagger$ by definition. They also satisfy the following anti-commutation relations: $\{c_i, c_j\} = 2\delta_{ij}$, $\{b_i^\alpha, b_j^\beta\} = 2\delta_{ij}\delta_{\alpha,\beta}$. And all other anti-commutation vanishes. We can make the following representation of

the spin operators:

$$\sigma_i^\alpha = ic_i b_i^\alpha, \qquad \alpha = x, y, z. \tag{C.3}$$

This representation enlarge the Hilbert space of spins from 2^N to 4^N (the dimension of one Majorana fermion is $\sqrt{2}$ while the dimension of a spin is 2)[53]. If we want to go back to the real physical space, the following constraint must be imposed: for any physical state $|\Psi\rangle_{phys}$, we have

$$D_i|\Psi\rangle_{phys} = |\Psi\rangle_{phys}, \qquad D_i \equiv c_i b_i^x b_i^y b_i^z. \tag{C.4}$$

And it can be proved that if we require $c_i b_i^x b_i^y b_i^z = 1$ for all the physical states (which is equivalent to say that $b^x b^y = b^z c = -cb^z$), we can have the representation (C.3) satisfies spin relation (3.1), which means that this is a faithful representation. In this appendix, we use the original notation of the Majorana fermions defined by Kitaev in Ref [23], note that such definition has the following correspondence with the definition we used in Sec 3.1.2 (more specifically Eq. (3.16)),

$$c_i \to \eta_i^t, \qquad b_i^\alpha \to \eta_i^\alpha, \qquad \alpha = x, y, z. \tag{C.5}$$

When applied to the model (4.1), we have the Hamiltonian can be written as [53]:

$$\mathcal{H} = \sum_{\alpha=x,y,z} J_\alpha \sum_{\langle ij\rangle_\alpha} ic_i \hat{u}_{\langle ij\rangle_\alpha} c_j, \tag{C.6}$$

in which we defined $\hat{u}_{\langle ij\rangle_\alpha} \equiv ib_i^\alpha b_j^\alpha$. Using the fact that $[b_i^\alpha b_j^\alpha, c_i c_j b_i^\beta b_j^\beta] = 0$, we can prove that

$$[\mathcal{H}, \hat{u}_{\langle ij\rangle_\alpha}] = 0. \tag{C.7}$$

This means that each bond operator $\hat{u}_{\langle ij\rangle_\alpha}$ is a conserved quantity for the model. This renders the theory being a free theory for c Majorana fermions, which can be solved completely for each distribution of the bond variables $\hat{u}_{\langle ij\rangle_\alpha}$. Thus each distribution of $\hat{u}_{\langle ij\rangle_\alpha}$ gives a completely separate family of states of c Majorana fermions. The ground state of the whole model exists in the sector where all $\hat{u}_{\langle ij\rangle_\alpha} = 1$.

It is easy to notice that the representation (C.3) has the following gauge redundancy $c_i \to \xi_i c_i, b_i^\alpha \to \xi_i^{-1} b_i^\alpha$. Due to the fact that Majorana fermions are "real", we can only

have $\xi_i = \pm 1$. This is a local Z_2 gauge symmetry rooted in the representation. Under this gauge transformation, we have $\hat{u}_{\langle ij\rangle_\alpha} \to \xi_i \hat{u}_{\langle ij\rangle_\alpha} \xi_j$, thus $\hat{u}_{\langle ij\rangle_\alpha}$ is identified as the gauge connection or "Wilson line" of the Z_2 gauge theory. Unlike the usual gauge field, this model has completely static gauge fields, it doesn't have dynamics. It can be checked that the W_p operator defined above satisfies $W_p \sim \Pi_{\langle ij\rangle \in \partial P} \hat{u}_{\langle ij\rangle}$ up to a sign. This is the lattice curl of the gauge connection, thus the W_p operator gives the fluxes of the gauge field in each plaquette.

For convenience, we can define the "bond-fermion" operator [53]:

$$\chi_{\langle ij\rangle_\alpha} = \frac{1}{2}(b_i^\alpha + i b_j^\alpha) \tag{C.8}$$

The gauge connection is related to the number operator of the bond fermion through:

$$\hat{u}_{\langle ij\rangle_\alpha} \equiv i b_i^\alpha b_j^\alpha = 2\chi^\dagger_{\langle ij\rangle_\alpha} \chi_{\langle ij\rangle_\alpha} - 1. \tag{C.9}$$

In terms of these bond fermions, we can write the spin operators as [53]:

$$\sigma_i^\alpha = i c_i (\chi_{\langle ij\rangle_\alpha} + \chi^\dagger_{\langle ij\rangle_\alpha}); \qquad \sigma_j^\alpha = c_j (\chi_{\langle ij\rangle_\alpha} - \chi^\dagger_{\langle ij\rangle_\alpha}). \tag{C.10}$$

C.2 Material realization of the Kitaev model

The material realization of Kiteav's honecomb lattice model is proposed by Ref. [54] in the iridium oxides A_2IrO_3. The Kitaev interaction is generated between two adjacent Ir sites with $j_{\text{eff}} = \frac{1}{2}$ through superexchange with the aid of the O atom in between. However, in real materials, it is too idealized to assume that the Kitaev model is the only spin interaction. As proposed by Ref. [141], the real effective spin Hamiltonian should be the following:

$$H = \sum_{\langle ij\rangle = \alpha\beta(\gamma)} \Big[J \boldsymbol{S}_i \cdot \boldsymbol{S}_j + K S_i^\gamma S_j^\gamma + \Gamma (S_i^\alpha S_j^\beta + S_i^\beta S_j^\alpha) \Big]. \tag{C.11}$$

The methodology of the bond labelling is defined in detail in Ref. [141]. The first term gives the isotropic Heisenberg interaction and the second term is the Kitaev interaction. The third is a novel spin exchange term which is similar to the Dzyaloshinskii-Moriya

terms.

While these three parameters J, K, Γ vary in the parameter space, various phases of the ground state might be possible in real materials. The phase structure is discussed in Ref. [141].

C.3 Complex fermion spectrum of Kitaev model

In our solution of the Kitaev model in Sec 4.1, it is possible to work out the spectrum of the complex fermion in a certain chosen gauge of the Z_2 gauge theory. On the other hand, in Kiaev's original solution discussed above, the free "c Majorana fermion" can also be paired up and form a system of complex fermions. The spectrum can thus be calculated in a certain gauge, and the results turn out to be identical as our solution using the SO(3) Majorana representation. Here we give the details of the calculation continuing with our discussion in Sec 4.1 using the SO(3) Majorana representation.

In terms of complex fermions introduced in Sec. 4.1.1, namely, Eq. (4.6), the Hamiltonian (4.5) becomes

$$\begin{aligned}\mathcal{H}'' = &\sum_{\boldsymbol{r}\in A}(-\tilde{J}_x)[(c^z_{\boldsymbol{r}} + c^{z\dagger}_{\boldsymbol{r}})(c^z_{\boldsymbol{r}+\boldsymbol{e}_1} - c^{z\dagger}_{\boldsymbol{r}+\boldsymbol{e}_1})] \\ &+ (-\tilde{J}_y)[(c^z_{\boldsymbol{r}} + c^{z\dagger}_{\boldsymbol{r}})(c^z_{\boldsymbol{r}+\boldsymbol{e}_2} - c^{z\dagger}_{\boldsymbol{r}+\boldsymbol{e}_2})] \\ &+ J_z(2c^{z\dagger}_{\boldsymbol{r}}c^z_{\boldsymbol{r}} - 1),\end{aligned} \tag{C.12}$$

in which $\tilde{J}_x = \pm J_x, \tilde{J}_y = \pm J_y$ depending on the eigenvalues of $\eta^y_i\eta^y_j$ and $\eta^x_i\eta^x_j$ on x- and y-bonds, respectively.

Next we perform a Fourier transformation of c fermions

$$c_{\boldsymbol{r}} = \frac{1}{\sqrt{N}}\sum_{\boldsymbol{k}} c_{\boldsymbol{k}}e^{i\boldsymbol{k}\cdot\boldsymbol{r}}; \qquad c^\dagger_{\boldsymbol{r}} = \frac{1}{\sqrt{N}}\sum_{\boldsymbol{k}} c^\dagger_{\boldsymbol{k}}e^{-i\boldsymbol{k}\cdot\boldsymbol{r}}, \tag{C.13}$$

where N denotes the total number of unit cells in the system. The sum in the k-space is taken over the entire first Brillouin Zone, labelled by BZ. However, for the Hamiltonian only half of the k-points are independent and thus we sum only over half of the BZ,

labelled by $BZ^{'}$. Therefore the Hamiltonian (C.12) is transformed into:

$$\mathcal{H}^{''} = \sum_{\boldsymbol{k}\in BZ'} \begin{pmatrix} c^{z}_{-\boldsymbol{k}} & c^{z\dagger}_{\boldsymbol{k}} \end{pmatrix} \mathcal{M}_{\boldsymbol{k}} \begin{pmatrix} c^{z\dagger}_{-\boldsymbol{k}} \\ c^{z}_{\boldsymbol{k}} \end{pmatrix}, \tag{C.14}$$

in which the coupling matrix $\mathcal{M}_{\boldsymbol{k}}$ is given by

$$\mathcal{M}_{\boldsymbol{k}} = \begin{pmatrix} -2\tilde{J}_x \cos(\boldsymbol{k}\cdot\boldsymbol{e}_1) - 2\tilde{J}_y \cos(\boldsymbol{k}\cdot\boldsymbol{e}_2) - 2J_z & 2i(\tilde{J}_x \sin(\boldsymbol{k}\cdot\boldsymbol{e}_1) + \tilde{J}_y \sin(\boldsymbol{k}\cdot\boldsymbol{e}_2)) \\ -2i(\tilde{J}_x \sin(\boldsymbol{k}\cdot\boldsymbol{e}_1) + \tilde{J}_y \sin(\boldsymbol{k}\cdot\boldsymbol{e}_2)) & 2\tilde{J}_x \cos(\boldsymbol{k}\cdot\boldsymbol{e}_1) + 2\tilde{J}_y \cos(\boldsymbol{k}\cdot\boldsymbol{e}_2) + 2J_z \end{pmatrix}. \tag{C.15}$$

Diagonalize this matrix, we obtain the energy spectrum for the c^z fermions which agrees with the one obtained in the Kitaev's solution [23],

$$E_{\boldsymbol{k}} = 2|\tilde{J}_x e^{i\boldsymbol{k}\cdot\boldsymbol{e}_1} + \tilde{J}_y e^{i\boldsymbol{k}\cdot\boldsymbol{e}_2} + J_z|. \tag{C.16}$$

Appendix D

Details of definitions in the quantum spin ice model

In this section, we give detailed definition of the variables defined in the quantum spin ice model in Chapter 5.

Firstly, the definition of the lattice vectors $\boldsymbol{\mu}$ is:

$$\hat{0} = \frac{+\hat{x}+\hat{y}+\hat{z}}{4}, \quad \hat{1} = \frac{+\hat{x}-\hat{y}-\hat{z}}{4},$$
$$\hat{2} = \frac{-\hat{x}+\hat{y}-\hat{z}}{4}, \quad \hat{3} = \frac{-\hat{x}-\hat{y}+\hat{z}}{4},$$

where $\hat{x}, \hat{y}, \hat{z}$ denote the global cubic axes. The local coordinates ($\hat{x}_\mu$, $\hat{y}_\mu$, $\hat{z}_\mu$) for the four sites (labeled as $\mu = 0, 1, 2, 3$) of a certain tetrahedron of the pyrochlore lattice are defined as

$$\begin{aligned}
\hat{x}_0 &= \frac{-2\hat{x}+\hat{y}+\hat{z}}{\sqrt{6}}, \hat{y}_0 = \frac{-\hat{y}+\hat{z}}{\sqrt{2}}, \hat{z}_0 = \frac{+\hat{x}+\hat{y}+\hat{z}}{\sqrt{3}}, \\
\hat{x}_1 &= \frac{-2\hat{x}-\hat{y}-\hat{z}}{\sqrt{6}}, \hat{y}_1 = \frac{+\hat{y}-\hat{z}}{\sqrt{2}}, \hat{z}_1 = \frac{+\hat{x}-\hat{y}-\hat{z}}{\sqrt{3}}, \\
\hat{x}_2 &= \frac{+2\hat{x}+\hat{y}-\hat{z}}{\sqrt{6}}, \hat{y}_2 = \frac{-\hat{y}-\hat{z}}{\sqrt{2}}, \hat{z}_2 = \frac{-\hat{x}+\hat{y}-\hat{z}}{\sqrt{3}}, \\
\hat{x}_3 &= \frac{+2\hat{x}-\hat{y}+\hat{z}}{\sqrt{6}}, \hat{y}_3 = \frac{+\hat{y}+\hat{z}}{\sqrt{2}}, \hat{z}_3 = \frac{-\hat{x}-\hat{y}+\hat{z}}{\sqrt{3}}.
\end{aligned} \tag{D.1}$$

In Eq.(5.1), the phase factors γ and ζ are defined as [81, 126]

$$\gamma_{\mu\nu} = \begin{pmatrix} 0 & 1 & \omega & \omega^2 \\ 1 & 0 & \omega^2 & \omega \\ \omega & \omega^2 & 0 & 1 \\ \omega^2 & \omega & 1 & 0 \end{pmatrix}_{\mu\nu} , \tag{D.2}$$

where $\omega = e^{2\pi i/3}$ and $\zeta_{\mu\nu} = -\gamma^*_{\mu\nu}$.

Appendix E

Glossary and Acronyms

Care has been taken in this thesis to minimize the use of jargon and acronyms, but this cannot always be achieved. This appendix defines jargon terms in a glossary, and contains a table of acronyms and their meaning.

E.1 Glossary

- **gauge theory** – A quantum field theory in which the field has local symmetry, the symmetry transformed field has identical physical meaning with the original one.
- **lattice gauge theory** – Gauge theory defined on lattice, originally introduced in particle physics for computer simulation. In recent years it has more and more application and relevance in condensed matter physics.
- **slave-particle representation** – Refers to the mapping between a spin operator and an operator in terms of bosonic or fermionic operators, including complex fermion representation and Majorana representation etc.
- **Majorana fermion** – A fermion which is its own antiparticle. The operators describing the Majorana fermions are real and anticommute with each other.
- **Majorana representation** – A kind of slave-particle representation defined in terms of Majorana fermions.

- **quantum spin liquid** – A special kind of ground state of interacting spin models in which no symmetry is broken.
- **Kitaev model** – An exactly solvable spin model on honeycomb lattice proposed by A. Kitaev. In its original solution, the Kitaev representation was applied.
- **Chern-Simons JW transformation** – The Jordan-Wigner transformation in 2D, involving Chern-Simons gauge theory.

E.2 Acronyms

Table E.1: Acronyms

Acronym	Meaning
QSL	Quantum spin liquid
QSI	Quantum spin ice
CS	Chern-Simons
QHE	Quantum Hall effect
HS	Hubbard-Stratonovich
JW	Jordan-Wigner
RVB	resonant-valence-bond
1D (1d)	one-dimensional or one dimension
2D (2d)	two-dimensional or two dimensions
PSG	Projective Symmetry Group
BHC	Baker-Hausdorff-Campbell
BZ	Brillouin Zone